TEC-0102

A Hyperspectral Gas Analysis System (HyGAS)

Pam Owensby
Juliana Lo
Jessica Sunshine
Stan Zisk

Science & Technology International
Grosvenor Center, Makai Tower
733 Bishop Street, 31st Floor
Honolulu, HI 96813

December 1997

U.S. Army Corps of Engineers
Topographic Engineering Center
7701 Telegraph Road
Alexandria, Virginia 22315-3864

US Army Corps of Engineers
Topographic Engineering Center

T E C

Destroy this report when no longer needed.
Do not return it to the originator.

The findings in this report are not to be construed as an official Department of the Army position unless so designated by other authorized documents.

The citation in this report of trade names of commercially available products does not constitute official endorsement or approval of the use of such products.

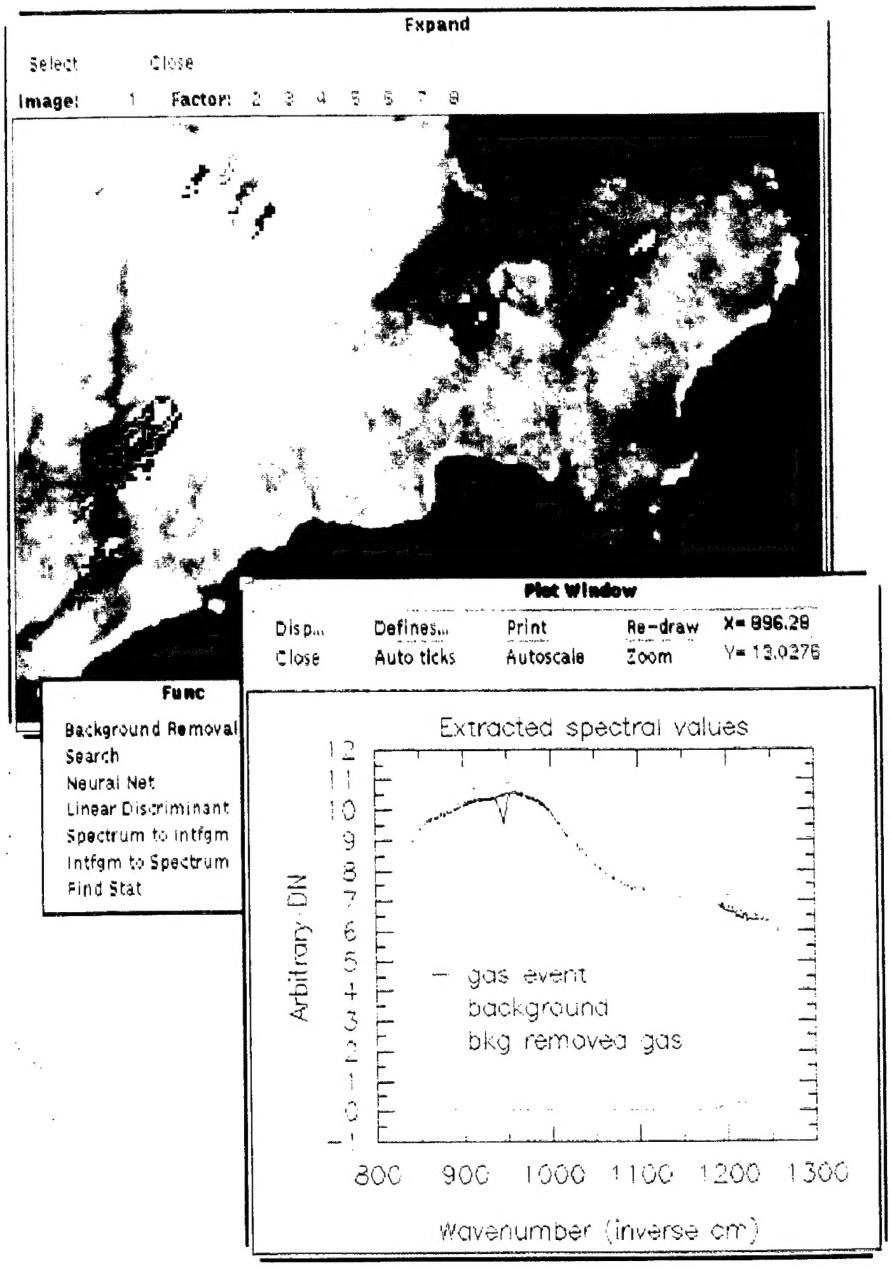

HyGAS

Hyperspectral Gas Analysis System

Final Report

For U. S. Army Topographic Engineering Center
Contract DACA 76-92-C-0037

sti

REPORT DOCUMENTATION PAGE

Form Approved
OMB No. 0704-0188

1. AGENCY USE ONLY *(Leave blank)*	2. REPORT DATE	3. REPORT TYPE AND DATES COVERED
	December 1997	Technical September 1992–November 1997

4. TITLE AND SUBTITLE

A Hyperspectral Gas Analysis System (HyGAS)

5. FUNDING NUMBERS

DACA76-92-C-0037

6. AUTHOR(S)

Pam Owensby Jessica Sunshine
Juliana Lo Stan Zisk

7. PERFORMING ORGANIZATION NAME(S) AND ADDRESS(ES)

Science & Technology International
Grosvenor Center, Makai Tower
733 Bishop Street, 31st Floor
Honolulu, HI 96813

8. PERFORMING ORGANIZATION REPORT NUMBER

9. SPONSORING / MONITORING AGENCY NAME(S) AND ADDRESS(ES)

U.S. Army Topographic Engineering Center
7701 Telegraph Road
Alexandria, VA 22315-3864

19. SPONSORING / MONITORING AGENCY REPORT NUMBER

TEC-0102

11. SUPPLEMENTARY NOTES

Block #7 - Performing Organization, Science & Technology International, was formerly known as: SETS Technology, Inc., 300 Kahelu Avenue, #10, Mililani, HI 96789.

12a. DISTRIBUTION / AVAILABILITY STATEMENT

Approved for public release; distribution is unlimited.

12b. DISTRIBUTION CODE

13. ABSTRACT *(Maximum 200 words)*

A prototype software hyperspectral gas analysis system (HyGAS) for standoff (remote) gas detection, identification, and analysis was designed for use with developing hyperspectral imaging spectrometer systems. HyGAS incorporates traditional (FFT, background removal and library search) and innovative (neural nets for gas identification and linear discriminants for gas detection) processing methods. Neural net and linear discriminant techniques are uniquely suited for low signal-to-noise ratio field applications, processing data quickly, and reducing data storage requirements, all important considerations for real-time exploitation and automated applications. HyGAS incorporates an interactive display-based system, where five spatial images and fifteen spectral plots can be displayed simultaneously. HyGAS applies spectral techniques of gas analysis to hyperspectral image cubes, providing a method of detecting and identifying gases and mapping regional extent and concen- tration. HyGAS is supplied with synthetic image cubes to simulate datasets collected by a hyperspectral imaging system over a possible gas release event covering the LWIR spectral region (~ 8-12 μm) with specifications selected to match the point spectronometers used to develop the neural net and linear discriminant techniques.

14. SUBJECT TERMS			15. NUMBER OF PAGES
Hyperspectral	Spectroscopy	Computer Image Processing	110
Remote Sensing	Gas Analysis		16. PRICE CODE

17. SECURITY CLASSIFICATION OF REPORT	18. SECURITY CLASSIFICATION OF THIS PAGE	19. SECURITY CLASSIFICATION OF ABSTRACT	20. LIMITATION OF ABSTRACT
UNCLASSIFIED	UNCLASSIFIED	UNCLASSIFIED	UNLIMITED

Table of Contents

Volume I:

Table of Contents

Volume I (continued):

REPORT DOCUMENTATION PAGE

Form Approved
OMB No. 0704-0188

1. AGENCY USE ONLY *(Leave blank)*	2. REPORT DATE	3. REPORT TYPE AND DATES COVERED
	December 1997	Technical September 1992-November 1997

4. TITLE AND SUBTITLE

A Hyperspectral Gas Analysis System (HyGAS)

5. FUNDING NUMBERS

DACA76-92-C-0037

6. AUTHOR(S)

Pam Owensby Jessica Sunshine
Juliana Lo Stan Zisk

7. PERFORMING ORGANIZATION NAME(S) AND ADDRESS(ES)

Science & Technology International
Grosvenor Center, Makai Tower
733 Bishop Street, 31st Floor
Honolulu, HI 96813

8. PERFORMING ORGANIZATION REPORT NUMBER

9. SPONSORING / MONITORING AGENCY NAME(S) AND ADDRESS(ES)

U.S. Army Topographic Engineering Center
7701 Telegraph Road
Alexandria, VA 22315-3864

19. SPONSORING / MONITORING AGENCY REPORT NUMBER

TEC-0102

11. SUPPLEMENTARY NOTES

Block #7 - Performing Organization, Science & Technology International, was formerly known as: SETS Technology, Inc., 300 Kahelu Avenue, #10, Mililani, HI 96789.

12a. DISTRIBUTION / AVAILABILITY STATEMENT

Approved for public release; distribution is unlimited.

12b. DISTRIBUTION CODE

13. ABSTRACT *(Maximum 200 words)*

A prototype software hyperspectral gas analysis system (HyGAS) for standoff (remote) gas detection, identification, and analysis was designed for use with developing hyperspectral imaging spectrometer systems. HyGAS incorporates traditional (FFT, background removal and library search) and innovative (neural nets for gas identification and linear discriminants for gas detection) processing methods. Neural net and linear discriminant techniques are uniquely suited for low signal-to-noise ratio field applications, processing data quickly, and reducing data storage requirements, all important considerations for real-time exploitation and automated applications. HyGAS incorporates an interactive display-based system, where five spatial images and fifteen spectral plots can be displayed simultaneously. HyGAS applies spectral techniques of gas analysis to hyperspectral image cubes, providing a method of detecting and identifying gases and mapping regional extent and concen- tration. HyGAS is supplied with synthetic image cubes to simulate datasets collected by a hyperspectral imaging system over a possible gas release event covering the LWIR spectral region (~ 8-12 μm) with specifications selected to match the point spectronometers used to develop the neural net and linear discriminant techniques.

14. SUBJECT TERMS

Hyperspectral Spectroscopy Computer Image Processing
Remote Sensing Gas Analysis

15. NUMBER OF PAGES

110

16. PRICE CODE

17. SECURITY CLASSIFICATION OF REPORT	18. SECURITY CLASSIFICATION OF THIS PAGE	19. SECURITY CLASSIFICATION OF ABSTRACT	20. LIMITATION OF ABSTRACT
UNCLASSIFIED	UNCLASSIFIED	UNCLASSIFIED	UNLIMITED

A HYPERPSECTRAL GAS ANALYSIS SYSTEM (HyGAS) FINAL REPORT

1.0 Summary

The Hyperspectral Gas Analysis System (HyGAS) Phase II project objective was to design and develop a software system for use with the Hyperspectral Image Processing System (HIPS)[1] to do standoff (remote) gas detection, identification and analysis.

To define practical specifications for HyGAS, we reviewed existing techniques for standoff gas analysis. Techniques developed by the U. S. Army for application in field scenarios (as opposed to laboratory settings) were given precedence for incorporation into HyGAS.

The following techniques from U. S. Army researchers were initially identified as operationally functional for limited standoff gas applications under actual field situations.

- gaussian spatial edge-detection, background clutter suppression, and multiple focal plane filters (M. Althouse, ERDEC[2])
- linear discriminant spectral detection (R. Kroutil, ERDEC)
- narrow-band infrared video camera (M. Norton, NVEOD[3])
- neural net spectral identification (P. Rauss, ARL[4])

The two spectral techniques (Kroutil and Rauss) were demonstrated using point FOV FTIR spectrometers. The remaining techniques (Althouse and Norton) were demonstrated using infrared spatial imaging arrays (FLIRs or IR video cameras), in conjunction with one or more associated narrow-band filters. Although each of these techniques holds in common the potential for real-time application, each is limited by currently available hardware to producing data in only two of the three-dimensions accommodated by a standard HIPS image cube[5].

We conceptualized HyGAS as an interactive software package for HIPS that would enable the user to interactively display and analyze both multiple images and multiple spectra. Spectral techniques could be applied interactively to selected spatial images; similarly, spatial techniques could be applied interactively to selected spectral bands.

After investigating each of the above techniques, only the two spectral techniques proved feasible for incorporation into the existing HIPS architecture of performing spectral operations on a traditional 2-D spatial scene. To simulate the use of these techniques with next-generation hardware systems capable of generating full 3-D hyperspectral image cubes, we created simulated hyperspectral image cubes based on the actual Government Furnished Information (GFI) field-acquired spectral data for each technique.

---

[1] Hyperspectral Image Processing System, developed under previous SBIR funding for the U.S. Army Topographic Engineering Center, Alexandria, Virginia.

[2] U. S. Army Edgewood Research Development and Engineering Center, Edgewood, Maryland.

[3] U. S. Army Night Vision and Electro-Optical Directorate, Ft. Belvoir, Virginia.

[4] U.S. Army Research Laboratory, Ft. Belvoir, Virginia

[5] a HIPS image cube is usually represented as a two-dimensional spatial image with full spectral data defined for each image pixel.

We then designed the interactive HyGAS user interface to incorporate each function necessary to apply these techniques. Details on supplied GFI datasets, gas databases, and creation of simulated cubes are given in the appendices of this report. Details on the functional use of HyGAS are given separately in the *HyGAS User's Manual/Tutorial.*

2.0 Technical Objectives

HyGAS is a software module prototype designed to meet the scientific requirements of standoff (remote) gas detection and exploitation for an *imaging* spectrometer system. HyGAS applies the methodologies used to process/analyze data from point spectrometers to process a hyperspectral image cube data set, i.e., a 2-D image with full spectral data for each image pixel.

HyGAS is designed to function within the framework of the existing HIPS software package.

The HyGAS Phase II effort was divided chronologically into two major parts:

(1) define the practical specifications required for HyGAS development, as built upon the Phase I background research and system requirements

(2) implement these specifications into the HyGAS prototype software system.

HyGAS development comprised four tasks:

Task 1—System Development

Task 2—Software Development

Task 3—Spectrum Database/Measurements Development

Task 4—Documentation

2.1 Task 1—System Development

The objectives of the system development task were:

(1) prepare a HyGAS conceptual design

(2) define the specifications necessary to implement this design

(3) incorporate these specifications into preliminary and final designs for the HyGAS system.

This task included reviewing the research conducted during Phase I and conducting new research, selecting suitable applications and requirements from that research, and defining the specifications required to implement software for these applications and requirements.

The HyGAS software system was developed for hardware systems that did not currently exist, but were expected to become available in the near future. The design of HyGAS was biased towards hardware systems that were currently under development, and systems that were likely to adapt well to existing methods of gas study. Such systems include imaging fourier transform infrared (FTIR) systems (FTS), and hyperspectral imaging (HSI) cameras. To adapt best to gas studies, such systems should operate in the 8-12 μm spectral region with a spectral resolution of at least 8 cm^{-1}. Systems such as

these will allow the application of novel techniques of gas detection and integration currently in use for point FTIR spectrometers and multispectral imaging (MSI) cameras.

HyGAS was designed to incorporate into HIPS current methods of standoff gas analysis using both spectral and spatial (image) processing techniques. Primary emphasis was gas/vapor cloud detection, i.e., "Is there a gas cloud present, and if so, where is it?" Secondary emphasis was gas identification, i.e., "If there is a gas contaminant present, what gas(es) is it?" Tertiary emphasis was gas analysis, i.e., "How much gas is there?", "Where, in detail, is the gas?" and/or "Where is the gas cloud likely to go?" Gas cloud detection was currently being done by both spectral (Kroutil) and spatial (Althouse) processing techniques. Gas identification was only being done by spectral (Rauss) techniques.

Gas analysis usually requires both spectral and spatial techniques as well as some sort of depth profiling technique (such as LIDAR), or some sort of time profiling technique (such as real time video synchronization, e.g. Norton). As delivered, only spectral techniques were implemented into HyGAS. Spatial techniques and depth and time profiling techniques should be considered for future implementation.

2.2 Task 2—Software Development

The objective of the software development task was to implement the software processes required to build the HyGAS system defined in Task 1. This task included acquisition of necessary hardware, acquisition and modification of necessary existing software, and coding of additional new software.

A *Gas Analysis* option was added to the HIPS main menu selection window. This *Gas Analysis* menu contains the individual gas analysis functions, which can be run non-interactively. It also includes the *Interactive HyGAS* module which incorporates all of these individual functions (and more) into the interactive gas analysis package. Individual HyGAS functions include Linear Discriminant Test (Kroutil gas detection algorithm), Background Removal (subtraction or division method), Interferogram to Spectrum and Spectrum to Interferogram (FFT and inverse FFT), Library Search and Neural Net search (gas identification/analysis), and image statistics. Most of these are spectral functions which can be applied either to an image cube or an individual spectrum (or interferogram). [Additional functions originally considered for incorporation, such as the spatial edge detection functions from M. Althouse, turned out not to be feasible for this implementation of HyGAS.]

2.3 Task 3—Spectral Database/Measurements Development

The objectives of the spectral database/measurements development task were to provide suitable data for testing and demonstrating the HyGAS system developed under Task 1, and for demonstrating and validating the performance of each software process developed under Task 2. This task included acquisition of existing datasets and/or data libraries, measurement of new datasets and/or data libraries, and/or modeling of theoretical datasets and/or data libraries. Datasets and gas libraries supplied (GFI) for use with HyGAS are described in detail in Appendices A and B.

Hyperspectral image data suitable for gas applications was not available for HyGAS. Therefore, we synthesized datasets to demonstrate and test the functionality of all HyGAS routines. These datasets are based on actual spectral data synthesized into a hyperspectral image cube format and are designed to approximate realistic acquisition applications. Details are given in Appendix C.

2.4 Task 4—Documentation

The objective of the documentation task was to manage, plan, track and provide proper closure of the project. This task included preparation and delivery of the items on the contract data requirements list (CDRL). This task also included the test and validation plans, training and demonstration, the Factory Acceptance Test (FAT) and the Site Acceptance Test (SAT).

Documentation included technical progress reports, work plans, software users manual and final technical report.

3.0 Review of Work Performed

3.1 Task 1—System Development

HyGAS was designed to process hyperspectral image data for standoff (remote) gas/vapor cloud detection, identification and analysis. During HyGAS development, no suitable hyperspectral imaging sensor systems were operational for these applications. Hyperspectral imaging systems did exist, but they had neither the spectral coverage nor the spectral resolution necessary for gas-specific applications. However, gas sensor systems with the required spectral coverage and resolution are in design and development stages, and the HyGAS project intent was to provide software for processing the data from such systems as soon as they become available.

Software routines developed for HyGAS were based on current state-of-the-art techniques developed for gas analysis using existing sensor systems. Existing sensor systems designed for standoff (remote) gas applications fall into one of the following system types: Type I—hyperspectral point spectrometers, or Type II—multispectral imaging cameras. Under development are hybrid systems of Type III—hyperspectral imaging systems.

All of these systems are designed to operate in the thermal IR spectral region (2–14μm), often referred to as the "fingerprint" spectral region for gas studies. Type I systems, hyperspectral point spectrometers, are usually Fourier Transform Spectrometer (FTS) systems. These systems produce sufficient (high resolution) spectral information for gas studies, but only for a single, usually wide, instantaneous spatial field of view (IFOV). Type II systems, multispectral imaging cameras, are usually Forward Looking Infrared Radiometers (FLIRs) or IR video cameras converted to "multispectral" spatial imagers. These systems produce sufficient spatial information, but only at a very few (2-3) relatively narrow spectral bands. Type III systems, hyperspectral imaging systems, are currently under design and development only as system prototypes. These systems will produce both sufficient spectral and spatial information for gas specific applications, but at the expense of time dependence in one dimension. Hyperspectral imaging hardware

systems, by the inherent restriction of a 2-D focal plane, must compromise one of the three dimensions (spatial-spatial-spectral) in a hyperspectral image cube, and collect that dimension as a function of time. Spatial analysis techniques are most useful for hardware that generates a spatial-spatial focal plane (i.e. imaging cameras). Spectral analysis techniques are most useful for hardware that generates a spatial-spectral focal plane (imaging spectrometers). The remaining dimension (spectral for imaging cameras, spatial for imaging spectrometers) must be collected (scanned) as a function of time. This naturally creates difficulties with time variable phenomena, which necessitates that integration times and time differentials be kept as short as possible.

In the HyGAS project, we integrated gas detection algorithms and techniques already in practice with Type I and II systems, into the existing HIPS software system designed to handle data from Type III systems. Thus HyGAS is an integrated software system ready to process data from hyperspectral spatial imaging sensor systems with the spectral resolution and range of coverage required for standoff gas applications.

During Phase II, we selected the techniques in use for Type I and II systems as most likely to be successfully implemented into HyGAS. A certain bias was assumed to support systems of Type III most likely to be available in the near future.

3.1.1. Type I systems—Hyperspectral point spectrometers

Spectral analysis of gases and vapors is traditionally done in the thermal infrared spectral region (700–5000 cm^{-1}, or 2–14 μm), at high spectral resolution (0.1–16 cm^{-1}, or $\Delta\lambda/\lambda \cong$ 0.0001–0.01), using integrated point field of view laboratory Fourier Transform Spectrometer (FTS) systems. The infrared spectral region is often referred to as the "fingerprint" region for gas identification: each molecule exhibits specific characteristic absorption (or emission) lines due to specific changes in energy associated with the electronic, vibrational or rotational state of the molecule. For gases, changes in vibrational and rotational states are most common. Changes in vibrational state exhibit broader bands than changes in rotational state (rotational fine structure), and the two are often superimposed, creating a vibration-rotation band. Rotational fine structure (lines of bandwidth ~0.1 cm^{-1}) is important primarily for the detailed study of small, symmetrical molecules. For the study of larger, more complicated molecules, so many broad, overlapping lines are generated due to vibrational changes, that high resolution gains very little over coarser resolution. For studies of these agents, resolutions on the order of 16 cm^{-1} can suffice.

Laboratory observations are generally conducted under carefully controlled atmospheres, with the major absorbing atmospheric constituents, water and carbon-dioxide, removed. For standoff field applications, the strength of the ambient atmospheric water vapor absorptions typically leave only the "window" spectral regions of 800–1200 cm^{-1} (~8–12 μm) and 2000–3000 cm^{-1} (~3–5μm) useful. Additionally, the reduced intensity of the background source radiation and the resultant reduced temperature differential between that source and the gas under study (ambient thermal background instead of a hot thermal laboratory source) reduces the signal-to-noise ratio to near detectability limits for ambient atmosphere field applications.

FTS systems, with their inherent Fellgett and Jacquinot advantages, are generally preferable to dispersive (grating) systems for low signal-to-noise scenarios. The *Fellgett advantage* refers to the inherent benefit achieved by an FTS system which can collect the energy from all spectral frequencies simultaneously, over that of a comparable single detector dispersive system, which could only collect the energy from each spectral band sequentially as the spectrum is scanned over the detector. This advantage is achieved with the FTS system by frequency-division multiplexing, providing wide wavelength coverage as well as greatly improved SNR (perhaps several orders of magnitude) over that of a comparable range scanning spectrometer. The *Jacquinot advantage* refers to the greater optical throughput (étendue, defined as the product of the beam area A and the solid angle Ω) achieved by an FTS system over a comparable resolution dispersive system. This advantage, shared also by Fabry–Perot interferometers, is realized mostly on practical considerations of the physical size of a reasonable beamsplitter element for an FTS system, as compared to the much larger grating required for a similar resolution dispersive system.

In the laboratory, FTS systems produce sufficiently high signal-to-noise data at high enough spectral resolution to make gas identification and analysis easy and practicable. Data collected in time (Fourier) domain are transformed into spectral (frequency or wavenumber) domain using a Fast Fourier Transform (FFT) technique. Data of both the target and a suitable background reference are required in order to remove instrumental or observational effects and isolate the spectral features of the target gas itself. This is referred to as background removal, and is typically performed on the target measurement by dividing by, or in some cases subtracting, the background measurement. By choosing an appropriately calibrated background reference, the resultant spectrum of the target can be calibrated to relative absorbance, and searched against a standard library of likely candidate materials to be identified based on traditional search and match techniques.

In the field, where the signal-to-noise ratio is much lower than in the laboratory, the traditional library search and match techniques fail. Two promising methods of dealing with this difficulty were selected for implementation into HyGAS: (1) a technique developed by R.T. Kroutil of the U.S. Army Edgewood Research and Development Engineering Center (ERDEC), which is applied to raw FTS interferograms to *detect* the presence or absence of a particular gas; and (2) a technique developed by Patrick J. Rauss of the U.S. Army Research Laboratory (ARL), which is applied to the transformed FTS spectra to *identify* an unknown gas.

3.1.1.1 Gas Detection

Kroutil developed a unique technique suitable for gas detection in actual real-time field scenarios, using raw FTS interferogram data. Based on a predetermined linear discriminant vector, a simple mathematical test is performed in the field on each interferogram acquired, detecting the presence or absence of one particular gas. The key to this technique is the advance determination of the linear discriminant vector. The accuracy of this method depends on the quality and universality of this vector. In theory, if one can measure a sufficiently diverse set of background materials in advance, both with and without gas presence, to define this vector with sufficient accuracy, one can attain a very high (~98%) positive detection ratio with very few false alarms. It is then a

simple mathematical task to use this discriminant in the field to detect the presence of the desired gas. The disadvantage of this technique is that a different discriminant vector must be determined for each particular gas one wants to search for.

This technique is very good at dealing with the difficulties of low signal-to-noise ratio and changing backgrounds common to typical field data collection scenarios. This technique also is fast because it operates on the raw FTS interferogram data, obviating any need to perform an FFT, and it is space efficient because, in general, it operates on only a small subset of the interferogram (i.e. 100 instead of 1000 channels). While not of particular importance to a point FTS system, this consideration becomes much more important for an imaging FTS system. The trade-off to obtain this speed of application is twofold: (1) extensive measurement and computation is required in advance of the actual field application in order to determine an accurate discriminant vector for any agent; and (2) the "search" is actually the detection likelihood of one single specific agent—"searching" against a "library" of agents would be very fast if such a library were to exist, but developing such a library would require the extensive advance measurement and computation effort for each individual agent included in the library. Although this technique is currently impracticable for more than a very few individual agents, future prospects may be improved by: (1) the use of suitable hyperspectral imaging spectrometers to collect a sufficient advance measurement database for each desired agent; and (2) the use of a super computer to speed up the advance computation time. Also, in practicality, the number of agents one would be searching for should be relatively small for most applications, and development of a suitable "library" of discriminant vectors would be for only a few agents.

For HyGAS, we designed the user interface for HIPS to perform the discriminant test using Kroutil's code and discriminants. We provide this "discriminant test" function for application to a raw interferogram "image" dataset. We generated a suitable input test dataset of interferograms from data we acquired from Kroutil. We provided for a small "library" of discriminants, which we populated with two discriminants for test purposes. We obtained these discriminants from Kroutil. [Details are given in Appendix E.] Standard HIPS routines for display can be used to identify and locate the detected agent in the image based on the results of the discriminant test.

For HyGAS, it was not practicable to implement the actual advance pattern recognition techniques developed by Kroutil to define a discriminant vector. This situation might be feasible if one acquired a Silicon Graphics machine of suitable compatibility to Kroutil's.

3.1.1.2 Gas Identification

Rauss developed a unique technique for gas identification using a trained backpropagation neural network to search a processed spectrum from an FTS system against a small but traditional spectral library. This technique was developed by training a pattern recognition technique to recognize noisy processed spectra based on a training dataset of library spectra corrupted with random noise.

For HyGAS, we incorporated this technique into the HyGAS package using a commercially available neural net package. We initially intended to acquire the trained net and identification code from Rauss. We acquired the FFT routine as part of the initial

code received from R. Kroutil to process any interferogram to yield a "spectrum." Data for both the target and a suitable background must be acquired, transformed, and then processed through a background removal technique. Given a suitable known background, spectral calibration can be performed, and the resultant spectrum can be searched using these special techniques "trained" on noisy library data to identify the unknown gas.

Additional details on this technique are given in Appendix D.

3.1.2 Type II systems—Multispectral imaging cameras

Image analysis of gases and vapors based on thermal IR spectral signatures is a relatively new developmental technique. Traditionally, image analysis uses various edge detection algorithms to detect, identify and analyze discrete targets: buildings, tanks, missiles, etc. These detection algorithms can sometimes use multispectral information to enhance their detection accuracy. Vapor clouds are nebulous entities, not discrete targets, and detection/identification algorithms that work for discrete targets will not work for vapor clouds. Also, with current imaging hardware, *identification* of unknown gases is not feasible because the spectral resolution is too low and the range of spectral coverage is too small; however, *detection* of specific gases is possible in cases where specific filters can be selected *a priori* to enhance the spectral contrast between a specific gas and most common backgrounds.

Current hardware systems researched for potential HyGAS applications were designed to be incorporated into existing forward looking infrared radiometer (FLIR) video systems, for use in the field in real-time (i.e. at the 30Hz frame rate of standard video systems), and with the intent to work eventually as part of an autonomous unmanned automatic sensor system. Hardware approaches were designed to convert existing raster scan FLIR thermal imaging systems into a sort of narrow bandpass spectrometer (multispectral imaging camera) by means of filtering the 8-12 μm input radiation before it reaches the FLIR detector. Typically, two or three specific filters are selected to "match" the spectral signatures of the known specific gas(es) to be studied. One filter, the "target" filter, is selected centered on a spectral feature contributed purely by the gas; and the other, the "background" filter, is selected just to one side of this spectral feature. The intent is to image the "target" gas in one filter and the "background" in the other filter(s), such that the image of the "background" filter can be subtracted from (or divided into) the image of the "target" filter, eliminating all background clutter except for the gas cloud.

Three different hardware systems were considered for potential HyGAS application. Two of these are pupil plane filtering techniques; the other is a focal plane filtering technique. Of the pupil plane filtering techniques, one uses traditional discrete interference filters; the other uses a tunable Fabry-Perot Etalon filter.

The focal plane filtering technique (developed by M. Althouse, ERDEC) deposits thin film coatings in discrete physical spectral filters directly on top of a linear detector array. Resulting video images are "multispectral" in that within each video frame, stripes across the image represent data collected at different spectral bands. In theory, a cloud with the suspect gas contamination would appear distinctly "striped" in the video image, while

everything else would appear nearly normal. Analysis of actual data of this type is somewhat difficult for humans, but almost trivial for computers.

The discrete filtered pupil plane technique (also developed by M. Althouse) uses one or more filters in a stepped or spinning filter wheel in front of the FLIR lens. The spinning of the filter wheel is synchronized to the video frame rate. Discrete filters are selected based on the gas(es) one expects to search for. Again, image analysis by computer is easier than image analysis by a human operator.

The tunable Fabry-Perot Etalon filtered pupil plane technique (developed by M. Norton of NVEOD) uses two circular variable filters (CVFs), one broad band and one narrow band, both placed in front of the FLIR lens. Again, the filter selection is synchronized to the video frame rate. However, in this case, the filters are not discrete filters, but are tunable to any position across the 8–12 μm spectral range. Theoretically, this means that tuning can be matched quickly and easily to any specific gas; this gives this type of system much more flexibility over discrete filtered systems. With this system, the minimum number of filters required to detect the gas are selected. This saves time and processing. The system is currently designed as an aid to visual detection of a vapor cloud in real time. One aid to the operator is an inverse video technique, such that a warm gas detected against a cool sky background may look bright, and against a warmer terrain background may look dark. With inverse video, the operator can make the gas look bright in both cases.

The practical difficulties of all of these systems are low signal to noise, and high background clutter. Different approaches have been selected to deal with these difficulties. Techniques that are designed to function with the standard FLIR video output for immediate analysis by an operator must operate fast, generally at the standard 30Hz video rate. For automatic applications, operations can conceivably be somewhat slower and significantly computer enhanced.

One simple technique for image enhancement is multiple frame averaging. More complicated techniques generally involve statistical methods for edge detection and background clutter suppression. M. Althouse has experimented with several edge detection and background clutter suppression techniques suitable for application to vapor clouds using multispectral images.

3.1.2.1 Target detection based on statistical concentration models

Althouse is currently developing statistical methods suitable for real-time autonomous target detection of chemical vapor clouds, using data from focal plane spectrally filtered FLIRs. Althouse has demonstrated that statistical Gaussian-distribution vapor concentration models developed by R.E. Warren can be successfully applied to low signal-to-noise bi-spectral (2-spectral bands) images to detect vapor clouds (i.e. targets with neither distinct edges nor distinct dimensions); however, these methods are rather time consuming to compute. Althouse has derived a recursive Kalman filtering technique based on the Warren model that computes much faster. He also has developed adaptive filtering preprocessing algorithms for suppression of background clutter to further enhance the usefulness of this technique in low signal-to-noise situations. Although also computationally time consumptive, the application of systolic array algorithms with

appropriate parallel processing hardware can reduce this computation time to the point of being real-time possible in a deployable FLIR package.

For HyGAS we decided that these techniques, although quite promising, were sufficiently developmental, and until they are further refined for application on realistic data, it was not practicable to incorporate them into the HyGAS system. We also decided that the concept of a focal plane multispectral filter was not compatible with the initial design concept of HyGAS. Further research of this technique would be required before it would be suitable for incorporation into HyGAS. However, this approach may eventually be applicable to pupil plane filtering techniques.

3.1.2.2. Other techniques developed by Althouse

Althouse also experimented with edge detection using multistage predictive coding (MPC), and also with image thresholding using relative entropy theory. These techniques were not selected for integration into HyGAS.

3.1.2.3. Target detection based on tunable Fabry-Perot filter FLIRs

Norton (NVEOD) experimented with tunable Fabry-Perot Etalon filters for vapor cloud detection using current FLIR systems. This approach used only very simple image processing techniques, such as image subtraction (or division) to do background removal, inverse video, and image coadding. These techniques already existed within the HIPS system, so applying them to HyGAS is simple. We developed these techniques into Interactive HyGAS to make them easier to use.

3.1.3 Type III systems: Hyperspectral imaging systems

Thermal infrared hyperspectral imaging systems suitable for gas studies were not yet available during HyGAS development. However, such systems are under design and development, and may be suitable for gas studies in the not too distant future. One potential system is a 3-5μm FTS system under modification at the University of Hawaii. Another potential FTS system is under development by Bomem.

For HyGAS, we unsuccessfully tried to acquire actual test data of a spatial scene collected in interferogram space to use as input for HyGAS functional testing.

3.1.4 Task 1 Summary

HyGAS incorporates methods of gas/vapor cloud detection and gas identification using primarily spectral rather than image (spatial) analysis techniques.

Gas detection in HyGAS can only be done spectrally (on raw interferograms using Kroutil's linear discriminant test). Gas detection using spatial techniques (on multispectral bands, using Althouse's statistical concentration model and a recursive Kalman filtering technique) should be kept under consideration for future implementations.

Gas identification can only be done spectrally (on transformed spectra, using Rauss's trained search technique). This technique is incorporated into HyGAS.

All of these methods are based heavily on statistical probabilities, and meaningful image display and interpretation may require additional information. One suggestion of the COTR is to allow for low spatial resolution analysis results to be superimposed on higher resolution image data. This is a technique that should be considered for future implementation.

3.2 Task 2—Software Development

HyGAS was designed to be part of the existing HIPS software package. This enables HyGAS to access all of the existing HIPS math functions, display routines, libraries and user interfaces. Hardware and software issues required compatiblity with the existing platform.

3.2.1 Hardware acquisition and basic system platform preparation

A SUN SPARCstation 10 was selected and purchased (GFE) as the HyGAS software system platform. This hardware was selected for compatibility with the existing HIPS platform, but with significantly increased speed to enable faster processing. This hardware initially arrived with the incorrect operating system, which caused some delays in getting the hardware operational. This difficulty was resolved when the correct software was supplied by the manufacturer.

HyGAS was designed to function as a module of the existing HIPS software system, which was developed on a SPARCstation 1 under the Sun O/S 4.1 operating system, using the original Kernighan and Ritchie C–compiler. The SPARCstation 10 runs the Solaris 2.3 operating system and uses the more universal standard ANSI C–compiler. This required all existing HIPS code to be modified to conform to ANSI C standards before it would compile properly on the SPARCstation 10. This process involved changing all function declarations from the Kernighan and Ritchie standard to ANSI C standard. Once this was completed, all HIPS routines had to be tested for any run-time errors caused by the new compiler.

The existing HIPS source code was transferred from the SPARCstation 1 onto the SPARCstation 10, and was converted to ANSI C. Most, but not all HyGAS HIPS (version 1.7) routines have been tested for run-time errors. Some HIPS modules may still contain run-time errors.

3.2.2 HyGAS software development

HyGAS software development concentrated on obtaining existing algorithms and code from other parties and manufacturers for incorporation into HyGAS/HIPS. Three primary efforts were made: (1) acquisition of suitable contour plotting and 3-D display software; (2) acquisition of suitable library search routines and/or detailed gas analysis software; and (3) acquisition of specialized source code, such as discriminant testing, etc.

3.2.2.1 Contour plotting and 3-D display software

Three commercially available software packages were acquired for testing on a trial basis: (1) S–Plus/Stat Sci; (2) NCAR; and (3) XRT/3d. None of these packages proved suitable for incorporation into HyGAS/HIPS. The S-Plus package did not provide

suitable results (we want labeled/identified contour levels), and the separate software library modules required to create a run-time package summed up to $5K. The NCAR package produced nice output, but was very slow. Also, this package produces a metafile, i.e. a computer generated graphics code file that with an appropriate driver can be plotted on the monitor screen. However, there is no way to overlay this file with a HIPS image file, and no way to access this file with any HIPS function. The XRT/3d package had severe limitations on the number of pixels it could handle, and it was very slow.

Given these difficulties, we elected not to pursue 3-D plotting for HyGAS.

Two options seem feasible for future consideration: the Interactive Data Analysis Language (IDL); and the Advanced Visualization System (AVS). Both of these packages are combined image processing and plotting packages, and ought to be able to handle contour plots and image overlays. (The three prior packages were just plotting packages, not imaging packages.) We anticipate that one or both of these packages should be able to do both image and contour overlays, but we would need to find out if the data formats are accessible to HIPS. They both have accessible software/display libraries, so they may prove suitable on both counts.

3.2.2.2 Library search routines and detailed gas analysis software

We purchased a PC-compatible software package for laboratory gas analysis called GRAMS/386 (previously referred to as SpectraCalc). Although this package is not UNIX compatible, we decided that since it was strongly suggested by both ERDEC and NVEOD, as well as other contacts (and referred to as the unofficial "Army standard" for spectral analysis), we would acquire it for possible interfacing with HyGAS. SpectraCalc is designed for use with laboratory spectrometers, primarily for FTS instruments. As such, it is designed to deal with high spectral resolution data. Its search routines are based on the premise that laboratory collected data will generally be at higher spectral resolution than library data, and matching the laboratory spectral resolution of the unknown agent to the standard resolution of the spectral library will be a process of high-to-low convolution (such that convolution can be done on the unknown spectrum to match the lower resolution library), or, if low-to-high convolution, not at significantly different resolutions (such that either linear or spline interpolation would not introduce significant discrepancies). This situation is not likely to be attained for imaging spectrometers in the near future, but the capability should not be dismissed. HyGAS was not designed to interface with SpectraCalc (as originally intended), to be able to extract spectra from a HIPS image and store them in standard SpectraCalc and/or JCAMP format. However, HyGAS was designed to export ASCII_XY data, so that any PC networked to the SPARCstation should be able to import these spectra directly to SpectraCalc for traditional gas analysis.

We researched the availability of traditional gas phase spectral libraries for use with HyGAS/HIPS. Traditional gas phase spectral libraries are available in PC-compatible format from several different vendors (Aldrich Chemical, Sadtler Research, Sprouse Scientific, Infrared Analysis, etc.). Many of these vendors supply copyrighted and/or encrypted libraries that can only be accessed with specific PC software packages. This

means HIPS cannot access these libraries, nor can we write translation routines. SpectraCalc can access all of these libraries (as well as any other library in "Galactic" format). [Galactic Industries is the manufacturer of the GRAMS/386 and the related SpectraCalc and LabCalc programs.] Very few of these libraries are available in SPARC/UNIX compatible format; a few are available in JCAMP format, for an additional fee. We approached Aldrich Chemical about obtaining their library(ies) in SPARC/UNIX compatible format, but were unable to reach a solution. Hence, for HyGAS we were unable to provide either search routines or access routines for such libraries.

We approached Aldrich about acquiring data access rights, perhaps by signing a non-disclosure agreement or by providing encryption protection within HyGAS/HIPS. The difficulty is that for HyGAS, we must provide for data collected at lower spectral resolution than that of the libraries (perhaps at substantially lower resolution, such that linear or spline interpolation methods would not be applicable). For encrypted and/or copyrighted libraries, this will only be possible if we can obtain the approval of the library supplier to not only access the library, but also to convolve it to lower resolutions and store the convolved library as a HIPS library. In the future, we should consider encryption of HIPS libraries, so that appropriate convolution of the library to the HyGAS/HIPS sensor can be performed without infringing on the manufacturer's restrictions. In the unlikely situation of HyGAS/HIPS resolution higher than that of a library, it is a simple matter to convolve the higher resolution HyGAS spectrum to the lower resolution of the library before performing the spectral search.

We acquired the novel search method using backpropagation neural nets developed by Rauss. Details of this approach are described in Appendix D.

3.2.2.3 Specialized source code

Specialized source code to perform the linear discriminant test was acquired from Kroutil in PC-compatible code. This code was transferred to the SPARCstation 10, and rewritten to conform to standard ANSI C. Graphics libraries accessed by the PC code were not available for the SPARC hardware, and a few required PC routines were rewritten to call standard X-window libraries.

Specialized code to actually determine the linear discriminant is available from Kroutil, but only in SiliconGraphics (SGI) C-code. This code accesses many of the specialized graphics display features available only on an SGI machine. For the future, we should consider acquiring this code and a low-end SGI machine to run it on. (Estimated GFE price for such a machine is ~$5K.) The intent would be to allow the user to select several image cube datasets, and run these datasets through the special pattern recognition algorithms developed by Kroutil to determine a less robust discriminant vector, but one that would likely be usable for subsequent datasets. [For example, Kroutil has spent months of CPU time determining a robust discriminant vector for one specific gas based on several hundred thousand spectra acquired with a point spectrometer (MIDAC FTS sensor). With a set of hyperspectral *images*, perhaps as few as 5 images carefully selected and defined would produce enough data to define a reasonably efficient discriminant. This discriminant could be determined off-line, using the SGI machine, and

the resultant discriminant could then be added to the library on the HyGAS machine for consideration in subsequent datasets.]

Specialized code to do image enhancement ("edge detection" for vapor clouds, and background clutter suppression) could be obtained from M. Althouse. We intended to incorporate these techniques into HyGAS, but were unable to do so.

3.2.3 Task 2 Summary

HyGAS appears under a *Gas Analysis* menu within HIPS. This menu contains the individual gas analysis functions, which can be run non-interactively, as well as the HyGAS module which incorporates them into an interactive package. Current functions include Linear Discriminant Test (gas detection), Background Removal (subtraction or division), Fast Fourier Transform (interferogram to spectrum) and reverse, and Library Search and Neural Net search (gas identification/analysis).

Analysis can be performed on raw instrumental interferograms or on transformed (or raw instrumental) spectra. Techniques developed by Kroutil to do gas detection by linear discriminant tests are performed in interferogram space. Spectral search techniques developed by Rauss are performed in spectral space. Data from an FTS may be processed through either or both techniques.

3.3 Task 3—Spectral Database/Measurements Development

Simulation of a test dataset required a significant effort in HyGAS. We acquired some data from R. Kroutil and from P. Rauss, but without much descriptive information.

We considered J. Salisbury (of Johns Hopkins University) as a source for alternative thermal IR data, along with the possibility of renting a MIDAC sensor to measure actual interferograms of realistic backgrounds to match Kroutil's data for use with his predetermined discriminants. Neither of these options was successful.

Full details on GFI databases and libraries, and a description of the use of these datasets to develop simulated test image cubes, are found in the appendices.

3.4 Task 4—Documentation

Since HyGAS was developed as a functional part of HIPS, the software documentation, or user's manual, for HyGAS was expected to become part of the *HIPS User's Manual.* This was the plan when the interim software documentation was set up as *Chapter 12—Gas Analysis*, in the standard format of the *HIPS User's Manual*, with preliminary function and parameter specification descriptions. However, as HyGAS progressed, we elected to create the User's Manual in the form of a tutorial, and we delivered the *HyGAS User's Manual/Tutorial* instead of the reference manual format of the *HIPS User's Manual.*

Complete details on the use of HyGAS with the provided and the simulated datasets is given in the *HyGAS User's Manual/Tutorial.*

4.0 Additional Information

Additional details on GFI datasets, GFI databases, creation of simulated image cubes, neural net and linear discriminants, are provided in the appendices.

APPENDIX A

HyGAS Field Instrument Datasets (GFI)

Two types of field instrument datasets were supplied (GFI) for use with HyGAS.

- Rauss_Howden spectral datasets
- Kroutil_MIDAC interferogram datasets

1. Rauss_Howden spectral datasets

The Rauss_Howden spectral datasets came from a field experiment by E. Howden of NVEOD. These measurements (11 and 12 August 1992) were collected using a point sensor FTIR spectrometer. Individual diskette listings are included below. Figures 1 and 2 show associated logbook notes. Table 1 lists the measurements of the better dataset (12 August) in chronological order; corresponding spectra are shown in Figures 3–5.

Rauss_Howden Field Data, Disk 1 Listing.

```
Volume in drive A is FIELDDATA
Volume Serial Number is 2C63-13F9
Directory of A:\

ACE1     SPC      365,824 08-12-92   2:30p
ACE2     SPC      365,824 08-12-92   2:38p
ACE3     SPC      365,824 08-12-92   2:21p
BG1      SPC        2,052 08-12-92   3:39p
BG2      SPC       36,784 08-12-92   2:08p
BG3      SPC       36,784 08-12-92   3:40p
BG4      SPC       36,784 08-12-92   4:31p
README   BAK          192 04-15-94   1:04p
README                1,028 04-15-94   2:54p
        9 file(s)     1,211,096 bytes
                        244,224 bytes free
```

Rauss_Howden Field Data, Disk 2 Listing.

```
Volume in drive A is FIELDDATA2
Volume Serial Number is 283A-14D0
Directory of A:\

MEK1     SPC      914,224 08-12-92   4:57p
MEK2     SPC      365,824 08-12-92   5:05p
        2 file(s)     1,280,048 bytes
                        177,152 bytes free
```

Rauss_Howden Field Data, Disk 3 Listing.

```
Volume in drive A is FIELDDATA3
Volume Serial Number is 0E2D-14E9

Directory of A:\

81292          <DIR>          04-15-94   1:40p
81192          <DIR>          04-15-94   1:44p
        2 file(s)              0 bytes

Directory of A:\81192

.              <DIR>          04-15-94   1:44p
..             <DIR>          04-15-94   1:44p
BG10     SPC       36,784 08-11-92   1:45p
BG11     SPC       36,784 08-11-92   2:03p
BG12     SPC       36,784 08-11-92   2:50p
BG13     SPC       91,624 08-11-92   3:21p
BG14     SPC       91,624 08-11-92   6:14p
BG15     SPC       91,624 08-11-92   6:22p
BGROUND4 SPC        5,708 08-11-92  10:22a
BGROUND5 SPC       36,784 08-11-92  10:49a
BGROUND6 SPC       36,784 08-11-92  11:00a
BGROUND7 SPC       36,784 08-11-92  11:02a
BGROUND8 SPC       36,784 08-11-92  11:06a
BGROUND9 SPC       36,784 08-11-92  11:19a
SF62     SPC       67,860 08-11-92  11:34a
       15 file(s)      642,712 bytes

Directory of A:\81292

.              <DIR>          04-15-94   1:40p
..             <DIR>          04-15-94   1:40p
SF61     SPC      365,824 08-12-92   3:59p
SF62     SPC      365,824 08-12-92   4:07p
README                63 04-15-94   1:42p
        5 file(s)      731,711 bytes

Total files listed:
       22 file(s)     1,374,423 bytes
                        79,872 bytes free
```

Rauss_Howden Field Data, Disk 4 Listing.

```
Volume in drive A is FIELDDATA4
Volume Serial Number is 0C3C-14F0
Directory of A:\

ACE1     SPC      914,224 08-11-92   3:52p
ACE2     SPC      365,824 08-11-92   4:00p
        2 file(s)     1,280,048 bytes
                        177,152 bytes free
```

Rauss_Howden Field Data, Disk 5 Listing.

```
Volume in drive A is FIELDDATA5
Volume Serial Number is 0410-15CA
Directory of A:\

ACE3     SPC      365,824 08-11-92   4:08p
ACE4     SPC      365,824 08-11-92   4:16p
ACE5     SPC      365,824 08-11-92   4:29p
SF61     SPC      183,024 08-11-92  11:32a
        4 file(s)     1,280,496 bytes
                        176,128 bytes free
```

Rauss_Howden Field Data, Disk 6 Listing.

```
Volume in drive A is FIELDDATA6
Volume Serial Number is 203A-15CE
Directory of A:\

SF63     SPC      914,224 08-11-92   2:35p
        1 file(s)       914,224 bytes
                        543,232 bytes free


Volume in drive A is FIELDDATA7
Volume Serial Number is 2F18-15D1
Directory of A:\

MEK1     SPC      914,224 08-11-92   7:00p
        1 file(s)       914,224 bytes
                        543,232 bytes free
```

Table 1. Summary of Rauss_Howden field data from 12 August 1992. The datasets listed here (in chronological order) were identified as preferable to those from 11 August 1992. Corresponding spectral plots for these datasets are shown in Figures 3–5.

BG2	SPC	36,784	08-12-92	2:08p
ACE3	SPC	365,824	08-12-92	2:21p
ACE1	SPC	365,824	08-12-92	2:30p
ACE2	SPC	365,824	08-12-92	2:38p
BG1	SPC	2,052	08-12-92	3:39p
BG3	SPC	36,784	08-12-92	3:40p
SF61	SPC	365,824	08-12-92	3:59p
SF62	SPC	365,824	08-12-92	4:07p
BG4	SPC	36,784	08-12-92	4:31p
MEK1	SPC	914,224	08-12-92	4:57p
MEK2	SPC	365,824	08-12-92	5:05p

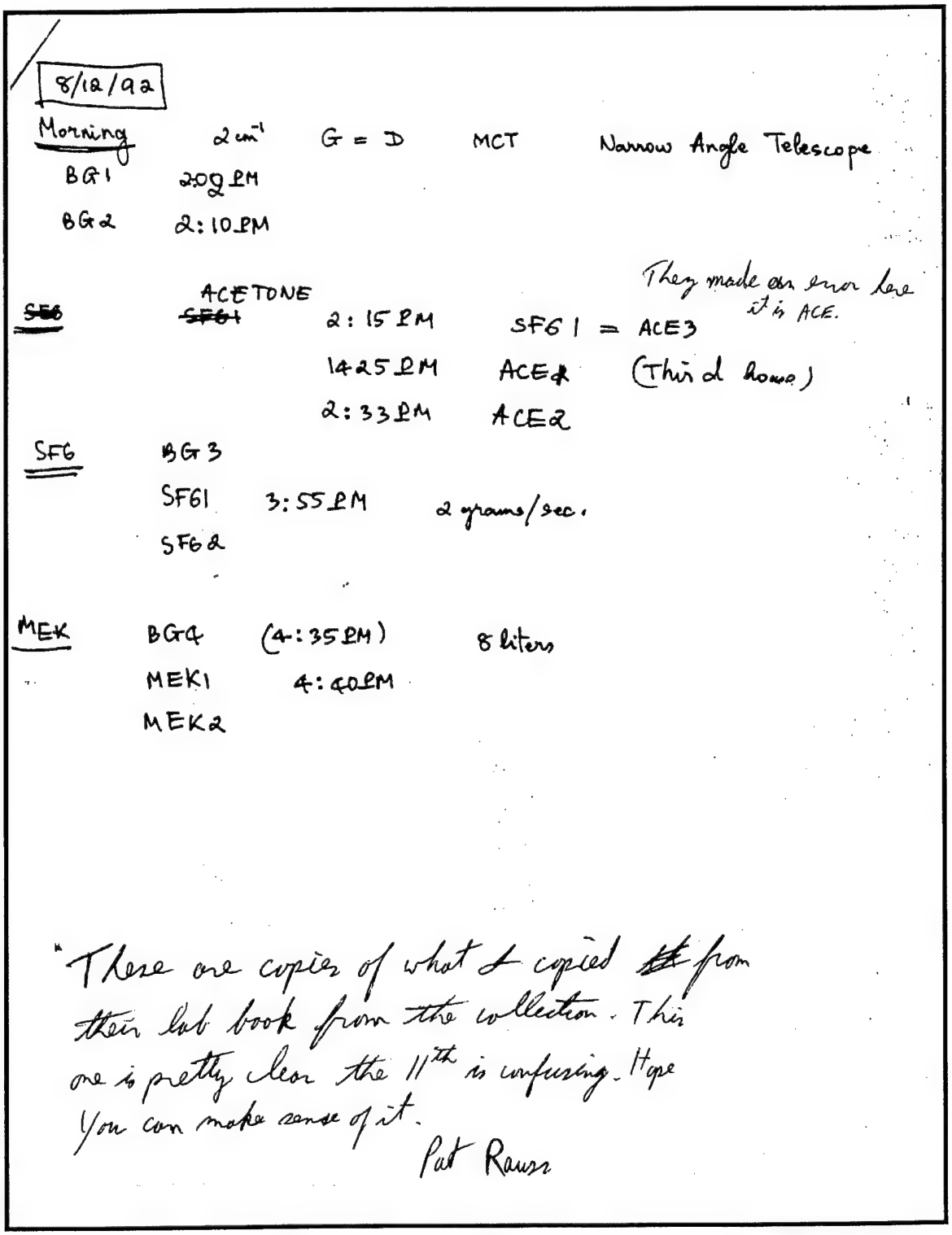

Figure 1. Logbook notes for Rauss_Howden experimental gas release on 12 August 1992. Annotations indicate this dataset is preferable to that of 11 August 1992.

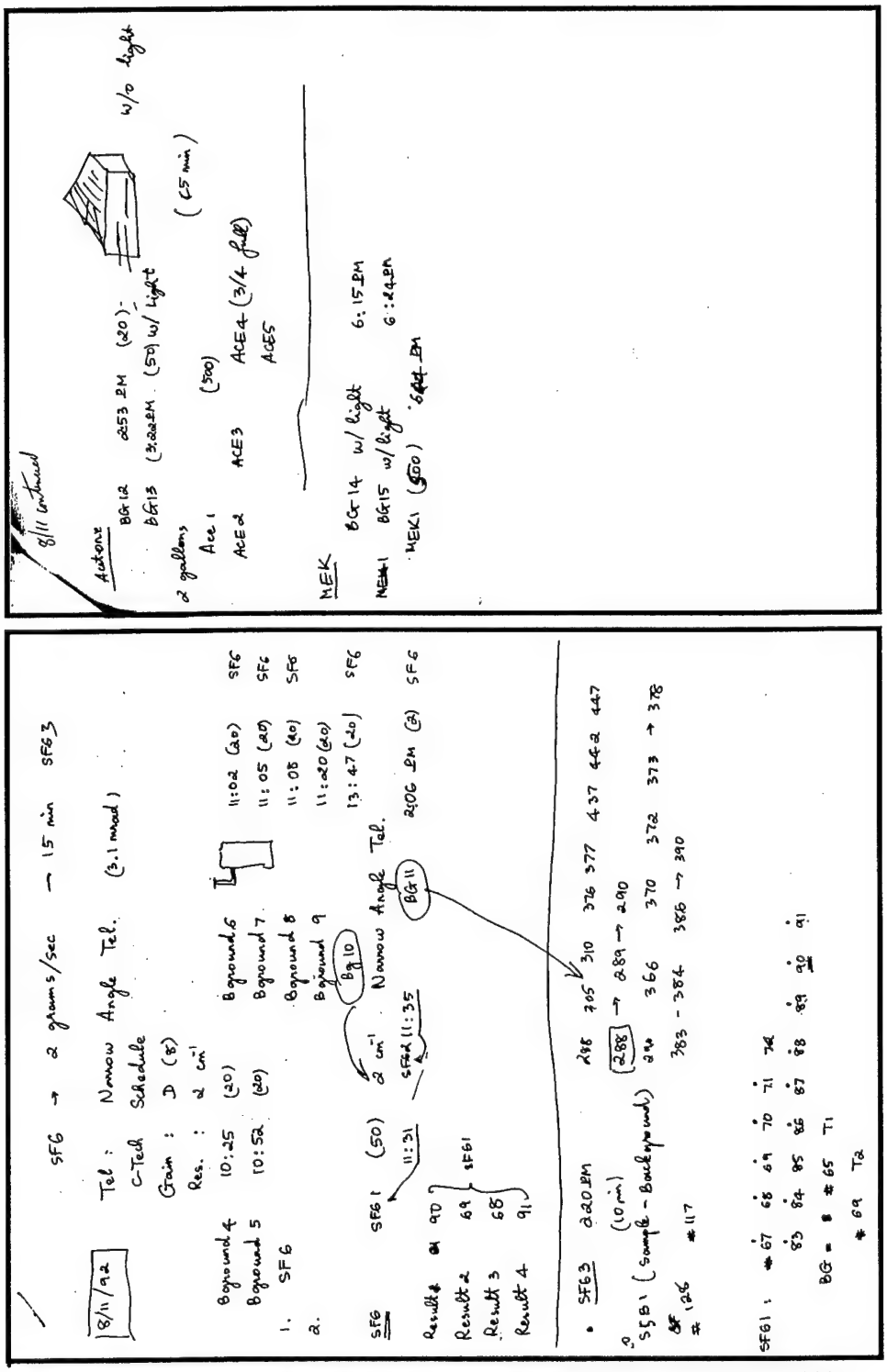

Figure 2. Logbook notes for Rauss_Howden experimental gas release on 11 August 1992.

These field measurements cover the spectral range 833–1265 cm^{-1} at 2 cm^{-1} resolution (449 datapoints each, Nyquist sampling at 1 cm^{-1} datapoint spacing). [Presumably, these spectra were originally collected as interferograms by an FTIR spectrometer, were subsequently transformed into the spectral domain, and then were trimmed to exclude

datapoints outside the given spectral range.] Laboratory absorbance spectra (at a coarser resolution of 12 cm^{-1} resolution) for these same gases are shown in Figure 6.

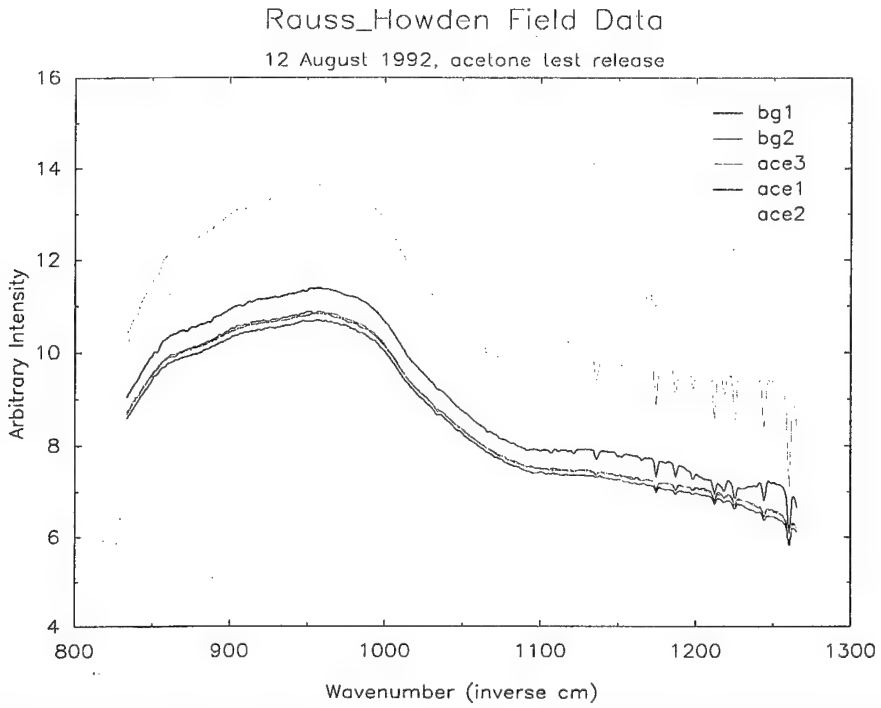

Figure 3. Spectral measurements for acetone and associated field backgrounds from 12 August 1992. Absorptions due to acetone are clearly visible in sample `ace1`.

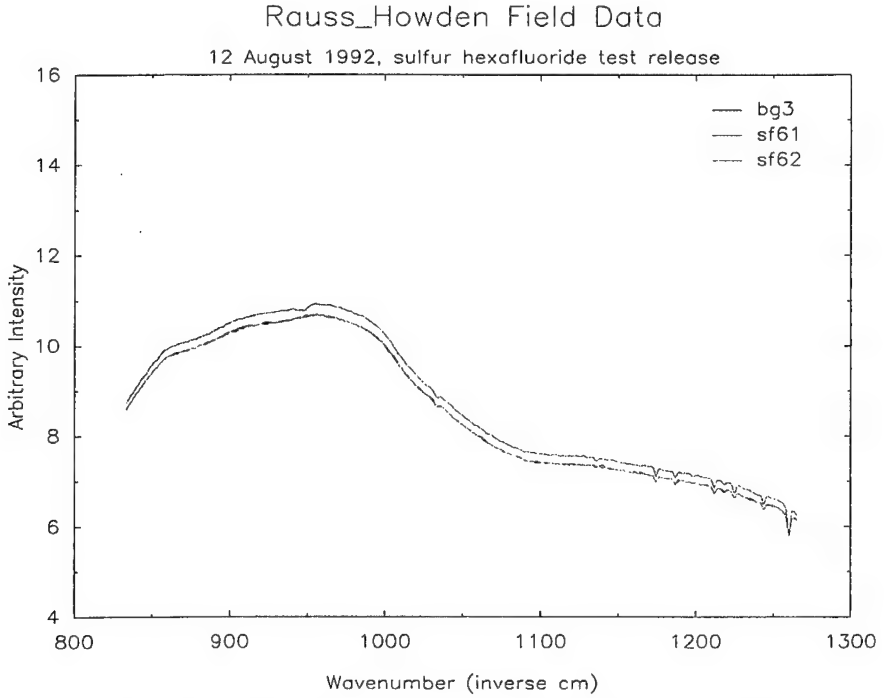

Figure 4. Spectral measurements for sulfur hexafluoride (SF_6) and associated field backgrounds from 12 August 1992. Absorptions due to SF_6 are barely discernible in sample `sf62`. [Refer to Figure 4 for corresponding laboratory absorbance spectra.]

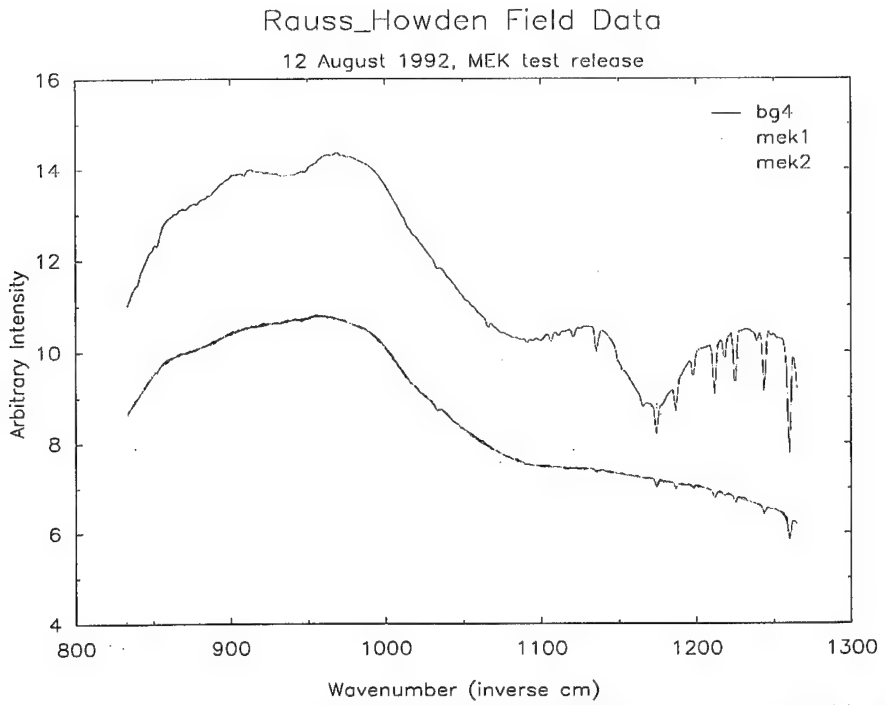

Figure 5. Spectral measurements for methyl-ethyl-ketone (MEK) and associated field backgrounds from 12 August 1992. Absorptions due to MEK are clearly visible in sample `mek2`. However, there is a significant difference in the overall radiance for this sample and the corresponding background, which *may* be caused by possible alterations in the instrumental gain settings.

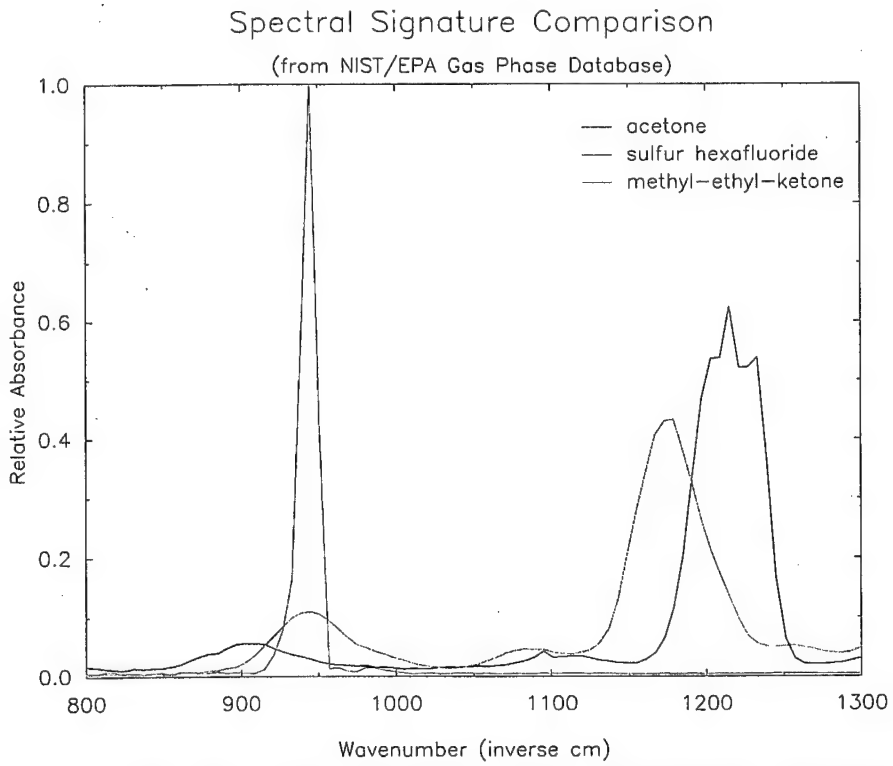

Figure 6. Laboratory absorbance spectra for acetone, sulfur hexafluoride and methyl-ethyl-ketone. These absorbance spectra came from the NIST/EPA Database 35, Gas Phase Infrared, and are measured at a significantly coarser spectral resolution (12 cm^{-1} spectral resolution) than the field data (at 2 cm^{-1}).

2. *Kroutil_MIDAC Interferogram Datasets*

The Kroutil_MIDAC interferogram datasets came from both field and laboratory experiments by R. Kroutil of ERDEC. All measurements [presumably] were collected using a MIDAC point sensor FTIR spectrometer, operated at 8 cm^{-1} spectral resolution. This mode of operation generates interferograms with 1024 datapoints, which correspond to spectra of 512 datapoints over the spectral range 0 to 1971 cm^{-1} wavenumbers.

Three interferogram datasets were supplied.

- *mdt01*
- *kft0002.dat*
- *kft0048.dat*

Dataset *mdt01* is [presumably] a series of field interferograms collected from a helicopter overflight during a ground test release of sulfur hexafluoride (SF_6). No additional details were supplied with this dataset. Unfortunately, since no discriminant coefficients to detect the presence of SF_6 were supplied with this dataset, we were unable to determine which records within this file included SF_6 and which were field background only.

Dataset *kft0002.dat* is [presumably] a collection of interferograms measured in a laboratory under controlled conditions, using a MIDAC spectrometer, a gas cell, and a laboratory thermal blackbody source. Various conditions (background source temperature, gas temperature, gas concentration) are presumably represented for situations with, and without, the gas MEK in the optical path. Discriminant coefficients for both acetone and MEK were supplied with this dataset. [However, no measurements of acetone were detected within this dataset.] No additional details were supplied with this dataset.

Dataset *kft0048.dat* is [presumably] a collection of laboratory background interferograms measured under various conditions, but all without the gas MEK. No additional details were supplied with this dataset.

Example interferograms from each dataset are shown superposed in Figure 7. Examples expanded about the centerburst region are shown in Figure 8. All interferograms from dataset *mdt01* appear nearly identical, suggesting a uniform field background differing only in the presence or absence of SF_6 in the optical path. Interferograms from the other two datasets exhibit comparable variability within distinct groups of contiguous measurements, but vary between groups. This suggests differences in the conditions under which each group of interferograms was collected, such as, perhaps, different temperatures for the background thermal source in each group. Details describing the different groups of measurements in each dataset were not available.

Individual diskette listings of the datasets (and programs) supplied by Kroutil are included below. Listings of the ERDEC dataset diskettes also are included.

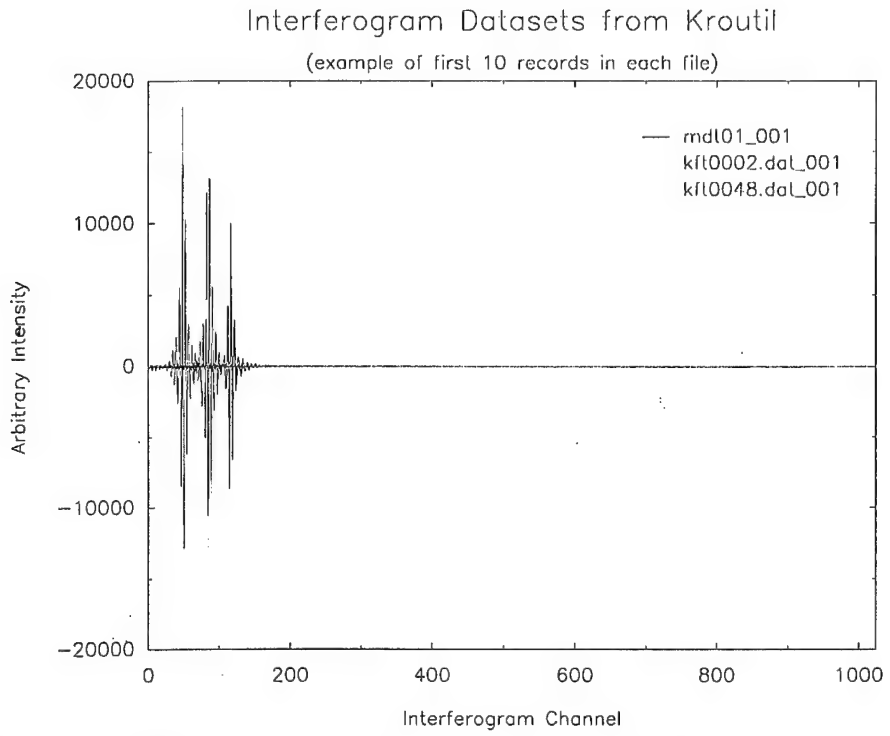

Figure 7. Example interferograms from datasets `mtd01`, `kft0002.dat`, and `kft0048.dat`. Overall intensity is comparable to the example shown for all records within `mtd01`, but varies between groups of comparable data for the other datasets.

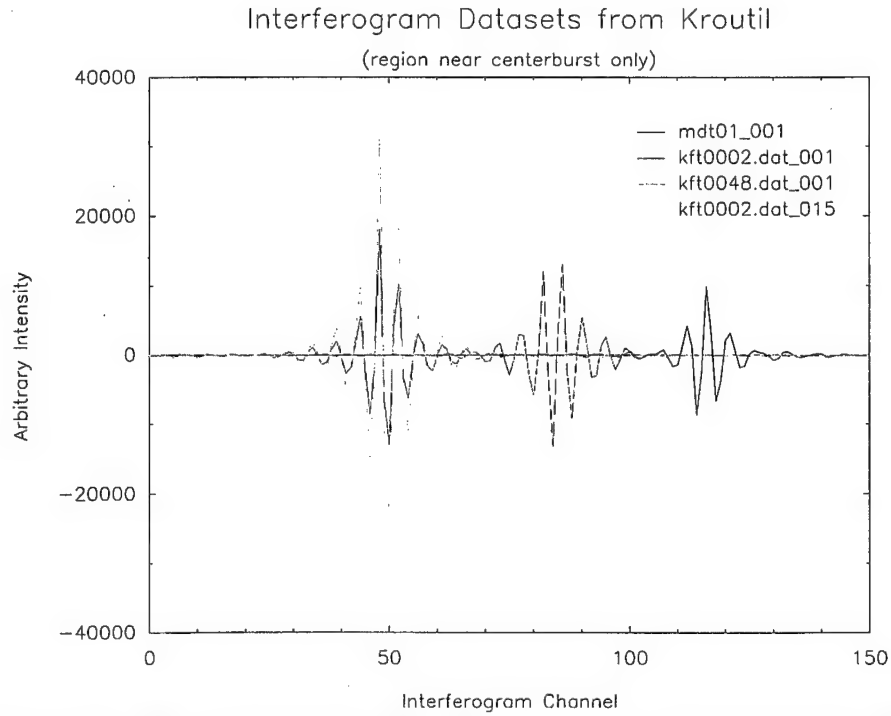

Figure 8. Example interferograms from datasets `mtd01`, `kft0002.dat`, and `kft0048.dat`, region near centerburst, only. The centerburst occurs at channel 116 for interferograms in `mtd01`, at channel 48 for `kft0002.dat`, and at channel 84 (a negative burst) for `kft0048.dat`. Example interfrograms from the first two groups of interferograms in `kft0002.dat` are shown.

Kroutil Disk 1, Collect Programs.

```
 Volume in drive A has no label

Directory of A:\

COLLECT      <DIR>        07-15-94  12:32p
        1 file(s)              0 bytes

Directory of A:\COLLECT

.            <DIR>        07-15-94  12:32p
..           <DIR>        07-15-94  12:32p
MIDCOL   EXE       54,173 12-29-93  12:20p
MIDCOL   V1        51,025 09-25-92   3:10p
REPLAY   EXE       42,394 05-03-93   8:51a
HEADERST DEF        2,505 05-04-92   9:34p
REPLAY   C         29,299 05-01-93   3:53p
OSCCONV  C          9,113 04-26-93   8:54a
ASM      BAT          745 05-16-92   7:57p
MIDCOL   BAT          135 08-15-92   9:07p
MIDDEF   H          2,816 07-24-92   7:13a
MIDCOLD  C         31,783 08-25-92   3:44p
MIDCOLD  BAT          138 08-25-92   3:46p
MIDCOLD  EXE       46,863 10-04-92   3:41p
HEADERS  DEF        1,578 09-27-92   2:36p
REPLAY   V1        23,775 11-05-92  11:46a
REPLAY   BAT          132 05-01-93  11:47a
INSTALL  BAT          267 10-13-92   2:50p
MIDLAB   C         68,692 02-17-93   8:26a
MIDLAB   EXE       54,019 02-17-93   8:22a
MIDCOL   V2        61,271 11-05-92  11:51a
MIDLAB   BAT          135 01-26-93   2:56p
MIDLAB   V1        61,752 02-05-93   9:51a
F5       FSP        2,072 02-13-93   7:51p
CONVINTF BAT          137 04-27-93   9:01a
F6       FSP        2,072 02-13-93   7:51p
F7       FSP        2,072 02-13-93   7:51p
F8       FSP        2,072 02-13-93   7:52p
REPLAY   V2        26,068 02-12-93   8:48p
SCCONV   C         14,719 04-30-93   9:22a
EXSCCONV DEF          381 04-27-93  10:01a
SCCONV   BAT           99 04-26-93   8:54a
SCALC    DEF          970 04-02-93   6:51p
CONVINTF EXE      239,818 04-27-93   1:37p
SCCONV   EXE      175,742 04-30-93   9:22a
MENU     H          2,084 01-18-90   6:46p
EXCONV   DEF          402 04-27-93   8:50a
EXREPLAY DEF          478 05-01-93  11:56a
CONVINTF C         11,915 05-03-93   9:07a
MIDCOLV  BAT          180 05-04-93   6:08a
MENU     C         11,208 01-18-90   6:44p
EXMIDCOL DEF          359 05-03-93   8:22p
MIDCOLV  EXE      190,247 12-29-93  12:32p
MIDCOL   C         68,434 12-29-93  12:19p
MIDCOLV  C         72,357 12-29-93  12:31p
       45 file(s)     1,366,496 bytes

Total files listed:
       46 file(s)     1,366,496 bytes
                         77,824 bytes free
```

Kroutil Disk 2, Pattern Recognition Programs.

```
Volume in drive A has no label
 Volume Serial Number is 2A4A-0FFC

Directory of A:\

MTRX         <DIR>        07-15-94  12:35p
        1 file(s)              0 bytes

Directory of A:\MTRX

.            <DIR>        07-15-94  12:35p
..           <DIR>        07-15-94  12:35p
MTRX     DEF          318 08-17-92  12:08a
MIDDEF   H          2,816 07-24-92   7:13a
AMTRX    EXE       52,843 04-15-93   9:52a
MTRXD    BAT          132 08-17-92   1:44p
AMTRXD   EXE       49,403 04-15-93   9:53a
MTRX     BAT          129 08-17-92   1:46p
HEADERS  DEF        1,578 09-27-92   2:36p
FILTER1  INC       28,285 04-02-93   2:01p
MATGRAPH EXE       45,034 10-02-92   3:52p
MATGRAPH BAT          112 10-01-92  10:45a
MTRXD    C         16,243 02-17-93  10:19a
DISCRIM1 INC        5,122 04-03-93   9:07a
MTRX     EXE       56,035 12-27-93   7:03p
MTRX2    EXE       65,443 12-27-93   7:02p
MTRXD    EXE       52,595 04-15-93   9:55a
MTRX2    BAT          132 02-09-93   3:37p
MATGRAPH C          5,516 02-17-93  10:18a
FILTER2  INC       18,421 04-02-93   2:21p
DISCRIM2 INC        5,122 04-03-93   9:06a
MFILTER  INC       28,285 04-02-93   2:01p
AFILTER1 INC       18,421 04-02-93   2:20p
AFILTER2 INC       18,421 04-02-93   2:21p
ADIS1    INC        5,122 04-03-93   9:04a
ADIS2    INC        5,122 04-03-93   9:06a
MDIS1    INC        5,122 04-03-93   9:07a
MTRX2    C         42,995 12-27-93   7:00p
MTRX     C         40,406 12-27-93   7:00p
       29 file(s)     569,173 bytes

Total files listed:
       30 file(s)     569,173 bytes
                      880,128 bytes free
```

Kroutil Disk 3, Datafile #1, kft0002.dat.

```
 Volume in drive A has no label
 Volume Serial Number is 192A-15F0

Directory of A:\

KFT0002  DAT     587,648 07-15-94  12:25p
        1 file(s)      587,648 bytes

Total files listed:
        1 file(s)      587,648 bytes
                       869,888 bytes free
```

Kroutil Disk 4, Datafile #2, kft0048.dat.

```
 Volume in drive A has no label
 Volume Serial Number is 3A15-1AEC

Directory of A:\

KFT0048  DAT   1,162,112 07-15-94   8:21a
        1 file(s)    1,162,112 bytes

Total files listed:
        1 file(s)    1,162,112 bytes
                       274,432 bytes free
```

Kroutil Disk 5, FTIR data collection software, version 2, update 1, 3/17/93.

```
 Volume in drive A has no label
 Volume Serial Number is 2A3C-12E7

Directory of A:\

COLLECT      <DIR>        07-06-88   4:50a
PCIDA        <DIR>        07-06-88   4:50a
DATA         <DIR>        07-06-88   4:51a
INSTALL  BAT          257 02-28-93   6:22p
READ     ME         1,306 02-28-93   6:25p
        5 file(s)         1,563 bytes

Directory of A:\COLLECT

.            <DIR>        07-06-88   4:50a
..           <DIR>        07-06-88   4:50a
MIDCOL   EXE       54,091 02-17-93   5:26p
REPLAY   C         29,155 02-28-93   5:26p
REPLAY   EXE       43,057 02-28-93   5:17p
HEADERST DEF        2,505 05-04-92   9:34p
REPLAY   BAT          135 08-25-92   3:48p
CONVINTF           42,852 04-26-93   8:56a
MIDCOL   BAT          135 08-15-92   9:07p
MIDDEF   H          2,816 07-24-92   7:13a
READ     ME           463 02-25-93   2:45p
MIDCOL   C         68,614 04-06-93   9:02a
HEADERS  DEF        1,578 09-27-92   2:36p
MIDDOC   TXT       21,479 10-13-92   2:38p
MIDDOC   WP        21,600 10-13-92   2:38p
F5       FSP        2,072 02-13-93   7:51p
F6       FSP        2,072 02-13-93   7:51p
F7       FSP        2,072 02-13-93   7:51p
F8       FSP        2,072 02-13-93   7:52p
SCALC    DEF          970 04-02-93   6:51p
       20 file(s)      297,738 bytes

Directory of A:\DATA

.            <DIR>        07-06-88   4:51a
..           <DIR>        07-06-88   4:51a
MDT01            361,664 02-20-93   5:29p
READ     ME          288 02-28-93   5:11p
        4 file(s)      361,952 bytes

Directory of A:\PCIDA

.            <DIR>        07-06-88   4:50a
..           <DIR>        07-06-88   4:50a
PCIDA    C          9,793 03-24-93  10:08a
TEMPS    C         14,472 07-22-92   2:18p
RMATH    C         18,771 07-23-92  10:44p
DEFINES  IDA          375 04-20-90  12:38p
EXTERNS  IDA          525 04-03-90   8:31a
HEADERS  IDA        1,504 07-20-90   9:58a
PCIDA    DOC        3,061 12-06-90  10:02a
INTF_TMP IDA       40,960 07-24-92   4:51p
SPEC_TMP IDA       20,480 07-24-92   4:51p
MICPRINT SMS        1,629 10-16-89  12:00p
```

```
ROMAN3     SMS       13,789 10-16-89   12:00p
SBO        SMS        4,669 10-16-89   12:00p
MATH       BAT           46 07-23-92   12:49p
IDA1       BAT           41 07-25-92   12:29p
PCIDA      EXE      128,754 04-19-93    1:55p
IDALINK    BAT           47 04-15-93    4:39p
BOB        FSP       17,408 07-22-92    2:56p
MATH       C         18,594 04-19-93   10:33a
HELP       IDA       15,809 03-24-93    9:39a
PCIDA      TXT          161 10-05-92    9:02a
GRAFIX     BAT           44 07-22-92    4:12p
IDAPRINT   BAT           24 07-25-92    1:03p
READ       ME           340 02-25-93    2:47p
DISK       C         21,600 02-12-93    3:56p
GRAFIX     C         15,692 02-12-93    3:49p
OUTPUT     C         24,085 03-24-93    9:39a
IDACOMP    BAT          205 04-19-93    1:43p
       29 file(s)      372,878 bytes

Total files listed:
       58 file(s)    1,034,131 bytes
                       407,040 bytes free
```

Kroutil Disk 6, Version 3 "C" code MIDCOL.

```
 Volume in drive A has no label
 Volume Serial Number is 411A-19D5

Directory of A:\

MIDCOL     EXE       54,091 02-17-93    5:26p
EXREPLAY   DEF          478 05-01-93   11:56a
REPLAY     BAT          132 05-01-93   11:47a
HEADERST   DEF        2,505 05-04-92    9:34p
REPLAY     C         29,299 05-01-93    3:53p
CONVINTF   BAT          137 04-26-93    8:53a
MIDCOL     BAT          135 08-15-92    9:07p
MIDDEF     H          2,816 07-24-92    7:13a
READ       ME           463 02-25-93    2:45p
CONVINTF   C         11,915 05-03-93    9:07a
HEADERS    DEF        1,578 09-27-92    2:36p
MIDDOC     TXT       21,479 10-13-92    2:38p
MIDDOC     WP        21,600 10-13-92    2:38p
F5         FSP        2,072 02-13-93    7:51p
F6         FSP        2,072 02-13-93    7:51p
F7         FSP        2,072 02-13-93    7:51p
F8         FSP        2,072 02-13-93    7:52p
SCALC      DEF          970 04-02-93    6:51p
MIDCOL     C         68,614 04-06-93    9:02a
CONVINTF   EXE      239,818 04-27-93    5:12p
EXCONV     DEF          402 04-27-93    8:50a
REPLAY     EXE       42,394 05-03-93    8:52a
MENU       H          2,084 01-18-90    6:46p
MIDCOLV    BAT          180 05-04-93    6:08a
MIDCOLV    EXE      190,141 05-07-93    6:48a
MENU       C         11,208 01-18-90    6:44p
EXMIDCOL   DEF          359 05-03-93    8:22p
MIDCOLV    C         71,963 05-07-93    6:46a
SCCONV     C         14,719 04-30-93    9:22a
SCCONV     BAT           99 04-26-93    8:54a
SCCONV     EXE      175,742 04-30-93    9:22a
       31 file(s)      973,609 bytes

Total files listed:
       31 file(s)      973,609 bytes
                       475,136 bytes free
```

Kroutil Disk 7, Version 3 PCIDA.

```
 Volume in drive A has no label
 Volume Serial Number is 382A-19D7

Directory of A:\

DISK       C         22,870 05-04-93   10:08p
RMATH      C         18,771 07-23-92   10:44p
OUTPUT     C         24,067 05-04-93    7:42p
HEADERS    IDA        1,504 07-20-90    9:58a
PCIDA      DOC        3,061 12-06-90   10:02a
INTF_TMP   IDA       40,960 07-28-93    9:22a
SPEC_TMP   IDA       20,480 07-28-93    9:22a
MICPRINT   SMS        1,629 10-16-89   12:00p
ROMAN3     SMS       13,789 10-16-89   12:00p
SBO        SMS        4,669 10-16-89   12:00p
MATH       BAT           46 07-23-92   12:49p
IDA1       BAT           41 07-25-92   12:29p
PCIDA      EXE      352,244 07-27-93    9:23p
IDALINK    BAT           47 04-15-93    4:39p
GRAFIX     C         15,908 05-04-93   10:44p
PCIDA      TXT          161 10-05-92    9:02a
GRAFIX     BAT           44 07-22-92    4:12p
IDAPRINT   BAT           24 07-25-92    1:03p
READ       ME           340 02-25-93    2:47p
IDACOMP    BAT          205 05-02-93    8:51p
EXTERNS    IDA          646 05-04-93    7:38p
HELP       IDA       15,809 05-04-93    7:58p
MATH       C         18,556 07-27-93    9:22p
DISK       BAT           34 05-04-93    5:38p
DEFINES    IDA          376 05-04-93   10:47p
TEMPS      C         14,697 05-04-93    9:05p
PCIDA      C         10,232 07-27-93    8:49p
       27 file(s)      581,210 bytes

Total files listed:
       27 file(s)      581,210 bytes
                       869,376 bytes free
```

Kroutil Disk 8, Version 3 MTRX source.

```
 Volume in drive A has no label
 Volume Serial Number is 0C42-19D4

Directory of A:\

MTRX       DEF          318 08-17-92   12:08a
MIDDEF     H          2,816 07-24-92    7:13a
AMTRX      EXE       52,843 04-15-93    9:52a
MTRXD      BAT          132 08-17-92    1:44p
AMTRXD     EXE       49,403 04-15-93    9:53a
MTRX       BAT          129 08-17-92    1:46p
HEADERS    DEF        1,578 09-27-92    2:36p
FILTER1    INC       28,285 04-02-93    2:01p
MATGRAPH   EXE       45,034 10-02-92    3:52p
MATGRAPH   BAT          112 10-01-92   10:45a
MTRXD      C         16,243 02-17-93   10:19a
DISCRIM1   INC        5,122 04-03-93    9:07a
MTRX2      C         42,997 04-15-93    9:56a
MTRX       EXE       56,035 04-15-93    9:56a
MTRX2      EXE       65,443 04-15-93    9:57a
MTRXD      EXE       52,595 04-15-93    9:55a
MTRX2      BAT          132 02-09-93    3:37p
MATGRAPH   C         5,516 02-17-93   10:18a
FILTER2    INC       18,421 04-02-93    2:21p
DISCRIM2   INC        5,122 04-03-93    9:06a
MFILTER    INC       28,285 04-02-93    2:01p
AFILTER1   INC       18,421 04-02-93    2:20p
AFILTER2   INC       18,421 04-02-93    2:21p
ADIS1      INC        5,122 04-03-93    9:04a
ADIS2      INC        5,122 04-03-93    9:06a
MDIS1      INC        5,122 04-03-93    9:07a
MTRX       C         40,409 04-15-93    9:51a
       27 file(s)      569,178 bytes

Total files listed:
       27 file(s)      569,178 bytes
                       881,152 bytes free
```

ERDEC Disk 1, Edgewood Chemical Database, Disk 1 of 2.

```
 Volume in drive A has no label

Directory of A:\

IRSPEC     EXE       72,610 02-02-88    8:17a
IRSPEC     LIR      610,100 10-21-93    9:35a
IRSPEC01   SPC        8,301 12-11-90    1:06p
IRSPEC02   SPC        8,225 12-11-90    1:08p
IRSPEC03   SPC        8,234 12-11-90    1:12p
IRSPEC05   SPC        8,226 12-11-90    2:21p
IRSPEC04   SPC        8,235 12-11-90    2:23p
IRSPEC06   SPC        8,279 12-11-90    2:23p
IRSPEC07   SPC        8,256 12-11-90    2:24p
IRSPEC08   SPC        8,481 12-11-90    2:24p
IRSPEC09   SPC        8,362 12-11-90    2:24p
IRSPEC10   SPC        8,478 12-11-90    2:25p
IRSPEC11   SPC        8,533 12-11-90    2:25p
IRSPEC12   SPC        8,556 12-11-90    2:26p
IRSPEC13   SPC        8,318 12-11-90    2:26p
IRSPEC14   SPC        9,232 12-11-90    2:27p
IRSPEC15   SPC        8,475 12-11-90    2:28p
IRSPEC16   SPC        9,647 12-12-90    9:34a
IRSPEC     BAK          675 12-12-90   11:36a
IRSPEC50   ASP       21,887 12-14-90    2:49p
IRSPEC51   ASP       21,887 12-14-90    2:49p
IRSPEC52   ASP       21,887 12-14-90    2:49p
IRSPEC53   ASP       21,887 12-14-90    2:49p
IRSPEC54   ASP       21,887 12-14-90    2:49p
IRSPEC55   ASP       21,887 12-14-90    2:49p
IRSPEC56   ASP       21,887 12-14-90    2:49p
IRSPEC57   ASP       21,890 12-14-90    2:49p
IRSPEC58   ASP       21,887 12-14-90    2:49p
IRSPEC59   ASP       21,887 12-14-90    2:49p
IRSPEC60   ASP       21,887 12-14-90    2:49p
IRSPEC     CNT          634 02-14-91    2:19p
README!!   DOC        1,008 02-14-91    2:27p
       32 file(s)    1,061,625 bytes

Total files listed:
       32 file(s)    1,061,625 bytes
                       388,096 bytes free
```

ERDEC Disk 2, Edgewood Chemical Database, Disk 2 of 2.

```
 Volume in drive A has no label

Directory of A:\

IRSPEC49   ASP       21,887 12-14-90    2:49p
IRSPEC48   ASP       21,887 12-14-90    2:49p
IRSPEC47   ASP       21,887 12-14-90    2:49p
```

```
IRSPEC46 ASP       21,887 12-14-90   2:49p
IRSPEC45 ASP       21,887 12-14-90   2:49p
IRSPEC44 ASP       21,887 12-14-90   2:48p
IRSPEC43 ASP       21,887 12-14-90   2:48p
IRSPEC42 ASP       21,899 12-14-90   2:48p
IRSPEC41 ASP       21,925 12-14-90   2:48p
IRSPEC40 ASP       21,903 12-14-90   2:48p
IRSPEC39 ASP       21,890 12-14-90   2:48p
IRSPEC38 ASP       21,911 12-14-90   2:48p
IRSPEC37 ASP       21,896 12-14-90   2:48p
IRSPEC36 ASP       21,887 12-14-90   2:48p
IRSPEC35 ASP       21,887 12-14-90   2:48p
IRSPEC34 ASP       21,887 12-14-90   2:48p
IRSPEC33 ASP       21,887 12-14-90   2:48p
IRSPEC32 ASP       21,887 12-14-90   2:48p
IRSPEC31 ASP       21,889 12-14-90   2:48p
IRSPEC30 ASP       22,156 12-14-90   2:48p
IRSPEC29 ASP       21,888 12-14-90   2:48p
IRSPEC28 ASP       21,887 12-14-90   2:48p
IRSPEC27 ASP       21,887 12-14-90   2:48p
IRSPEC26 ASP       21,889 12-14-90   2:48p
IRSPEC25 ASP       21,887 12-14-90   2:48p
IRSPEC24 ASP       21,888 12-14-90   2:47p
IRSPEC23 ASP       21,887 12-14-90   2:47p
IRSPEC22 ASP       21,887 12-14-90   2:47p
IRSPEC21 ASP       21,887 12-14-90   2:47p
```

```
IRSPEC20 ASP       21,956 12-14-90   2:47p
IRSPEC19 ASP       21,887 12-14-90   2:47p
IRSPEC18 ASP       21,887 12-14-90   2:47p
IRSPEC17 ASP       21,887 12-14-90   2:47p
IRSPEC16 ASP       21,887 12-14-90   2:47p
IRSPEC15 ASP       21,887 12-14-90   2:47p
IRSPEC14 ASP       21,887 12-14-90   2:47p
IRSPEC13 ASP       21,887 12-14-90   2:47p
IRSPEC12 ASP       21,887 12-14-90   2:47p
IRSPEC11 ASP       21,887 12-14-90   2:47p
IRSPEC10 ASP       21,887 12-14-90   2:47p
IRSPEC09 ASP       21,887 12-14-90   2:47p
IRSPEC08 ASP       21,887 12-14-90   2:47p
IRSPEC07 ASP       21,887 12-14-90   2:47p
IRSPEC06 ASP       21,898 12-14-90   2:47p
IRSPEC05 ASP       21,888 12-14-90   2:46p
IRSPEC04 ASP       21,904 12-14-90   2:46p
IRSPEC03 ASP       21,899 12-14-90   2:46p
IRSPEC02 ASP       21,887 12-14-90   2:46p
IRSPEC01 ASP       21,887 12-14-90   2:46p
       49 file(s)     1,072,950 bytes

Total files listed:
       49 file(s)     1,072,950 bytes
                        378,368 bytes free
```

APPENDIX B

Gas Library Databases (GFI)

Two gas library databases were obtained (GFI) for use with HyGAS.

- Rauss_Sprouse database
- ERDEC_Emery database

1. Rauss_Sprouse database

The Rauss_Sprouse database (Table 1) was supplied by P. Rauss of the U.S. Army Research Laboratories (ARL), Ft. Belvoir, Virginia. This database contains 80 spectra. This includes the absorbance spectra for 78 different gas species at 2 cm^{-1} spectral resolution. (Nyquist sampling for 2 cm^{-1} spectral resolution requires a datapoint spacing of 1 cm^{-1}.) One gas was measured at two concentrations (ethylene dibromide, at 259.13 ppm and 12.4 ppm); one gas was measured at two spectral resolutions (sulfur hexafluoride, at 2 cm^{-1} and 0.5 cm^{-1}).

This database was supplied in Spectra Calc™/GRAMS™ (trademarks of Galactic Industries Corporation) binary format, which we converted into standard JCAMP format and/or ASCII_XY format, for incorporation into a HIPS spectral library. Each of the spectra at 2 cm^{-1} resolution contains 4150 datapoints (the 0.5 cm^{-1} spectrum contains 14730 datapoints), decreasing in x-value from 4400 cm^{-1} to 400 cm^{-1} wavenumbers; the y-value is in absorbance units. The original measurements for this gas database were done by Sprouse Scientific Systems, to specifications defined by Rauss.

Table 1. HyGAS GFI Rauss_Sprouse database. The 80 spectra included in the Sprouse database are listed numerically by filename (`spec[nn][r]`). Original filenames (i.e. `spec#1.spc`) included the extension "`.spc`" (indicating the Spectra Calc/GRAMS format of Galactic Industries Corporation), and a "#" character in the title, which was not recognized as a valid filename by GRAMS. Descriptions were extracted from the converted JCAMP format header. Cross-reference index numbers for each derived HyGAS library are listed. [Note indexing starts at 0 for HIPS spectral libraries, and 1 for the HyGAS Neural Net.] Files `spec44a` and `spec44b` refer to two different species; `spec58` and `spec58r` are the same species, as are `spec71` and `spec71r`. [This explains the original index numbers ranging from 1–77 rather than the expected 1–80.]

Title	Description	Sprouse_80 HIPS Library Index	Rauss-Sprouse_65 HIPS Library Index	HyGAS Neural Net Index
spec_01	METHYL CHLORIDE, 800 ppm	0	0	1
spec_02	ETHYL CHLORIDE, 800 ppm	1	1	2
spec_03	ISOPROPYL CHLORIDE, 49.54 ppm	2	2	3
spec_04	DIMETHYL ETHER, 200 ppm	3	3	4
spec_05	DIMETHYL DISULFIDE,	4	4	5
spec_06	PINACOLYL ALCOHOL, 193.50 ppm	5	5	6
spec_07	2-CHLOROETHANOL,	6	6	7
spec_08r	FORMAMIDE, 404 ppm, T=60 deg C	7	7	8
spec_09	TRIMETHYL PHOSPHITE, 19.00 ppm	8	8	9
spec_10r	PYRIDINE, 144 ppm, T=25 deg C	9	9	10
spec_11r	ALLYL CHLORIDE, 352 ppm, T=25 deg C	10	10	11
spec_12	DIMETHYL METHYLPHOSPHONATE, 46.52 ppm, T=45 deg C	11	11	12
spec_13	DIETHYL METHYLPHOSPHONITE, 26.88 ppm, T=45 deg C	12	12	13
spec_14	DIETHYL METHYLPHOSPHONATE, 40.24 ppm, T=45 deg C	13		
spec_15	TRIISOPROPYL PHOSPHITE, 14.68 ppm, T=45 deg C	14	13	14
spec_16	DIISOPROPYL METHYLPHOSPHONATE, 22.96 ppm, T=45 deg C	15	14	15
spec_17	DIETHYL METHYLPHOSPHONOTHIOATE,	16	15	16
spec_18r	ACETONITRILE, 1696 ppm, T=25 deg C	17	16	17
spec_19r	ACETONE, 146 ppm, T=25 deg C	18	17	18
spec_20	THIODIGLYCOL, 10,837.67 ppm, T=250 deg C	19	18	19
spec_21	DIISOPROPYL AMINOETHANOL, 96.61 ppm, T=73 deg C	20	19	20
spec_22r	BROMOBENZENE, 152 ppm, T=60 deg C	21	20	21
spec_23r	ALLYLBENZENE, 284 ppm, T=25 deg C	22	21	22
spec_24r	BROMOETHANE, 468 ppm, T=25 deg C	23	22	23
spec_25r	NITROMETHANE, 99 ppm, T=25 deg C	24	23	24
spec_26r	CYCLOHEXANONE, 87 ppm, T=25 deg C	25	24	25
spec_27r	ACETIC ANHYDRIDE, 49 ppm, t=25 deg C	26	25	26
spec_28r	ACETIC ACID, 129 ppm, T=25 deg C	27	26	27
spec_29r	BENZYL CHLORIDE, 242 ppm, T=25 deg C	28	27	28
spec_30r	ETHYL PHENYL KETONE, 205 ppm, T=60 deg C	29	28	29

Title	Description	Sprouse _80 HIPS Library Index	Rauss-Sprouse _65 HIPS Library Index	HyGAS Neural Net Index
spec_31	THIONYL CHLORIDE, 61.72 ppm	30	29	30
spec_32	PHOSPHORUS TRICHLORIDE, 19.26 ppm, T=45 deg C	31	30	31
spec_33	PHOSPHOROUS OXYCHLORIDE, 216.30 ppm, T=45 deg C	32	31	32
spec_34	DIMETHYLPHOSPHORAMIDIC DICHLORIDE, 70.60 ppm, T=73 deg C=	33		
spec_35	DIMETHYLPHOSPHITE, 54.97 ppm, T=45 deg C	34		
spec_36	DIISOPROPYL HYDROGEN PHOSPHITE, 20.22 ppm, T=45 deg C	35	32	33
spec_37r	TETRAHYDROFURAN, 133 ppm, T=25 deg C	36	33	34
spec_38r	ETHYL ACETATE, 45 ppm, T=25 deg C	37	34	35
spec_39r	METHACRYLATE, 80 ppm, T=25 deg C	38	35	36
spec_40	METHYLPHOSPHONYL DICHLORIDE, 36.37 ppm, T=45 deg C	39	36	37
spec_41r	FORMIC ACID, 119 ppm, T=25 deg C	40	37	38
spec_42	METHYL DICHLOROPHOSPHINE, 103.07 ppm, T=45 deg C	41	38	39
spec_43	HYDROGEN SULFIDE, 20,000 ppm	42	39	40
spec_44a	SULFUR DICHLORIDE, 53.46 ppm, T=45 deg C	43		
spec_44b	SULFUR MONOCHLORIDE, 63.02 ppm, T=45 deg C	44		
spec_45	ETHYLENE, 55.7 ppm	45	40	41
spec_46	METHANOL, 52.8 ppm	46	41	42
spec_47	ETHANOL, 69.1 ppm	47	42	43
spec_48	ISOPROPANOL, 34.9 ppm	48	43	44
spec_49	VINYL CHLORIDE, 49.20 ppm	49	44	45
spec_50	ETHYLENE OXIDE, 55.8 ppm	50	45	46
spec_51	DIMETHYLAMINE, 400 ppm	51	46	47
spec_52	TRIETHYLAMINE, 38.59 ppm	52	47	48
spec_53	CARBON TETRACHLORIDE, 11.1 ppm	53		
spec_54	CHLOROFORM, 20.1 ppm	54	48	49
spec_55	HYDROGEN CHLORIDE, 100ppm	55		
spec_56	PARATHION, 4,293.97 ppm, T=200 deg C	56	49	50
spec_57	DIETHYL ETHER, 172.59 ppm	57	50	51
spec_58	SULFUR HEXAFLUORIDE, 5.01 ppm	58	51	52
spec_58r	SULFUR HEXAFLUORIDE, 5.01 ppm, T=25 deg C, 0.5 cm-1 Resolution	59		
spec_59	METHANE, 50.30 ppm	60	52	53
spec_60	ETHANE, 48.50 ppm	61	53	54
spec_61	PROPANE, 54.50 ppm	62		
spec_62	PROPYLENE, 56.20 ppm	63	54	55
spec_63	1,3-BUTADIENE, 200 ppm	64	55	56
spec_64	n-BUTANE, 52.5 ppm	65	56	57
spec_65	cis-2-PENTENE, 83.09 ppm	66	57	58
spec_66	ETHYL MERCAPTAN, 363.21 ppm	67	58	59
spec_67	BUTYL MERCAPTAN, 133.92 ppm	68	59	60
spec_68	BENZENE, 20.2 ppm	69	60	61
spec_69	SULFUR DIOXIDE, 49.8 ppm	70	61	62
spec_70	NITROUS OXIDE, 47.2 ppm	71	62	63
spec_71	ETHYLENE DIBROMIDE, 259.13	72	63	64
spec_71r	ETHYLENE DIBROMIDE, 12.4 ppm, T=25 deg C	73		
spec_72r	NITROETHANE, 62 ppm, T=25 deg C	74	64	65
spec_73	CARBON DIOXIDE, 40.4 ppm	75		
spec_74	CARBON MONOXIDE, 50.40 ppm	76		
spec_75	WATER, 1,492.30 ppm, T=45 deg C	77		
spec_76	n-HEXANE, 89 ppm, T=25 deg C	78		
spec_77	n-HEPTANE, 79 ppm, T=25 deg C	79		

2. *ERDEC_Emery database*

The ERDEC_Emery database (Table 2) was supplied by R. Kroutil of the U.S. Army Edgewood Research Development and Engineering Center (ERDEC), Edgewood, Maryland. This database contains 60 spectra. This includes absorbance spectra for selected chemical warfare (CW) agents, CW agent simulators, and potential contaminants such as engine vapors, smoke and dust, all at 2 cm^{-1} spectral resolution.

This database was supplied in a generic ASCII format, which we converted into ASCII_XY format for incorporation into a HIPS spectral library. Each of the original spectra contains 2184 datapoints, increasing in x-value from 388 cm^{-1} to 2500 cm^{-1} wavenumbers; y-values are in optical cross-section units. Not all spectra include valid datavalues over the full spectral range. Ranges of datapoints with y-values of zero were omitted, defining the valid subset spectral range for each spectrum; minimum and maximum wavenumbers for each spectrum are indicated in the appropriate columns of Table 2. The original measurements for this database were [presumably] done by ERDEC, to specifications defined by the Army, and were compiled into this database by Silvio Emery, at ERDEC.

Table 2. HyGAS GFI Emery database. The 60 spectra included in the Emery database are listed by original filename (`irspec[nn]`). Descriptions were extracted from the original ASCII header. Index numbers for the derived HyGAS library also are included, for cross-reference by library index number. Minimum and maximum wavenumber values are included for each spectrum, indicating the effective range of valid datavalues.

Title	Description	HIPS Library Index	min wavenumber cm^{-1}	max wavenumber cm^{-1}
irspec01	EA0001_GA_(LIQUID)	0	396	2500
irspec02	EA0002_GA_(VAPOR)	1	427	2500
irspec03	EA0003_GB_(LIQUID)	2	404	2500
irspec04	EA0004_GB_(VAPOR)	3	411	2500
irspec05	EA0005_GD_(LIQUID)	4	419	2500
irspec06	EA0006_GD_(VAPOR)	5	427	2500
irspec07	EA0007_VX_(LIQUID)	6	411	2500
irspec08	EA0008_CS_(LIQUID)	7	466	2500
irspec09	EA0009_CN_(LIQUID)	8	473	2500
irspec10	EA0010_HD_(LIQUID)	9	481	2500
irspec11	EA0011_HQ_(LIQUID)	10	489	2500
irspec12	EA0012_HD_(VAPOR)	11	496	2500
irspec13	EA0013_DM_(LIQUID)	12	396	2500
irspec14	EA0014_HC_(VAPOR)	13	396	2500
irspec15	EA0015_HC_(PARTICULATES)	14	404	2500
irspec16	EA0016_GREEN_SMOKE_(VAPOR)	15	411	2500
irspec17	EA0017_GREEN_SMOKE_(PARTICULATES)	16	419	2500
irspec18	EA0018_RED_SMOKE_(VAPOR)	17	427	2500
irspec19	EA0019_RED_SMOKE_(PARTICULATES)	18	435	2500
irspec20	EA0020_YELLOW_SMOKE_(VAPOR)	19	401	2500
irspec21	EA0021_YELLOW_SMOKE_(PARTICULATES)	20	450	2500
irspec22	EA0022_VIOLET_SMOKE_(VAPOR)	21	458	2500
irspec23	EA0023_VIOLET_SMOKE_(PARTICULATES)	22	466	2500
irspec24	EA0024_GRASS_SMOKE_(VAPOR)	23	473	2500
irspec25	EA0025_GRASS_SMOKE_(PARTICULATES)	24	481	2500
irspec26	EA0026_COTTON_SMOKE_(VAPOR)	25	489	2500
irspec27	EA0027_COTTON_SMOKE_(PARTICULATES)	26	496	2500
irspec28	EA0028_RUBBER_SMOKE_(VAPOR)	27	504	2500
irspec29	EA0029_WOOL_SMOKE_(VAPOR)	28	512	2500
irspec30	EA0030_WOOL_SMOKE_(PARTICULATES)	29	388	2500
irspec31	EA0031_PAPERS_(VAPOR)	30	527	2500
irspec32	EA0032_GASOLINE_ENGINE_EXHAUST	31	404	2500
irspec33	EA0033_GASOLINE_(VAPOR)	32	411	2500
irspec34	EA0034_ORANGE_SMOKE	33	419	2500
irspec35	EA0035_WHITE_SMOKE	34	427	2500
irspec36	EA0036_BLUE_SMOKE	35	435	2500
irspec37	EA0037_METHYLCELL	36	442	2500
irspec38	EA0038_DICDI	37	504	2500
irspec39	EA0039_THIOLAMINE	38	512	2500
irspec40	EA0040_DIMP_(LIQUID)	39	700	1350
irspec41	EA0041_DMMP_(VAPOR)	40	701	1350
irspec42	EA0042_DMMP_(LIQUID)	41	700	1350
irspec43	EA0043_ETHANOL_(VAPOR)	42	726	1350
irspec44	EA0044_FT._BENNING_DUST	43	435	1608
irspec45	EA0045_FT._BENNING_DUST	44	450	1608
irspec46	EA0046_SALT_LAKE_CITY_DUST	45	427	1613
irspec47	EA0047_PANAMA_DUST	46	435	1613
irspec48	EA0048_SINGLEEDON_DUST	47	401	1605
irspec49	EA0049_SOUTH_MIAMI_DUST	48	466	1613
irspec50	EA0050_PANAMA_DUST	49	401	1605
irspec51	EA0051_SINGLEEDON_DUST	50	401	1605
irspec52	EA0052_FT._MCCLELLEN_DUST	51	401	1600
irspec53	EA0053_FT._BENNING_DUST	52	401	1601
irspec54	EA0054_FT._BENNING_DUST	53	401	1599
irspec55	EA0055_WP_(VAPOR)	54	741	1428
irspec56	EA0056_NEUTRAL	55	388	2500
irspec57	EA0057_UNKNOWN	56	747	1303
irspec58	EA0058_UNKNOWN	57	708	1400
irspec59	EA0059_UNKNOWN	58	666	1400
irspec60	EA0060_UNKNOWN	59	699	1400

3. HyGAS Spectral Libraries

For use with HyGAS, three HIPS spectral libraries were created from these databases.

- `HyGAS_Sprouse_80`
- `HyGAS_Rauss-Sprouse_65`
- `HyGAS_ERDEC_Emery`

The first two of these libraries are derived from the Sprouse database; the third library is derived from the ERDEC Emery database. Descriptions for these libraries are listed in Table 3.

Table 3. HyGAS HIPS Spectral Library Descriptions. This information is extracted from the HIPS ASCII file `$DOD_DIR/LIBRARY/tables/General.lib`. Included for each library is a list of HIPS spectral sensors to which the library has been resampled.

```
Name        :   HyGAS_Sprouse_80
Description :   "Gas Spectra (2cm-1 resolution) measured by Sprouse Scientific
                Systems for P. Rauss of US Army NVEOD, 4150 pts., 4400-400 cm-
                1, DECREASING wavenumber; (also includes SF6 at 0.5cm-1
                resolution)"
Directory   :   /usr/HIPS/LIBRARIES/HyGAS_Sprouse_80
Mode        :   420
Sensors     :   Rauss_449_spec.sensor Kroutil_513_spec.sens
                Kroutil_113_spec.sens

                ------------------------------------------

Name        :   HyGAS_Rauss-Sprouse_65
Description :   "Gas Spectra (2cm-1 resolution) measured by Sprouse Scientific
                Systems for P. Rauss of US Army NVEOD, selected 65 items, 449
                pts., 833-1265 cm-1, sorted by increasing wavenumber,
                NORMALIZED 0 to 1"
Directory   :   /usr/HIPS/LIBRARIES/HyGAS_Rauss-Sprouse_65
Mode        :   420
Sensors     :   Rauss_449_spec.sensor

                ------------------------------------------

Name        :   HyGAS_ERDEC_Emery
Description :   "Wavenumber vs. optical cross section of chemicals stored in
                the IRSPEC database V.1.0 received from Edgewood Arsenal and
                compiled by Dr. Silvio L. Emery"
Directory   :   /usr/HIPS/LIBRARIES/HyGAS_ERDEC_Emery
Mode        :   420
Sensors     :   Rauss_449_spec.sensor Kroutil_113_spec.sens
```

The HIPS spectral library `HyGAS_Sprouse_80` includes all 80 spectra from the Sprouse database, at original spectral resolution and at original absorbance units. Spectra included in this library are referenced by HIPS library index (0–79) in Table 1.

The HIPS spectral library `HyGAS_Rauss-Sprouse_65` includes 65 selected spectra from the full Sprouse database. For this library, data values outside the spectral region of interest (~8–12 μm, or ~800–1250 cm^{-1}) were eliminated. Gas species with no significant spectral features in this region also were eliminated, as were any replicated species. The y-axis values for the remaining 65 spectra were then scaled (minimum to maximum within each spectrum) to lie within the arbitrary range 0 to 1. [This is a standard technique for creating spectral search library datasets, and is the method used by Rauss for his neural net training library. This method also maximizes the variability in absorbance as a function of wavelength, which is the primary identifying metric for any gas species (i.e. its unique and characteristic "fingerprint" spectral signature).] Spectra included in this library are referenced by HIPS library index (0–64) in Table 1. These are the same spectra included in the HyGAS Neural Net search library, also referenced in Table 1. [Note the Neural Net index values are 1–65, while the corresponding HIPS library index values are 0–64.]

The HIPS library `HyGAS_ERDEC_Emery` includes all 60 spectra in the original Emery database, but only within the defined valid spectral range. This range is indicated in Table 2. Although this range varies, all spectra include the primary spectral region of interest (~8–12 μm, or ~800–1250 cm^{-1}) for HyGAS.

4. HIPS Sensor Files

HIPS can associate a spectral sensor characteristics (or INSTRUMENT) file with any HIPS dataset (Table 4). Such a file will define a spectral value for each spectral channel (or index) in a HIPS dataset. This is useful for spectral plots, when the HIPS user needs to assign a physical meaning to the spectral axis, particularly so in instances where the functional relationship between the spectral channels is not a simple linear function.

HIPS also uses the spectral sensor characteristics, albeit not directly, when applying a library search algorithm. Mathematically, HIPS compares the unknown spectrum to the library spectrum, channel by channel. In practice, this means the spectral channels in a spectral library should correlate directly with the spectral channels in the unknown. If a spectral library is created with the same spectral sensor characteristics as the unknown, HIPS can simply search against the so-called `Raw Spectrum` in the library. If, however, the samples in a spectral library are not consistent (such as is the case with the Emery library), or there is not a 1:1 correlation between the spectral channels of the unknown and the spectral channels in the library, the library must first be "convolved," or resampled to match the spectral sensor characteristics of the unknown species. In this case, HIPS creates an additional binary version(s) of the library, with data values resampled to match the spectral characteristics of the specified sensor(s).

Table 4. Associating a HIPS spectral sensor characteristics file. This is an example `abs` file in a HIPS dataset directory, which defines the parameters of the associated HIPS data file `data.xys`. The `INSTRUMENT` field indicates an associated spectral sensor characteristics file `Rauss_449_spec.sensor` which defines the spectral axis values for each of the 449 spectral channels. This sensor must exist in the directory `$DOD_DIR/LIBRARY/sensors`, for HIPS plotting functions to assign values to the independent variable, or spectral axis, in a spectral plot.

```
OWNER = "hardy:"
DATE  = "Thu Sep 8 11:54:58 1994"
DATATYPE = float
X_AXIS_SIZE = 240
Y_AXIS_SIZE = 150
S_AXIS_SIZE = 449
INSTRUMENT = Rauss_449_spec.sensor
```

The sensors supplied for use with HyGAS are listed in Table 5. These sensors were defined to match specific HyGAS test datasets, either for use with HyGAS plotting functions, or for use with the HyGAS search libraries. For HyGAS, each of the spectral libraries has been resampled to match the spectral sensor characteristics for appropriate simulated HyGAS test datasets. Table 3 indicates the sensors for which each of these libraries has been resampled to match.

The sensor `Kroutil_1024_intf.sen` was defined to match the characteristics of the field data supplied by Kroutil as GFI for use with HyGAS. This data was supplied as 1024 data point interferograms, at unit channel spacing, ranging from channel index 0 to channel index 1023. This sensor was defined for use during plotting only, and is not applicable for use with spectral libraries (no interferogram domain spectral libraries were attempted).

The sensor `Kroutil_513_spec.sens` was defined to match the recommended Spectra Calc functional translation of the Kroutil_MIDAC interferograms. Spectra Calc

generates a spectral domain of 513 data points from the raw interferograms of 1024 data points. This sensor was defined both for plotting and for preliminary testing with a spectral library. Only the Sprouse_80 library was resampled to this sensor. With a spectral range of 0 to 1974.75 cm^{-1} wavenumbers (at 8 cm^{-1} spectral resolution, Nyquist sampling requires a datapoint spacing of 4 cm^{-1}), much of the spectral data for this sensor falls outside the range of valid library spectral data (typically 400 cm^{-1} to 4400 cm^{-1} wavenumbers); in fact, in order to function with this sensor, such a spectral library must be extrapolated, essentially "padded" with invalid zero-data-value filler points, on one end of its valid spectral range, to match the spectral characteristics of the sensor. This approach is not recommended in practice, and was applied for testing purposes only.

The sensor `Kroutil_512_spec.sens` was defined to match an in-house developed FFT method, which generated an identical spectral domain to that for the Kroutil FFT code, but with one less data point. The sensor `Kroutil_512.spec` is functionally identical to this sensor, and is included purely for backwards compatibility with an outdated version of the HyGAS code.

The sensor `Kroutil_113_spec.sens` is a subset of the other Kroutil spectral domain sensors, which eliminates those datapoints outside the primary spectral region of interest (~8–12 μm, or ~800–1250 cm^{-1}) to HyGAS. Restricting this sensor to the primary spectral region of interest avoids any difficulties associated with trying to extrapolate beyond the range of valid spectral data for the library. The Emery library and the Sprouse_80 library are both resampled to this sensor, at 8 cm^{-1} resolution. (Since the Rauss-Sprouse_65 library already is a spectral subset of the Sprouse_80 library, little if anything is to be gained by duplicating this sensor for the subset Rauss-Sprouse_65 library. The sole difference would be in the values associated with the re-scaled y-axis, and this difference can be tested using the Rauss_449 sensor, described below.)

The sensor `Rauss_449_spec.sensor` is defined to match the spectral characteristics of the field data (from the Rauss-Howden spectrometer) supplied by Rauss as GFI for use with HyGAS. These data were supplied as 449 data points ranging from 1265 cm^{-1} to 833 cm^{-1} wavenumbers, at 2 cm^{-1} spectral resolution (Nyquist sampling at 1 cm^{-1} datapoint spacing). All three HyGAS spectral libraries were resampled to this sensor resolution.

A detailed listing of the sensor files defined for HyGAS is given in Table 6. This listing details the format of a HIPS sensor file; however, only the first five and last five channels of each sensor are listed.

Table 5. Sensors supplied for use with HyGAS. This is a listing of the HIPS directory `$DOD_DIR/LIBRARY/sensors`. Sensor names include a reference to a HyGAS simulation cube test dataset (Kroutil or Rauss), the number of spectral channels, and a reference to whether the sensor is an interferogram domain sensor, or a spectral domain sensor. The sensor `Kroutil_512.spec.tbl` is functionally identical to the sensor `Kroutil_512_spec.sens.tbl`, and is included for backwards compatibility with an outdated version of the HyGAS code. Actual sensor names omit the suffix `.tbl`.

```
Kroutil_1024_intf.sen.tbl
Kroutil_513_spec.sens.tbl
Kroutil_512_spec.sens.tbl
[Kroutil_512.spec.tbl]
Kroutil_113_spec.sens.tbl
Rauss_449_spec.sensor.tbl
```

Table 6. Detailed format listing of HIPS sensor files for HyGAS. Only the first five and last five channels of each sensor are included.

```
==> Kroutil_1024_intf.sen.tbl <==
Name                          : Kroutil_1024_intf.sen
Description                   : "Kroutil MIDAC 1024pt interferogram, 0-1023"
Channels                      : 1024
Band Table                    :
0.000000  0.100000  1.000000  0.000000
1.000000  0.100000  1.000000  0.000000
2.000000  0.100000  1.000000  0.000000
3.000000  0.100000  1.000000  0.000000
4.000000  0.100000  1.000000  0.000000

1019.000000  0.100000  1.000000  0.000000
1020.000000  0.100000  1.000000  0.000000
1021.000000  0.100000  1.000000  0.000000
1022.000000  0.100000  1.000000  0.000000
1023.000000  0.100000  1.000000  0.000000


==> Kroutil_113_spec.sens.tbl <==
Name                          : Kroutil_113_spec.sens
Description                   : "Kroutil spectral sensor, 113pts, 833-1265cm-1 (channels 217-329 in 512 or 513pts
spectra)"
Channels                      : 113
Band Table                    :
833.099976  3.860000  1.000000  0.000000
836.950012  3.860000  1.000000  0.000000
840.809998  3.860000  1.000000  0.000000
844.669983  3.860000  1.000000  0.000000
848.530029  3.860000  1.000000  0.000000

1249.650024  3.860000  1.000000  0.000000
1253.500000  3.860000  1.000000  0.000000
1257.359985  3.860000  1.000000  0.000000
1261.219971  3.860000  1.000000  0.000000
1265.069946  3.860000  1.000000  0.000000


==> Kroutil_512_spec.sens.tbl <==
Name                          : Kroutil_512_spec.sens
Description                   : "simulated spectral sensor for Kroutil/MIDAC FTIR spectrometer, for use with HyGAS FT
function that generates 512 datapoints from a 1024 point interferogram"
Channels                      : 512
Band Table                    :
0.000000  3.860000  1.000000  0.000000
3.860000  3.860000  1.000000  0.000000
7.710000  3.860000  1.000000  0.000000
11.570000  3.860000  1.000000  0.000000
15.430000  3.860000  1.000000  0.000000

1955.469971  3.860000  1.000000  0.000000
1959.319946  3.860000  1.000000  0.000000
1963.180054  3.860000  1.000000  0.000000
1967.040039  3.860000  1.000000  0.000000
1970.890015  3.860000  1.000000  0.000000


==> Kroutil_513_spec.sens.tbl <==
Name                          : Kroutil_513_spec.sens
Description                   : "Kroutil spectral sensor, 513pts, 0-1974.75cm-1 "
Channels                      : 513
Band Table                    :
0.000000  3.860000  1.000000  0.000000
3.860000  3.860000  1.000000  0.000000
7.710000  3.860000  1.000000  0.000000
11.570000  3.860000  1.000000  0.000000
15.430000  3.860000  1.000000  0.000000

1959.319946  3.860000  1.000000  0.000000
1963.180054  3.860000  1.000000  0.000000
1967.040039  3.860000  1.000000  0.000000
1970.890015  3.860000  1.000000  0.000000
1974.750000  3.860000  1.000000  0.000000

==> Rauss_449_spec.sensor.tbl <==
Name                          : Rauss_449_spec.sensor
Description                   : "simulated Howden field sensor, 449 spectral channels, 833-1265 inverse cm, from data
supplied by Rauss as GFI, bandwidth defined by datapoint spacing"
Channels                      : 449
Band Table                    :
833.000000  0.964000  1.000000  0.000000
833.960022  0.964000  1.000000  0.000000
834.929993  0.964000  1.000000  0.000000
835.890015  0.964000  1.000000  0.000000
836.859985  0.964000  1.000000  0.000000

1261.130005  0.964000  1.000000  0.000000
1262.099976  0.964000  1.000000  0.000000
1263.060059  0.964000  1.000000  0.000000
1264.020020  0.964000  1.000000  0.000000
1265.000000  0.964000  1.000000  0.000000
```

5. Additional notes

The HIPS spectral libraries supplied with HyGAS can be plotted, listed and accessed using the standard HIPS functions.

Sample HIPS command lines used to create these libraries and add the spectra to them are given in Tables 7 and 8. These command line files were supplied with HyGAS. The respective files are in directory paths

`$hygas/Rauss/Sprouse_data/ascii_xy/xstuff`

and

`$hygas/Emery/ascii_xy/xstuff`.

Subdirectory references are indicated relative to these path names.

Table 7. Sample HIPS command lines for creating HIPS spectral libraries for HyGAS. These command lines can be executed as UNIX shell scripts (ex. `sh do_crlib_Sprouse_80`) from the appropriate HyGAS directory.

```
==> do_crlib_Sprouse_80 <==
crlib -t "Gas Spectra (2cm-1 resolution) measured by Sprouse Scientific Systems for P. Rauss of US Army NVEOD, 4150
pts., 4400-400 cm-1, DECREASING wavenumber; (also includes SF6 at 0.5cm-1 resolution)" -S -G -d /usr/HIPS/LIBRARIES
HyGAS_Sprouse_80

==> do_crlib_Sprouse_65 <==
crlib -t "Gas Spectra (2cm-1 resolution) measured by Sprouse Scientific Systems for P. Rauss of US Army NVEOD, selected
65 items, 449 pts., 833-1265 cm-1, sorted by increasing wavenumber, NORMALIZED 0 to 1" -S -G -d /usr/HIPS/LIBRARIES
HyGAS_Rauss-Sprouse_65

==> do_crlib[_ERDEC_Emery] <==
crlib -t "Wavenumber vs. optical cross section of chemicals stored in the IRSPEC database V.1.0 received from Edgewood
Arsenal and compiled by Dr. Silvio L. Emery" -S -G -d /usr/HIPS/LIBRARIES HyGAS_ERDEC_Emery
```

Table 8. Sample HIPS command lines for adding spectra to HIPS spectral libraries for HyGAS. Only the first ten lines of each sample file are listed. These command lines can be executed as UNIX shell scripts (ex. `sh do_add2lib_Sprouse_80`) from the appropriate HyGAS directory.

```
==> do_add2lib_Sprouse_80 <==
add_spectrum -f 2 -t "METHYL CHLORIDE, 800 ppm" -L HyGAS_Sprouse_80 -n spec_01 ../unsorted_4150/spec_01.prn
add_spectrum -f 2 -t "ETHYL CHLORIDE, 800 ppm" -L HyGAS_Sprouse_80 -n spec_02 ../unsorted_4150/spec_02.prn
add_spectrum -f 2 -t "ISOPROPYL CHLORIDE, 49.54 ppm" -L HyGAS_Sprouse_80 -n spec_03 ../unsorted_4150/spec_03.prn
add_spectrum -f 2 -t "DIMETHYL ETHER, 200 ppm" -L HyGAS_Sprouse_80 -n spec_04 ../unsorted_4150/spec_04.prn
add_spectrum -f 2 -t "DIMETHYL DISULFIDE," -L HyGAS_Sprouse_80 -n spec_05 ../unsorted_4150/spec_05.prn
add_spectrum -f 2 -t "PINACOLYL ALCOHOL, 193.50 ppm" -L HyGAS_Sprouse_80 -n spec_06 ../unsorted_4150/spec_06.prn
add_spectrum -f 2 -t "2-CHLOROETHANOL," -L HyGAS_Sprouse_80 -n spec_07 ../unsorted_4150/spec_07.prn
add_spectrum -f 2 -t "FORMAMIDE, 404 ppm, T=60 deg C" -L HyGAS_Sprouse_80 -n spec_08r ../unsorted_4150/spec_08r.prn
add_spectrum -f 2 -t "TRIMETHYL PHOSPHITE, 19.00 ppm" -L HyGAS_Sprouse_80 -n spec_09 ../unsorted_4150/spec_09.prn
add_spectrum -f 2 -t "PYRIDINE, 144 ppm, T=25 deg C" -L HyGAS_Sprouse_80 -n spec_10r ../unsorted_4150/spec_10r.prn

==> do_add2lib_Sprouse_65 <==
add_spectrum -f 2 -t "METHYL CHLORIDE, 800 ppm" -L HyGAS_Rauss-Sprouse_65 -n spec_01 ../scaled_0_to_1/spec_01
add_spectrum -f 2 -t "ETHYL CHLORIDE, 800 ppm" -L HyGAS_Rauss-Sprouse_65 -n spec_02 ../scaled_0_to_1/spec_02
add_spectrum -f 2 -t "ISOPROPYL CHLORIDE, 49.54 ppm" -L HyGAS_Rauss-Sprouse_65 -n spec_03 ../scaled_0_to_1/spec_03
add_spectrum -f 2 -t "DIMETHYL ETHER, 200 ppm" -L HyGAS_Rauss-Sprouse_65 -n spec_04 ../scaled_0_to_1/spec_04
add_spectrum -f 2 -t "DIMETHYL DISULFIDE," -L HyGAS_Rauss-Sprouse_65 -n spec_05 ../scaled_0_to_1/spec_05
add_spectrum -f 2 -t "PINACOLYL ALCOHOL, 193.50 ppm" -L HyGAS_Rauss-Sprouse_65 -n spec_06 ../scaled_0_to_1/spec_06
add_spectrum -f 2 -t "2-CHLOROETHANOL," -L HyGAS_Rauss-Sprouse_65 -n spec_07 ../scaled_0_to_1/spec_07
add_spectrum -f 2 -t "FORMAMIDE, 404 ppm, T=60 deg C" -L HyGAS_Rauss-Sprouse_65 -n spec_08r ../scaled_0_to_1/spec_08r
add_spectrum -f 2 -t "TRIMETHYL PHOSPHITE, 19.00 ppm" -L HyGAS_Rauss-Sprouse_65 -n spec_09 ../scaled_0_to_1/spec_09
add_spectrum -f 2 -t "PYRIDINE, 144 ppm, T=25 deg C" -L HyGAS_Rauss-Sprouse_65 -n spec_10r ../scaled_0_to_1/spec_10r

==> do_add2lib[_ERDEC_Emery] <==
add_spectrum -f 2 -t "GA (LIQUID) EA0001" -L HyGAS_ERDEC_Emery -n GA_liquid ../irspec01.asc
add_spectrum -f 2 -t "GA (VAPOR) EA0002" -L HyGAS_ERDEC_Emery -n GA_vapor ../irspec02.asc
add_spectrum -f 2 -t "GB (LIQUID) EA0003" -L HyGAS_ERDEC_Emery -n GB_liquid ../irspec03.asc
add_spectrum -f 2 -t "GB (VAPOR) EA0004" -L HyGAS_ERDEC_Emery -n GB_vapor ../irspec04.asc
add_spectrum -f 2 -t "GD (LIQUID) EA0005" -L HyGAS_ERDEC_Emery -n GD_liquid ../irspec05.asc
add_spectrum -f 2 -t "GD (VAPOR) EA0006" -L HyGAS_ERDEC_Emery -n GD_vapor ../irspec06.asc
add_spectrum -f 2 -t "VX (LIQUID) EA0007" -L HyGAS_ERDEC_Emery -n VX_liquid ../irspec07.asc
add_spectrum -f 2 -t "CS (LIQUID) EA0008" -L HyGAS_ERDEC_Emery -n CS_liquid ../irspec08.asc
add_spectrum -f 2 -t "CN (LIQUID) EA0009" -L HyGAS_ERDEC_Emery -n CN_liquid ../irspec09.asc
add_spectrum -f 2 -t "HD (LIQUID) EA0010" -L HyGAS_ERDEC_Emery -n HD_liquid ../irspec10.asc
```

6. Notes on resampling libraries for HyGAS sensors

For HyGAS, resampling of the spectral libraries to the various HyGAS sensors was done manually, because of a problem with the `add_sensor` function in an interim version of

the HIPS code. The interim version did not work correctly with the specific HyGAS spectral libraries, which differed from previous HIPS libraries in ways such as having more spectral channels, being in cm^{-1} wavenumber units rather than μm wavelength units, and not necessarily being arranged in monotonic increasing spectral order. To get around these difficulties, a temporary library was created with spectral resolution characteristics matched for each of the desired HyGAS sensors. The appropriate matched sensor was then added to each temporary library, using the normal HIPS `add_sensor` function. Since there was no change in spectral resolution for this contrived situation of exactly matched sensor and raw library spectrum, the HIPS `add_sensor` function had no problems. The sensor portion of each temporary library was then moved to the appropriate HyGAS spectral library, under the appropriate sensor name.

Manual spectral resampling was done in one of two ways. For the case of matched spectral resolutions, differing simply in wavelength center positions (i.e. for Emery and Rauss, both at 2 cm^{-1} spectral resolution), values for the new sensor band positions were evaluated using a spline interpolation function applied to the original values. For the case of mismatched spectral resolutions (i.e., resampling Rauss from the original 2 cm^{-1} to the reduced resolution of 8 cm^{-1} for the Kroutil sensor), a simple average of four consecutive datapoints was performed. For this case, every four x-values were averaged, giving a resultant 8 cm^{-1} resolution band centered on the Kroutil sensor band centers. For use in a spectral search library, the four corresponding y-values can nearly equivalently be either summed (integrated) or averaged without altering the spectral signature. With HyGAS, and purely for ease of comparison with the original spectra when doing HIPS spectral plots, we chose to use the y-value averages rather than the integral sums.

Numerous batch command files were created to perform the spectral resampling steps required for the various sensors. These files are located in the directories referenced for Tables 7 and 8. These files can be executed as UNIX shell scripts. Any additional executables required by these command files, along with associated source code, are provided with HyGAS. Executables and source files are located in the `~pamo/bin` and `~pamo/src` directories, respectively.

APPENDIX C

HyGAS Simulation Image Cubes

Image cubes with sufficient spectral and spatial resolution for exploitation of the standoff gas scenarios selected for HyGAS were not available at the time of this effort. Therefore, we simulated appropriate image cubes for testing, validation and demonstration of the HyGAS software. (Use of these simulation image cubes with the various HyGAS software routines, demonstrating HyGAS in various application scenarios, is discussed in detail in the *HyGAS User's Manual/Tutorial*, Section 9, Interactive HyGAS.)

The HyGAS simulation image cubes were generated by assigning appropriate spectral information for a simulated HyGAS sensor to each pixel in a simple two-dimensional spatial scene. Included in the scene would be pixels with, and without, the spectral signature of various gases. [We could have constructed a simplistic block diagram image (as was done for an earlier synthetic cube project for this customer); however, we elected to create a more visually appealing and spectrally realistic image by using a real dataset from a multispectral imaging sensor, and assigning simulated hyperspectral signatures instead of the actual multispectral signatures to the various materials present in the scene.]

1. Selecting a spatial scene.

The spatial scene we selected was a Landsat image of an unpopulated and sparsely vegetated island, consisting primarily of natural components, i.e. soil, vegetation and water. From our existing library of local area Landsat images, we selected the small Hawaiian island of Kahoolawe (Figure 1). We selected a relatively cloud-free subset of this image, over the southeast portion of the island (boxed area in Figure 1).

2. Defining the materials present in the scene.

We created a multispectral signature model (a spectral mixture model) of this scene using a spectral Linear Mixing Model (LMM) algorithm. We processed the selected subset image of SE Kahoolawe, with six Landsat spectral bands (visible through near infrared), using the HIPS LMM algorithm and the interactive HIPS function STARS.[1] The interactive STARS procedure allows the user to select appropriate spectral endmembers representative of the various spectrally distinct materials available in the scene. The function then generates a corresponding model of the scene by combining solely these endmembers in a linearly additive fashion. For each spectral endmember, a fractional image plane is generated, representing for each pixel the percentage composition attributed to that particular endmember. A sum of all the fractional image planes should total 100 percent for each individual pixel. A residual image also is calculated, to display the difference between the calculated model and the original dataset.

A common method of selecting spectral endmembers is to start with two endmembers, review the resulting residuals to determine how best to revise the existing endmembers or add new endmembers, and then iterate on this procedure. A model with the fewest endmembers required to yield a reasonably randomly patterned residual image is the recommended iteration stopping point. The maximum number of endmembers cannot

[1] Spectrometric Target Analysis and Recognition System

exceed the quantity one greater than the number of available spectral bands; however, fewer endmembers can often model the scene adequately.

Typically, a representative bright and a representative dark pixel are selected as the first two spectral endmembers. These are often the pixel uniformly brightest, and the pixel uniformly darkest, in all available spectral channels. To a first order, the uniformly dark pixel represents a basic shade component, which can be added in various percentages to any pixel, to change its overall apparent albedo without altering its spectral signature. The uniformly bright pixel, again to a first order, represents any dominant spectral signature, if only in terms of being the brightest albedo. (In a case such as ours, where there is contamination by, for example, a bright cloud, a uniformly bright pixel in an uncontaminated region should be selected instead of the contaminated pixel.)

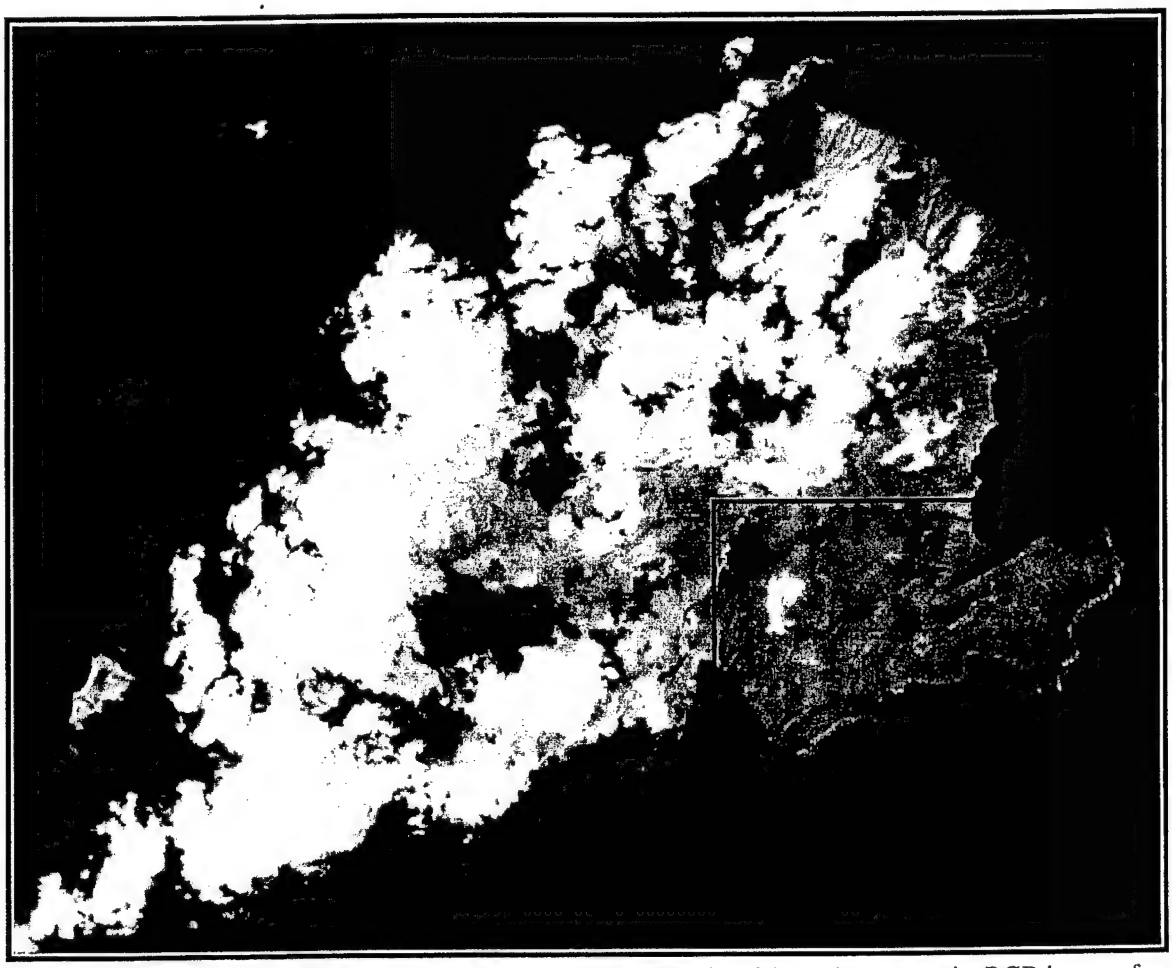

Figure 1. Landsat view of Kahoolawe, 5 January 1989. This is a false-color composite RGB image of Kahoolawe (a dry, uninhabited island in the Hawaiian Island chain). Three Landsat bands (bands 4, 5 and 2, arbitrarily scaled from 12–50, 5–70 and 20–100 DNs, respectively) are combined to form the false-color RGB image. For the simulated HyGAS image cube, we selected the relatively cloud-free SE area of the island (red box, 240 x 150 pixels). This area is composed primarily of natural elements— soil, vegetation and water.

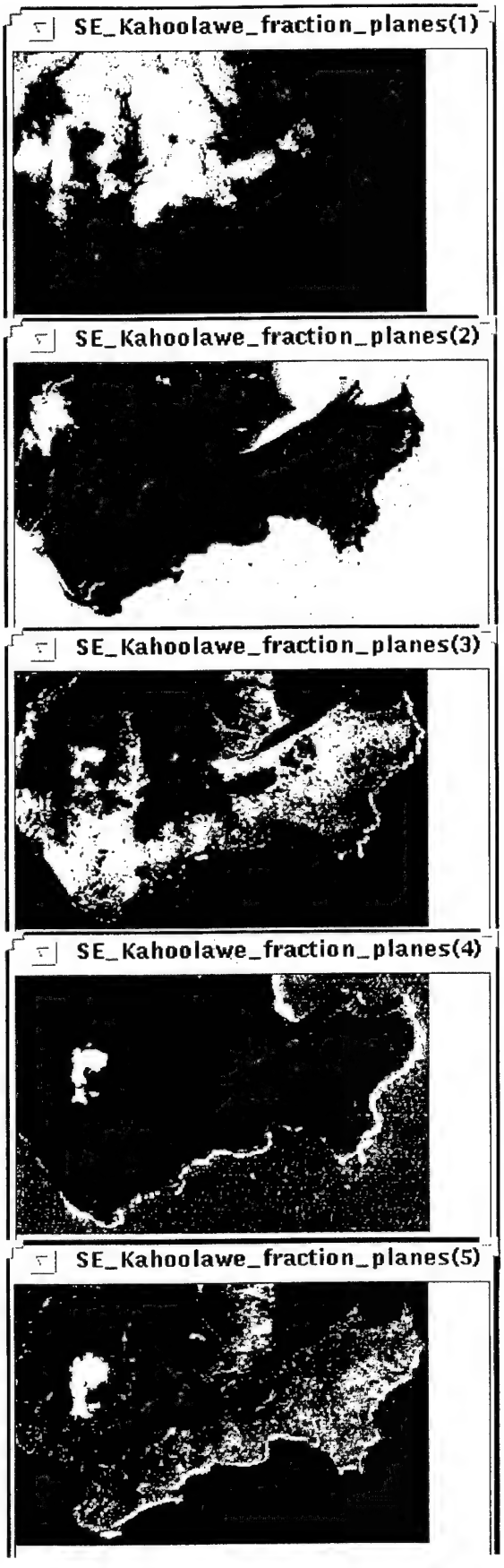

Figure 2 (left). Fraction planes from Linear Mixing Model (LMM) representing the various spectral endmembers selected to model the simulated image cube for HyGAS. The LMM function in HIPS was used to select representative spectral endmembers for this scene. From top to bottom are fraction planes representing (1) bright, red soil, (2) dark water/shade, (3) generic vegetation, (4) bright shoreline component, and (5) an additional darker soil or vegetation component. In each fraction plane, bright represents a higher percentage of the specific material. (Each fraction plane is displayed over the same range, 0–1 display minimum to display maximum, representing 0% to 100% fractional composition.) Although not necessarily representative of physical reality, these endmembers represent an approximation suitable for creating a synthetic image cube for use with HyGAS. Note the cloud and its shadow (apparent in fraction plane 2 as a dark patch and a bright patch, respectively), and how it appears as a bright or dark anomaly in each fraction plane.

Figure 3. False-color fraction plane image for simulated HyGAS image cube. For this composite, the first three fraction plane images (soil, vegetation and water) were combined into a single RGB color image. A fraction plane image such as this is useful to emphasize the spatial distribution of the various endmembers. Since only three endmembers can be combined at any one time in a simple RGB image, some false impressions can occur because of the excluded endmembers.

For our scene, we selected our first two endmembers as (1) a bright non-cloud pixel in a region that appeared in the false color RGB image as reddish soil (red kaolinitic clay soils are very common in the arid upland plateau regions of Hawaii), and (2) the uniformly darkest pixel in the scene. Iteratively selecting endmembers, based on the appearance of the residual image and an *a priori* assumption about the native materials appropriate for the scene (various soils, sparse vegetation and water), we selected three additional endmembers to model our specific scene: (3) a likely vegetation endmember, occurring on upper slopes and in valleys, (4) a bright shoreline component (possibly beach sand, white water or sea foam), and (5) a darker lower slopes component (most likely, a different type of soil or a different type of vegetation). Fractional image planes for all five endmembers are shown in Figure 2.

A false-color RGB composite image using the first three endmembers (soil, vegetation and water) is shown in Figure 3. Fraction plane images displayed in this manner are often used to emphasize the spatial location or spatial distribution of one or more specific endmembers. While not necessarily a complete picture (using only three colors to represent five endmembers), this picture certainly highlights the regions of red soil, green vegetation and blue water.

3. Defining simulated hyperspectral signatures for selected materials

Once the spectral endmembers have been determined from the multispectral scene, appropriate hyperspectral signatures must be defined for each endmember. A recombined image cube can then be constructed using this new spectral information and the appropriate fraction plane images for each spectral endmember. The new image cube will contain the same spatial characteristics as the Landsat image, but will have a simulated hyperspectral sensor response function appropriate for gas applications, instead of the original broadband response functions of the six Landsat bands.

Simulated hyperspectral signatures for each endmember were approximated to match both types of field data supplied to us (GFI) for use with HyGAS, namely (1) the Rauss_Howden field data, and (2) the Kroutil_MIDAC field data.

The Rauss_Howden field data [presumably] came from an experiment by E. Howden of NVEOD, using a point sensor FTIR spectrometer. An example of selected background spectra from this field spectrometer is shown in Figure 4. These spectra cover the spectral range 833–1265 cm^{-1} at 2 cm^{-1} resolution, with 449 data points each.

The Kroutil_MIDAC field data came from an experiment by R. Kroutil of ERDEC, using a MIDAC point sensor FTIR spectrometer. An example of a background interferogram from this spectrometer (prior to performing the FFT) is shown in Figure 5. These interferograms contain 1024 data points each. An example of the corresponding spectrum (calculated by performing an FFT on the example interferogram) is shown in Figure 6. These spectra cover the spectral range 0–1971 cm^{-1} at 8 cm^{-1} resolution, with 512 data points each. [Much of this spectral range, however, is outside the region of sensitivity of the sensor (roughly 600–1600 cm^{-1}). For example, only 113 data points fall within the corresponding spectral region (833–1265 cm^{-1}) for the Rauss_Howden sensor.]

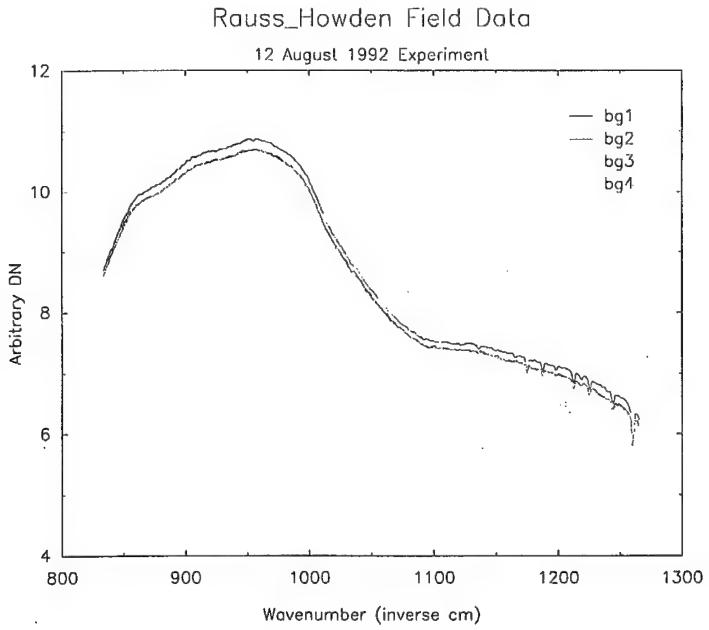

Figure 4. Example Rauss_Howden field sensor datasets. Example background datasets (bg1–bg4) from the Rauss-Howden field sensor (from experiments on 12 August 1992) are shown. In general, these spectra represent the overall blackbody radiation emitted by the background, uncontaminated by any target gases. Spectral absorptions caused by the intervening atmosphere in the optical path between the sensor and the background are present, however. All spectra were supplied (GFI) in SpectraCalc format, as 449-data point spectra over the spectral range 833–1265 cm^{-1} wavenumbers, at 2 cm^{-1} resolution (Nyquist sampling of 1 cm^{-1} data point spacing); spectra were translated into JCAMP and ASCII_XY format using the GRAMS software package, for incorporation into HyGAS.

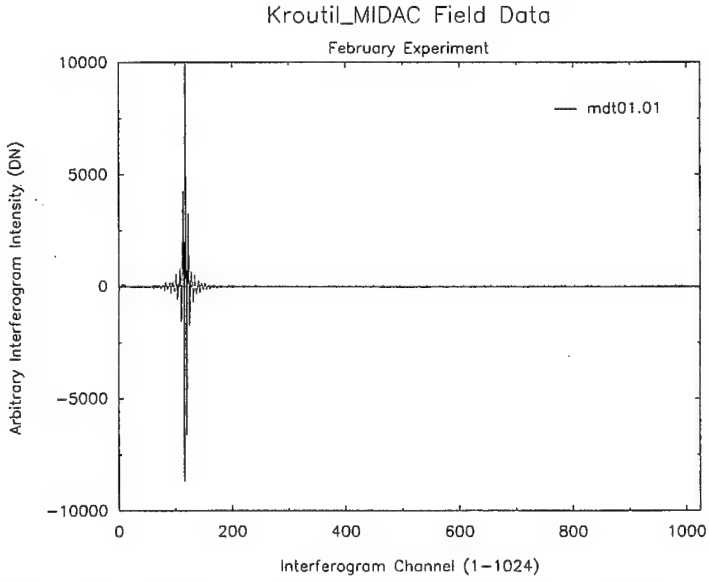

Figure 5. Example Kroutil_MIDAC field sensor dataset in original interferogram domain. An example background dataset (mdt01, record #1) from the Kroutil_MIDAC field sensor (from experiments in February, of undetermined year) is shown. This is an example interferogram from an FTIR spectrometer, showing the strong centerburst intensity response typical for a broadband thermal source. The broadband source in this case is the overall blackbody radiation emitted by the background, uncontaminated by any target gases. These datasets (1024-data point interferograms) were supplied in binary format, readable by the *pcida* software supplied (GFI) by Kroutil. (The corresponding spectrum generated from this interferogram is shown in Figure 6.)

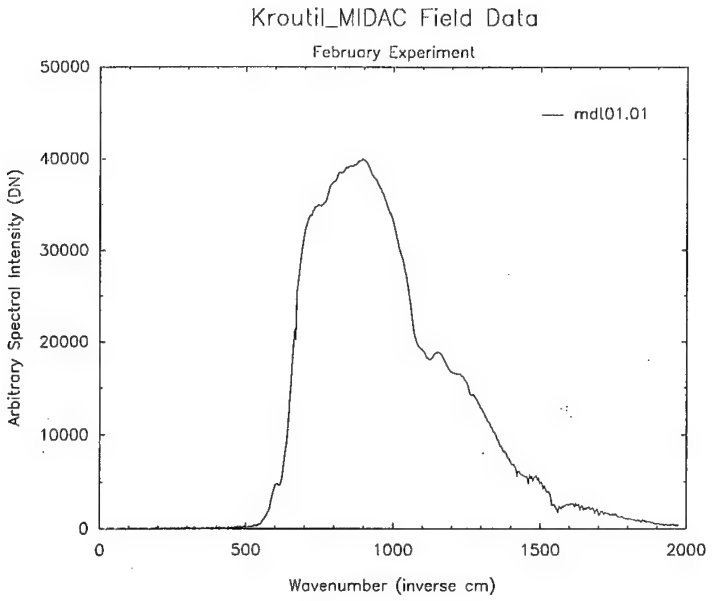

Figure 6. Example Kroutil-MIDAC field sensor dataset in transformed (FFT) spectral domain. The spectrum shown here was generated from the interferogram above (Figure 5), using the *pcida* software supplied (GFI) by Kroutil. This spectrum represents the overall blackbody radiation emitted by the background, uncontaminated by any target gases. Spectral absorptions caused by the intervening atmosphere in the optical path between the sensor and the background are present, however. Interferograms from this sensor are converted by *pcida* into spectra with 512 data points covering the spectral range 0–1971 cm^{-1} wavenumbers, at 8 cm^{-1} resolution (Nyquist sampling of 4 cm^{-1} data point spacing). The spectral region below 500 cm^{-1} falls outside the region of the responsivity of the sensor, and therefore lies near zero intensity.

The datasets for both experiments were supplied to us with no additional information regarding the sensor or the experimental setup. Given this situation, we made several assumptions in order to use these datasets as the basis to generate simulated hyperspectral signatures for the selected spectral endmembers.

For each experimental setup, the basic measurement setup represents passive thermal measurements of the respective field background. (Passive measurements use no added artificial source; the radiating field background *is* the thermal source.) These measurements, to a first order, are simply a function of the thermal background temperature (modified by the emissivity characteristics of the specific background material), the transmission characteristics of the intervening atmosphere between the source (the thermal background) and the sensor, and the overall spectral response function of the sensor. [No target gases are present in the intervening optical path for any dataset selected as a field background; however, the intervening atmospheric constituent gases (primarily nitrogen, oxygen, argon and water vapor, along with a host of minor constituents) function as absorbing gases since the atmosphere is usually slightly cooler than the ambient field surface background.]

If the spectral response function of the sensor (i.e., gain and offset) and the characteristics of the intervening atmosphere (i.e., optical path-length) are not known, their combined effect can be approximated by estimating the temperature and the emissivity of the background and comparing these values to an actual background measurement. [The spectral emissivity of a surface is defined as the ratio of the radiance emitted by the surface to that emitted by a blackbody of the same temperature.]

Essentially, the measured data number (DN) generated by the instrument is the sum of the instrumental offset (bias) and the product of the instrumental gain and the radiance at the sensor (L_s).

$$\mathrm{DN} = \mathrm{offset} + (\mathrm{gain} \times L_s) \tag{1}$$

The radiance at the sensor is the product of the emissivity (ε_s) of the surface material, the blackbody radiance (B_s) of the same temperature, and the transmission (τ_{atm}) of the intervening atmosphere.

$$L_s = \varepsilon_s \times B_s \times \tau_{atm} \tag{2}$$

This translates to

$$\mathrm{DN} = \mathrm{offset} + (\mathrm{gain} \times \varepsilon_s \times B_s \times \tau_{atm}) \tag{3}$$

or, combining the factors representing the sensor response function and the atmosphere,

$$\mathrm{gain} \times \tau_{atm} = (\mathrm{DN} - \mathrm{offset}) / (\varepsilon_s \times B_s) \tag{4}$$

The instrumental offset (usually a bias voltage applied to the A/D converter to register a very small positive voltage under conditions of zero signal input) can be assumed to be roughly constant for all wavelengths, for a constant bandwidth sensor. This value can be estimated from the instrumental output (DN) from a spectral region with little or no signal received at the sensor (i.e. shortwards of 500 cm^{-1} in Figure 6). If such data is not available, as for the Rauss_Howden sensor, this offset can only be assumed to be negligible. The combined atmosphere-sensor factor then simplifies to

$$\mathrm{gain} \times \tau_{atm} = \mathrm{DN} / (\varepsilon_s \times B_s) \tag{5}$$

For an opaque material (absorption only, no transmission), the spectral emissivity (ε_s) is related to the hemispherical spectral reflectance (ρ_s), by means of Kirchhoff's law,

$$\varepsilon_s = 1 - \rho_s \tag{6}$$

Substituting Eq. 6 into Eq. 5 yields

$$\mathrm{gain} \times \tau_{atm} = \mathrm{DN} / ((1 - \rho_s) \times B_s) \tag{7}$$

The DN in Eq. 7 is obtained from the spectral measurements of the field background (Figure 4 and Figure 6).

The field background is assumed to be grass, which can be represented by any generic grass for which the spectral reflectance properties (ρ_s) are known (Figure 7).

The temperature for Eq. 7 is estimated qualitatively by comparing the raw spectral measurements of the field background to a Planck blackbody function at a temperature appropriate for each experiment. The Rauss_Howden dataset was collected during the summer; the Kroutil_MIDAC dataset was collected during the winter. Figure 8 shows the relative spectral emittance for a blackbody at an estimated summer temperature of 300K (80° F, 27° C) and at an estimated winter temperature of 273K (32° F, 0° C). Plotted on the same scale are the calculated spectral radiance for grass at each temperature, and the corresponding field backgrounds for the Rauss_Howden and Kroutil_MIDAC experiments—all intensities are scaled relative to the peak spectral radiance for a blackbody at 300K.

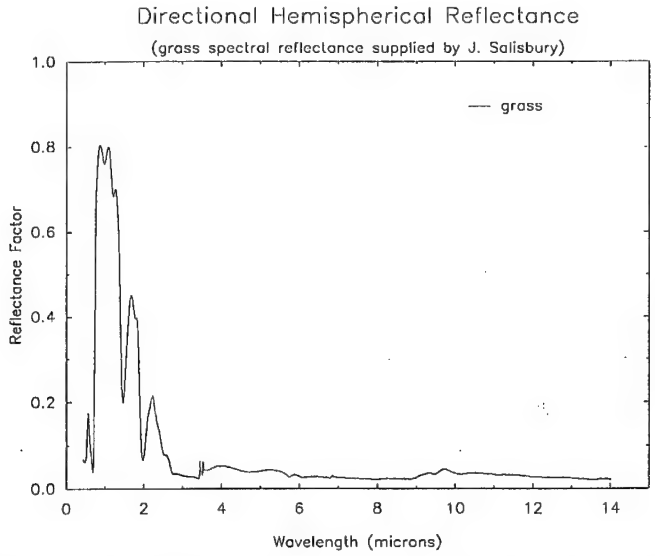

Figure 7. Hemispherical reflectance for grass. The directional hemispherical spectral reflectance for grass was provided by J. Salisbury (private communication). This generic grass can be used as a rough approximation of the background material for each of the field experiments, for purposes of determining the emissivity of the field background from the hemispherical reflectance using Kirchhoff's law.

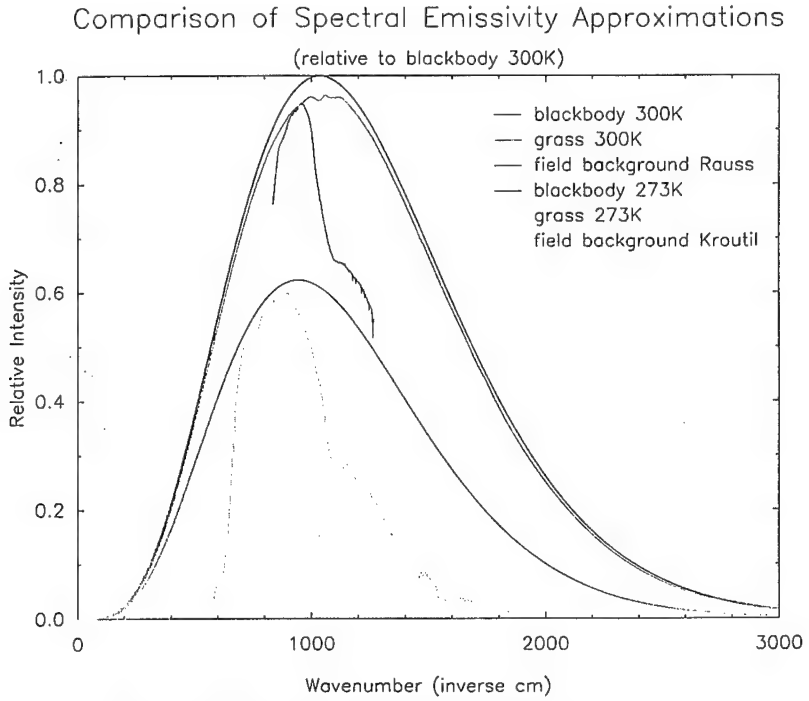

Figure 8. Comparison of Spectral Emissivity Approximations. The spectral radiance for a blackbody at 300K and at 273K are scaled to the maximum spectral radiance for the blackbody at 300K. These temperatures, selected as appropriate for summer and winter, best matched a rough convex-hull approximation of the raw background spectra from the Rauss_Howden and the Kroutil_MIDAC experiments. The spectral radiance for grass at these same temperatures also is plotted, similarly scaled to the blackbody at 300K. The raw background spectra are arbitrarily scaled to match the appropriate temperature grass background.

These temperatures were selected to match the *shape* of the background spectra near the peak spectral response—we estimated a convex-hull approximation for the raw spectra over a small region near the peak response, selected a blackbody temperature appropriate

for the season, and then altered this temperature by increments of 5° C to select the temperature with the best match to this shape. The initial temperature estimates of 300K and 273K appeared to be the closest matches. [Theoretically, the Wien Displacement Law can be used to determine the temperature of a blackbody source from the wavelength corresponding to the peak of the spectral radiation curve; however in practice, the spectral shape of the atmospheric transmittance in this spectral region, along with the spectral response function of the sensor, can skew the wavelength position of the apparent maximum of the measured radiation, resulting in erroneous estimates of temperature.]

As shown in Figure 8, the deviation between a blackbody emitter and the actual measured background is more a function of the transmission of the atmosphere and the sensor response than of the emissivity of the background material. The ratio of the measured DN to the calculated radiance of the background at the appropriate temperature, i.e. the combined atmosphere-sensor factor as specified by Eq. 7, is shown for the Rauss_Howden simulation in Figure 9, and for the Kroutil_MIDAC simulation in Figure 10. Figure 11 superposes both factors on a single plot, scaled to unity at the maximum value.

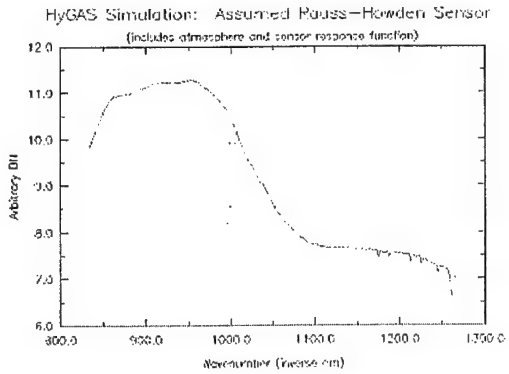

Figure 9. Combined sensor-atmosphere factor for Rauss_Howden simulation. This factor was calculated using Equation 7, substituting the measured DN of `bg3` (Figure 4), the spectral reflectance of grass (Figure 7), and an estimated temperature of 300K.

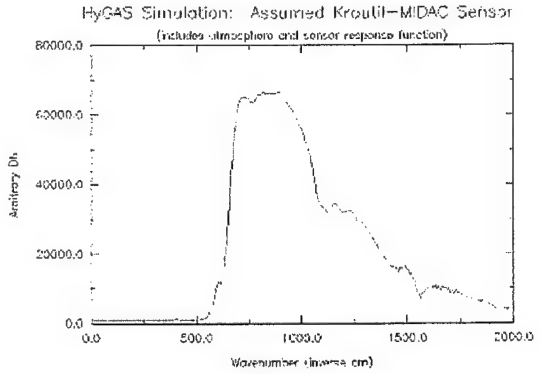

Figure 10. Combined sensor-atmosphere factor for Kroutil_MIDAC simulation. This factor was calculated using Equations 4 and 6, substituting the measured DN of `mdt01_01` (Figure 6), an estimated offset value of 75 DN, the spectral reflectance of grass (Figure 7), and an estimated temperature of 273K.

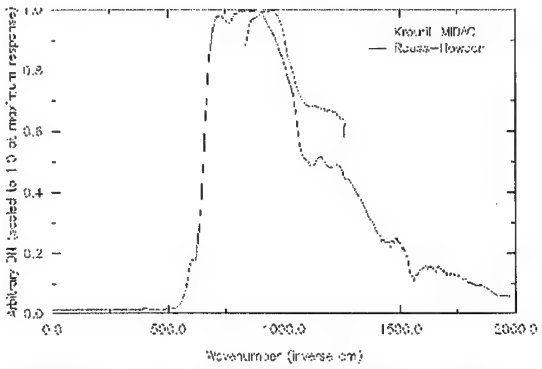

Figure 11. Comparison of combined sensor-atmosphere factors for both simulations. The plots of Figures 9 and 10 are scaled to unity at maximum response and superposed for comparison.

Once the combined sensor-atmosphere factor (and offset, if appropriate) has been determined for each experiment, estimated DN values (i.e. hyperspectral signatures) at whatever temperatures are desired can be calculated for any material whose spectral reflectance is known, by combining Equations 3 and 6.

Spectral reflectance values for the five materials selected to represent the five endmembers are shown in Figure 12. Corresponding emissivity values (over the 8–12 μm spectral region only) are detailed in Figure 13.

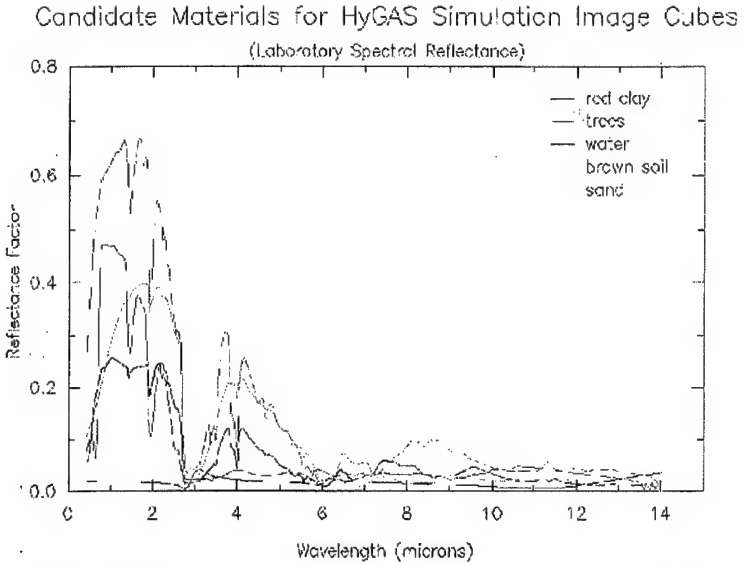

Figure 12. Hemispherical reflectance values for spectral endmembers selected for use in HyGAS simulation image cubes. Candidate materials with existing hemispherical reflectance spectra were selected to represent each of the five spectral endmembers defined from the Landsat multispectral image subset of Kahoolawe. These materials were selected from various in-house databases. Three materials came from the Spectral Library: red clay (0150UUUSOL), sand (0454UUUSOL) and brown soil (0216UUUSOL), representing endmember 1, bright red soil; endmember 4, bright shoreline component; and endmember 5, darker soil. [Sample 0150UUUSOL is a reddish brown silty clay, representing a suitable analog for the bright red kaolinitic clays characteristic of the arid upland plateau regions of Hawaii. Sample 0454UUUSOL is a light brown sandy soil with high carbonate content, representing a suitable analog for a calcareous beach sand mixed with kaolinitic clay. Sample 0216UUUSOL is a gray silty clay with some montmorillonitic and kaolinitic clays mixed with some minor darker organic material; this represents a suitable analog for a soil near vegetation. Although these samples were selected for their spectral variability and approximate composition, their actual composition and relation to physical reality have no impact on their function in the simulated image cube.] Water and vegetation came from separate databases (GFI from J. Salisbury), for endmembers 2, water; and endmember 3, vegetation. [The water spectrum we used is the same dataset available in the NEF database; the vegetation spectrum is a sample of sugar maple. Again, the actual composition of the vegetation and its relation to physical reality have no impact on the function of vegetation in the simulated image cube.]

For simulated image cubes for HyGAS, we selected an estimated base temperature of 300K for all materials except water/shade, which we selected to be 5° C cooler (295K). Calculated radiance values using these temperatures are shown for all five endmembers (along with a reference blackbody at 300K) in Figure 14. [For HyGAS simulations, we made the gross assumption that the combined factor representing the sensor response and the atmosphere is constant across the simulated scene.] These same materials are shown corrected to the sensor-atmosphere function for a Rauss_Howden sensor (Figure 15) and a Kroutil_MIDAC sensor (Figure 16). Corresponding interferograms for the Kroutil_MIDAC sensor are shown at full scale in Figure 17 and expanded in Figure 18.

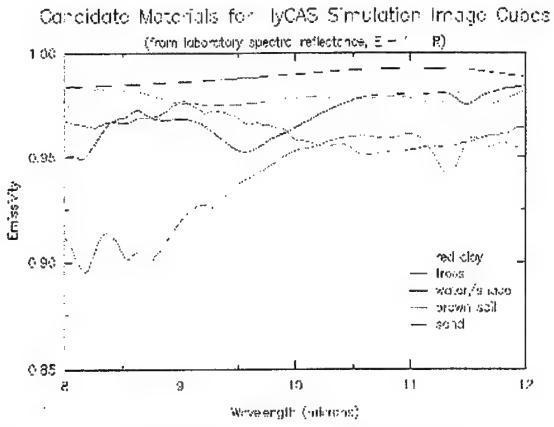

Figure 13. Emissivity values for selected endmember materials. The emissivity values are derived from the spectral reflectance values shown in Figure 12. Only the 8–12 μm spectral region is displayed.

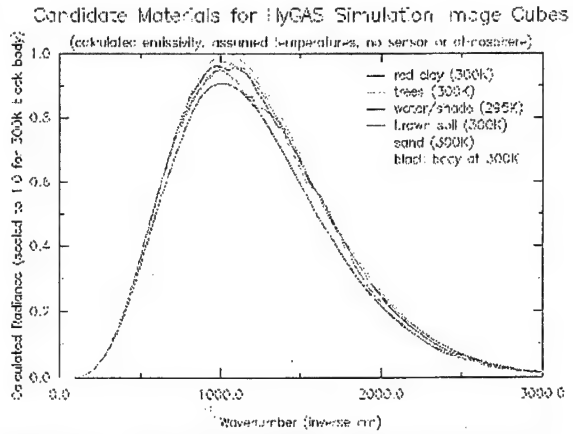

Figure 14. Calculated radiance for endmember materials for HyGAS simulations. All materials were assumed to be 300K except water/shade at 295K. A 300K blackbody is plotted for reference. All values are scaled to unity at the peak response for the 300K blackbody emitter.

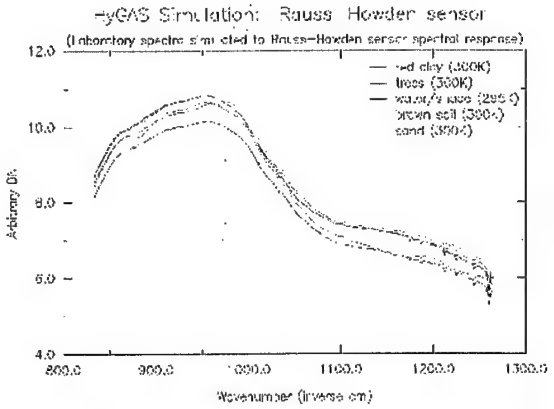

Figure 15. HyGAS endmembers for simulated Rauss_Howden sensor.

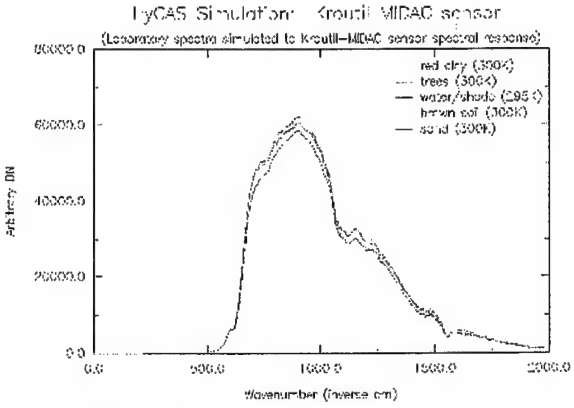

Figure 16. HyGAS endmembers for simulated Kroutil_MIDAC sensor, spectral domain.

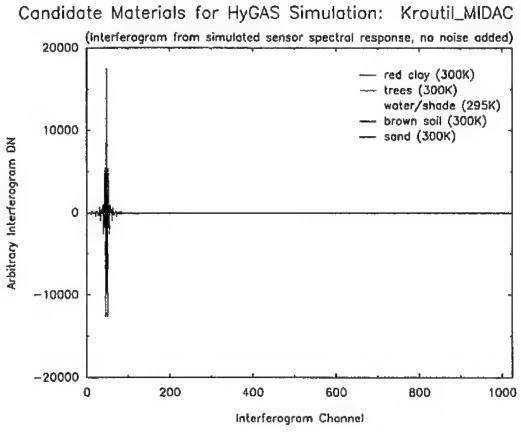

Figure 17. HyGAS endmembers for simulated Kroutil_MIDAC sensor, interferogram domain.

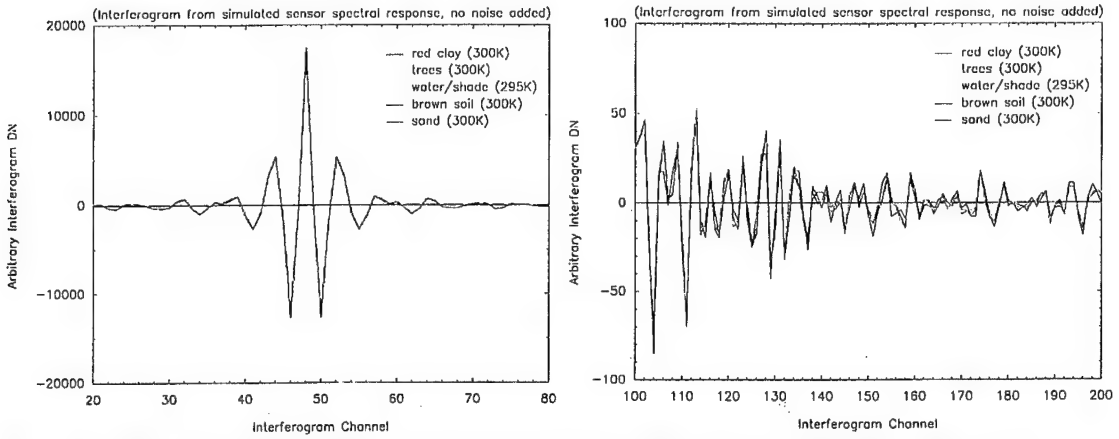

Figure 18. HyGAS endmembers for simulated Kroutil_MIDAC sensor, interferogram domain expanded. Differences in the interferograms for endmembers are slightly more distinguishable further out in the interferogram wings (right) than near the centerburst (left).

It should be noted that these interferograms (Figures 17 and 18) are modeled with a centerburst response at channel 48, compared with a centerburst response at channel 116 for the earlier interferogram example (Figure 5). A centerburst at channel 48 was selected to match the dataset *kft001.dat* supplied for testing with associated linear discriminants. [The discriminant test operates on a small subset of the full 1024-point interferograms; this subset is specified in channel space limits relative to the centerburst channel. For this reason, the position of the desired output centerburst is one of the input specifications required for the spectrum-to-interferogram function in HyGAS.]

It also should be noted that these calculated interferograms (Figure 17, 18), representing *ideal* interferograms, are symmetric about the centerburst, unlike actual measured interferograms (Figure 5), which are asymmetric. This measurement error, called phase error or sampling error, is usually corrected by comparing the shape of a measured interferogram on both sides of the centerburst, and estimating a corrected interferogram that is truly symmetric about the centerburst. This symmetric interferogram is then processed to generate the corresponding spectrum. For HyGAS simulations, we used the calculated symmetric interferograms, without any simulated sampling error.

4. Recombining hyperspectral endmember signatures into a synthetic image cube

Once hyperspectral signatures were generated for all five endmembers for both the Rauss_Howden and the Kroutil_MIDAC sensors (Figure 15 and Figure 17), we proceeded to create a simulated HyGAS hyperspectral image cube for each sensor by recombining the appropriate set of hyperspectral endmembers according to the previously defined fraction planes (Figure 2). A special command-line-only HIPS function (*simcub*) was created to generate these image cubes, given an appropriate hyperspectral endmember file for each sensor and a fraction plane image cube. [Command files, executable as UNIX shell scripts, to generate these cubes were supplied with HyGAS—`do_simcub.rauss` and `do_simcub.kroutil` in the directory `~HyGAS/simulations/cubes/xstuff`.]

To simulate potential variations due to instrumental noise, next we estimated a noise level from the DN variation between two comparable background measurements for each sensor. For the Rauss_Howden sensor, we estimated the average (~peak to peak)

difference in spectral domain at ±0.025 (floating point DN values); for the Kroutil_MIDAC sensor, we estimated this difference in interferogram domain at ±4 (integer DN values). We then used the `create cube` function in HIPS to generate a random number pattern "noise" image cube, evaluated within this DN range, which we added to each "no_noise" image cube to estimate a revised image cube for each sensor.

5. Adding gas signatures into the synthetic image cubes

We created an arbitrary spatial overlay map for the SE_Kahoolawe scene to simulate the presence of various gas clouds. Four large clouds were created with four contour levels each, and four smaller clouds with one contour level each. We used the HIPS display function `create mask` to sketch in the proposed spatial distributions for the gases as shown in Figure 19.

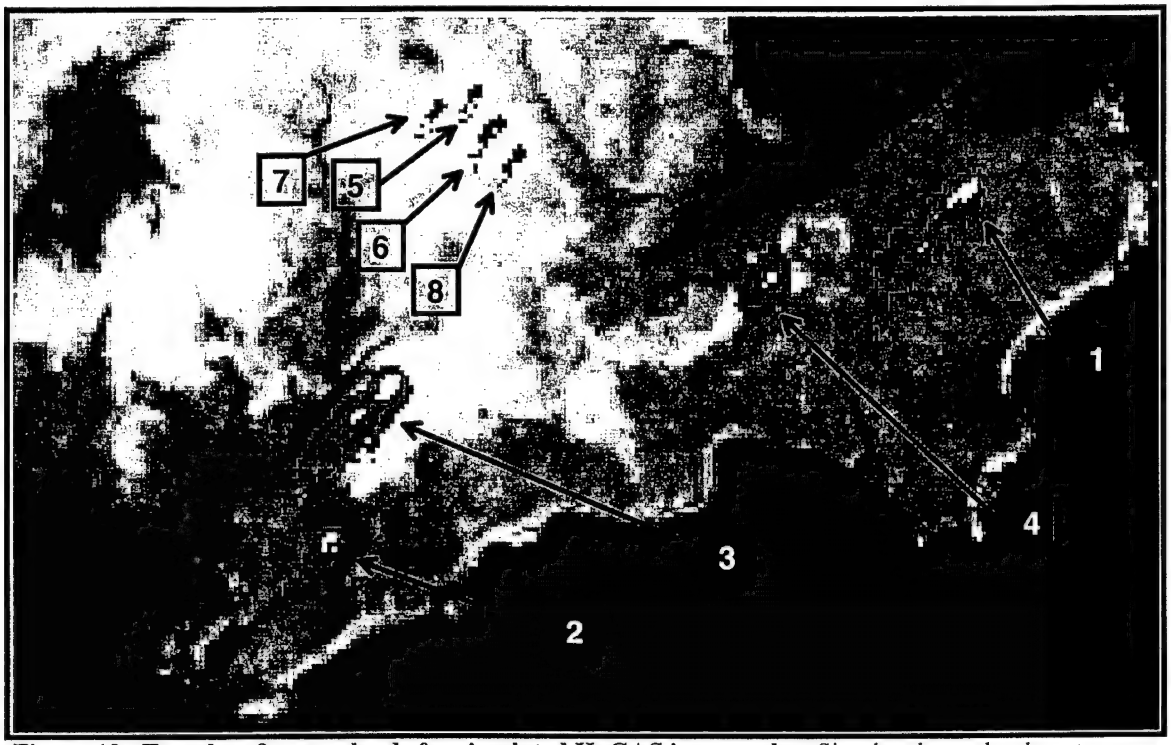

Figure 19. Template for gas clouds for simulated HyGAS image cube. Simulated gas cloud contours were created for inserting gases into the simulated HyGAS image cube. Four clouds with four contour levels, and four smaller clouds with a single contour level, were created. These contours represent a simulated dispersion with a prevailing wind pattern (light NE trade winds). Table 1 identifies the gases inserted into the clouds referenced by number here.

For each sensor, we selected two gases to insert into the scene, with each gas represented under both absorbing (gas colder than the background) and emitting (gas hotter than the background) conditions. Three common gases were used in the Rauss_Howden and the Kroutil_MIDAC experiments— sulfur hexafluoride (SF_6), acetone and methyl-ethyl-ketone (2–butanone, or MEK). All three gases were released during the Rauss_Howden field experiment; only SF_6 was released in the Kroutil_MIDAC field experiment. [Sulfur hexafluoride is a non-toxic gas, commonly used as a long wave IR marker gas, with a single very strong and narrow absorption at ~10.6 μm (940 cm^{-1}). Acetone and MEK are common solvents with relatively low vapor pressure, also with fairly strong and narrow vapor phase absorptions, at ~8–9 μm (1150–1250 cm^{-1}). Acetone also is used in copious

amounts in the chemical production of cocaine, and has related potential in demonstrating one commercial application of HyGAS.]

5.1 Acetone and Sulfur Hexafluoride

Since only acetone and sulfur hexafluoride were included in the Sprouse spectral database, we selected these two gases for insertion into the scene for both simulations. Table 1 indicates which gas was inserted into each cloud identified by number in Figure 19. Spectral absorbance values for acetone and sulfur hexafluoride (from the Sprouse database) are shown in Figure 20.

Table 1. Identification of gases inserted into each cloud numbered in Figure 19.

Large cloud	Small cloud	Gas Inserted	Absorption/Emission
1	5	Acetone	Absorption
2	6	Sulfur hexafluoride	Absorption
3	7	Acetone	Emission
4	8	Sulfur hexafluoride	Emission

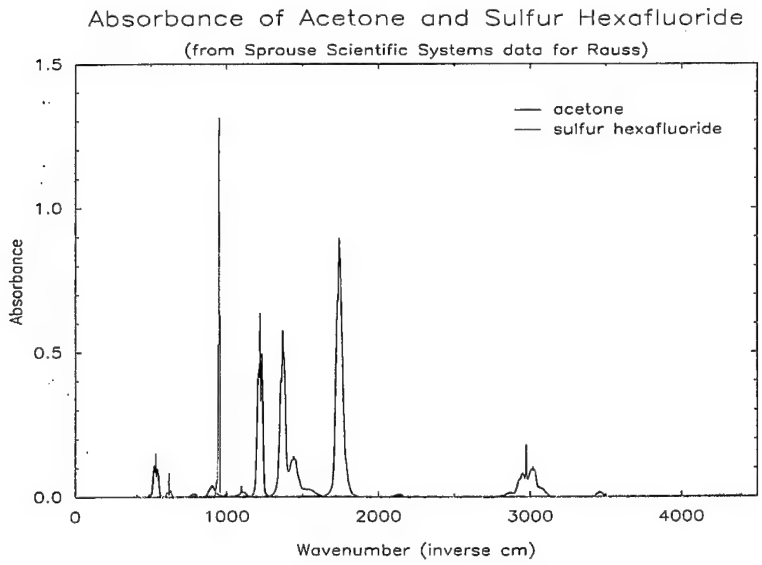

Figure 20. Absorbance for Acetone and Sulfur Hexafluoride. These laboratory spectra, measured by Sprouse Scientific Systems under contract to Rauss, were supplied to us (GFI) for use with HyGAS. Rauss needed measurements suitable for quantitative applications, i.e., gases measured at known concentration, at $2cm^{-1}$ resolution, and at roughly ambient temperature and pressure. These measurements were presumably done using a 1-meter length gas-cell. Header information included with the data cite a temperature of 25° C and concentrations of 146 ppm for acetone and 5.01 ppm for sulfur hexafluoride.

For HyGAS, we elected to treat the Sprouse absorption spectra for acetone and sulfur hexafluoride as appropriate relative absorptions for these two gases. We also elected to ignore any quantitative implications related to temperature, pressure, concentration and optical path-length, and elected simply to consider the total absorbance, i.e., the combined product of the absorption coefficient, the concentration and the optical path-length (Beer's Law). In effect, we elected to assign arbitrary amounts of radiance contributions because of the gas, and treat the gas as simply an additive (emission) or subtractive (absorption)

effect on the radiance of the underlying background reference. [This approximation is the basis of the classic approach of measuring the background reference with the unknown target gas in the intervening optical path, along with a basic background reference with no target gas in the intervening optical path, and subtracting the measurements of the background-alone from the background-with-gas to calibrate the measurements of the unknown target gas. With adequate background removal, a measurement containing a target gas calibrated in this way approximates the laboratory absorbance spectrum of the target gas alone.]

To approximate estimated radiance contributions from gases for realistic scenarios, and to compare with the supplied field data from the Rauss_Howden experiment and the Kroutil_MIDAC experiment, we estimated a lower level of detectability at ~1 percent radiance contribution because of a target gas (Kroutil, private communication). We calculated this percent radiance contribution for acetone and sulfur hexafluoride by rescaling the Sprouse database absorbance values for each gas (Figure 20) to unity at the peak for SF_6, and multiplying these values by the radiance DN values predicted for each simulated dataset. We defined the result as 100 percent radiance contribution for each gas. We then multiplied this result by the desired radiance contribution (1 percent) we wanted to be attributed to the gas, and then added (for emission, or subtracted for absorption) this result to the original DN of the background pixel for each pixel contaminated by a gas cloud (Figure 19).

We inserted acetone and sulfur hexafluoride into each simulated cube at a level representing 1 percent radiance contribution because of gas, for the outermost contour level of clouds 1–4, and for all of clouds 5–8, as specified in Table 1. For testing purposes, we specified increasing percentages (10 percent, 50 percent, even an impossibly high 100 percent, purely for tests, assuming the percentages would be reduced to something more reasonable at a later date) for the interior contours of clouds 1–4. [We used the custom HyGAS routine `simmask` to insert the appropriate spectral contributions defined for these gases.] Figures 21 and 22 show representative examples of the 1 percent, 10 percent and 50 percent absorption contributions for both acetone and sulfur hexafluoride for the Rauss_Howden and the Kroutil_MIDAC simulated image cubes. [The effect of the impossibly high 100 percent contribution can be inferred from these figures.] Figure 23 shows a section (channels 100–200) of the corresponding interferograms calculated from these spectra for the Kroutil_MIDAC simulation.

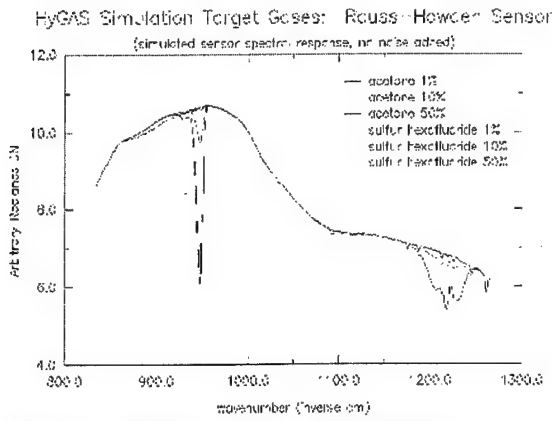

Figure 21. Effect of gas in absorption on Rauss_Howden simulation.

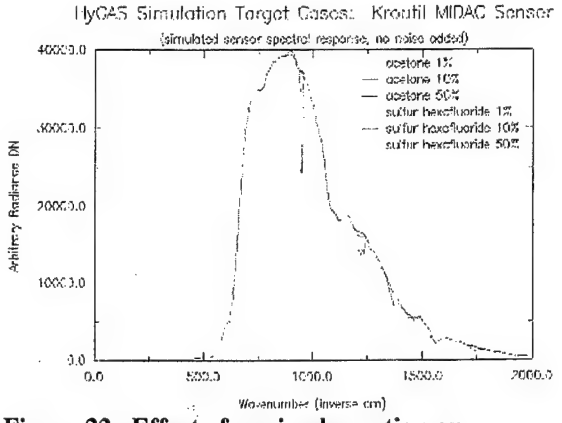

Figure 22. Effect of gas in absorption on Kroutil_MIDAC simulation, spectral domain.

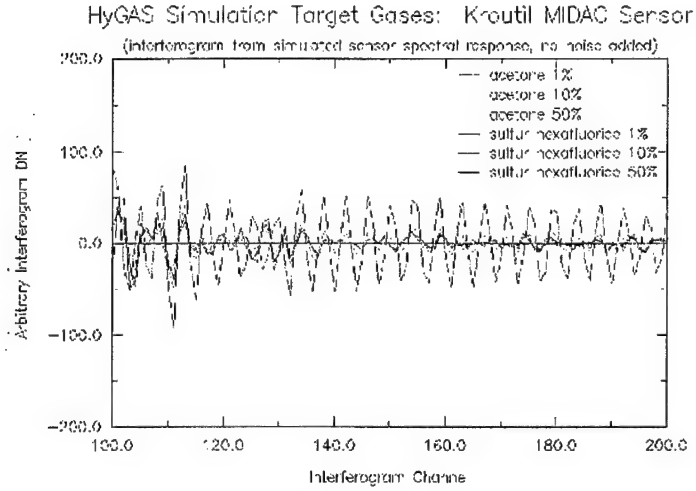

Figure 23. Effect of gas in absorption on Kroutil_MIDAC simulation, interferogram domain.

The effect of a narrow spectral feature on the outer regions of an interferogram is clearly apparent in the strong sinusoidal pattern shown for the 50 percent radiance contribution for SF_6 (Figure 23). This is in marked contrast to the identical interferogram region for the same background with acetone (Figure 24) and the various individual backgrounds with no gas at all (Figure 25). This is the basis of the linear discriminant approach developed by Kroutil to detect specific gases using specific sections of the original interferogram.

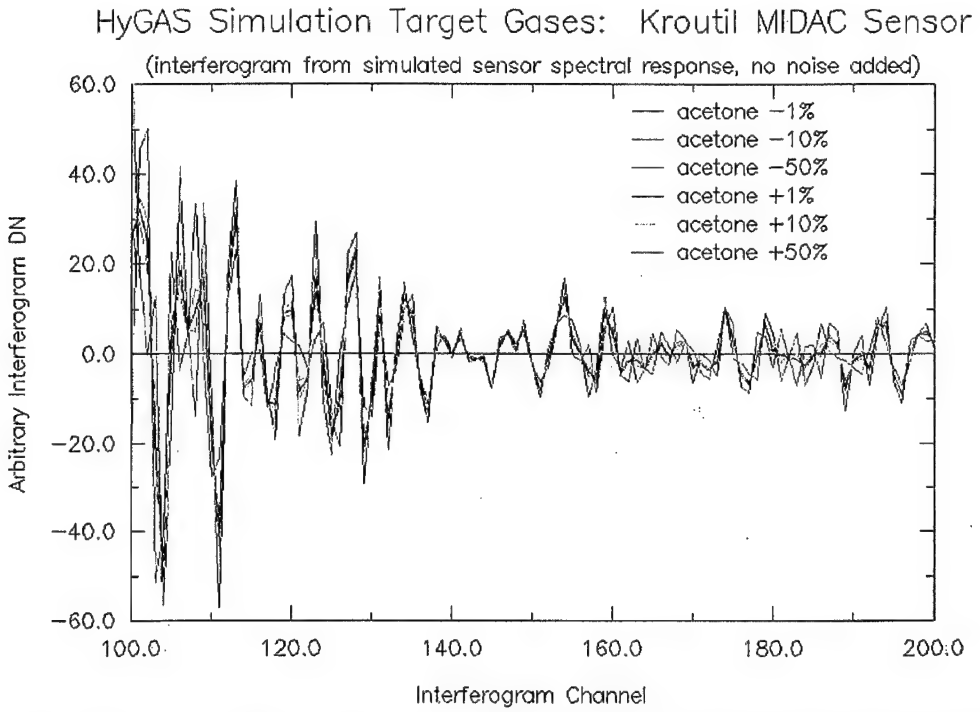

Figure 24. Interferogram subset for background with acetone. The same interferogram channels are displayed as in Figure 23, but the y-axis is expanded.

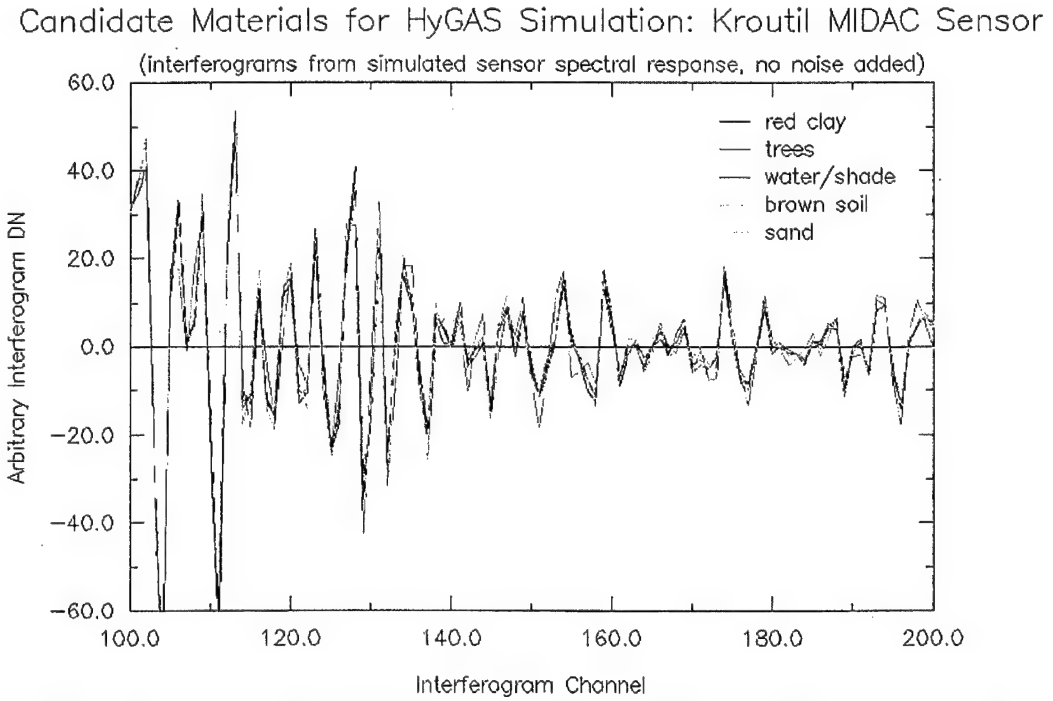

Figure 25. Interferogram subset for backgrounds with no gas. The same interferogram channels are displayed as in Figure 23, but the y-axis is expanded. The y-axis scale here is the same as for Figure 24.

5.2 Methyl-Ethyl-Ketone (MEK)

For the Kroutil_MIDAC simulation, we investigated the possibility of substituting MEK, for which we had a set of discriminant coefficients, for SF_6, for which no discriminants

were available. MEK was not included in the Sprouse database, so we attempted to get a suitable MEK spectrum from the dataset (`kft0001.dat`) provided to us for testing with the MEK discriminants.

This dataset [presumably] represents various laboratory gas-cell measurements, both with and without MEK in the optical path. We selected two measurements from this dataset (records 96 and 97) to represent measurements of a background with no MEK, and a background with MEK (Figure 26). A ratio of these two measurements generated a cursory approximation of the absorbance of MEK, but with significant differences from what we expected for a laboratory measured absorbance. We elected to treat these differences as an inadequate background removal. We then estimated a correction factor as a smooth curve baseline approximation, fit to the points outside the spectral absorptions attributed to MEK (Figure 27). Removing this baseline approximation yielded the estimate of the absorbance spectrum of MEK shown in Figure 28. [Alternatively, we could have assumed the background without MEK and the background with MEK to have been measured at different temperatures, and estimated a correction based on the estimated absolute temperatures; however, for a first approximation, our baseline estimate correction appeared sufficient.]

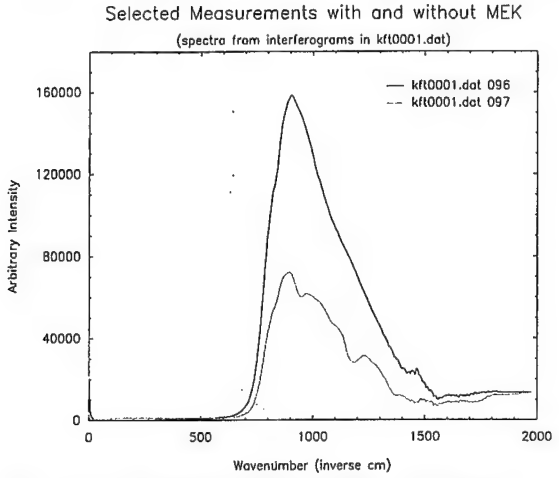

Figure 26. Selected measurements with and without MEK from file `kft0001.dat`. These spectra were computed from interferograms 096 and 097. Record 096 represents measurements of the background source with no MEK; record 097 represents a measurement with MEK.

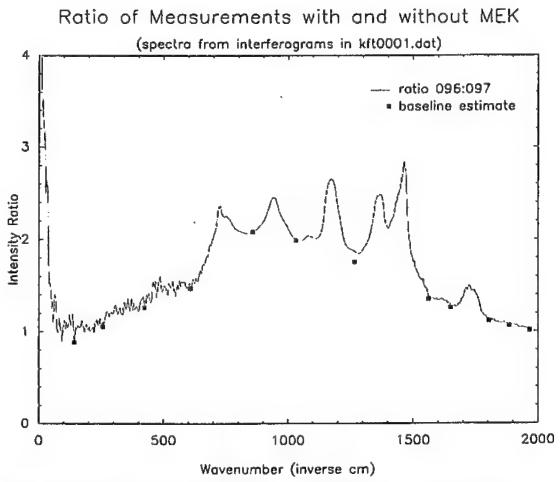

Figure 27. Estimate of baseline correction to initial ratio of background without MEK to background with MEK. We elected to estimate a baseline correction by fitting a smooth curve to the points marked, which we assumed to be outside the absorptions because of MEK.

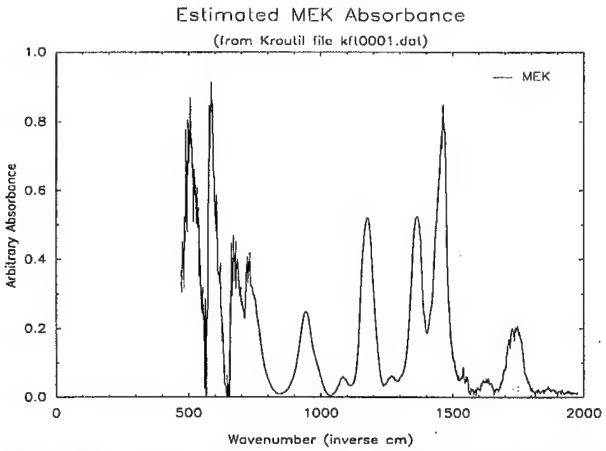

Figure 28. Estimated MEK absorbance spectrum. This estimated absorbance spectrum for MEK was generated by a ratio of spectra computed from interferograms 96 and 97 in the test datafile `kft0001.dat`. The remaining baseline was estimated by fitting a smooth curve to the points presumed to be unaffected by the absorptions because of MEK, and removing this estimated baseline from the calculated ratio. Although noisy in the regions of low original signal, we expect data within the spectral region 800–1500 cm^{-1} to be a fair estimate of the absorbance of MEK, albeit at an arbitrary y-axis scale.

Unfortunately, the provided MEK discriminants did not perform very well on any interferograms computed using this estimated MEK spectrum. We attributed this failure to the strong apparent but erroneous absorptions below 800 cm^{-1}, caused by the low signal levels of the raw spectrum in this region. We tried setting the spectrum for MEK to zero below 800 cm^{-1}, but this failed to improve the performance of the discriminants. We next tried to approximate the spectrum in this region, and also above 1600 cm^{-1}, by comparing it with another absorbance spectrum for MEK (Figure 29).

The comparison MEK spectrum came from the NIST/EPA Gas Phase Infrared Database.[2] This database is supplied as a spectral *search* library, and as such is arbitrarily scaled (on the absorption axis) to unity at the maximum absorption for each individual gas species. This precludes the quantitative use of such a database, or any comparison of the relative intensity of absorptions for different species, although it preserves the qualities required for spectral identification, namely the uniqueness of the positions of the spectral absorptions and their relative intensity within any single species. This database is also supplied at 12 cm^{-1} resolution, which would have to be resampled to a *higher* resolution (violating the Nyquist rule) to be used with the Kroutil_MIDAC simulation. In regions with no significant spectral absorptions approaching the Nyquist resolution limit, however, resampling to a higher resolution is reasonable. To correct the problem, spectral regions in the estimated MEK spectrum from `kft0001.dat` (Figure 28), we resampled the NIST/EPA spectrum of MEK to 8 cm^{-1} resolution, and substituted this resampled NIST/EPA spectrum for the `kft0001.dat` spectrum shortwards of 850 cm^{-1} and longwards of 1790 cm^{-1}. A comparison of the `kft0001.dat` and NIST/EPA spectra for MEK, along with the combined version, is shown in Figure 29.

Unfortunately, the supplied MEK discriminants failed to perform adequately with any of the estimated MEK spectra. Based on these failures, we abandoned any approaches intending to use MEK for image cube simulations.

[2] NIST Standard Reference Database 35, Version 1.0.

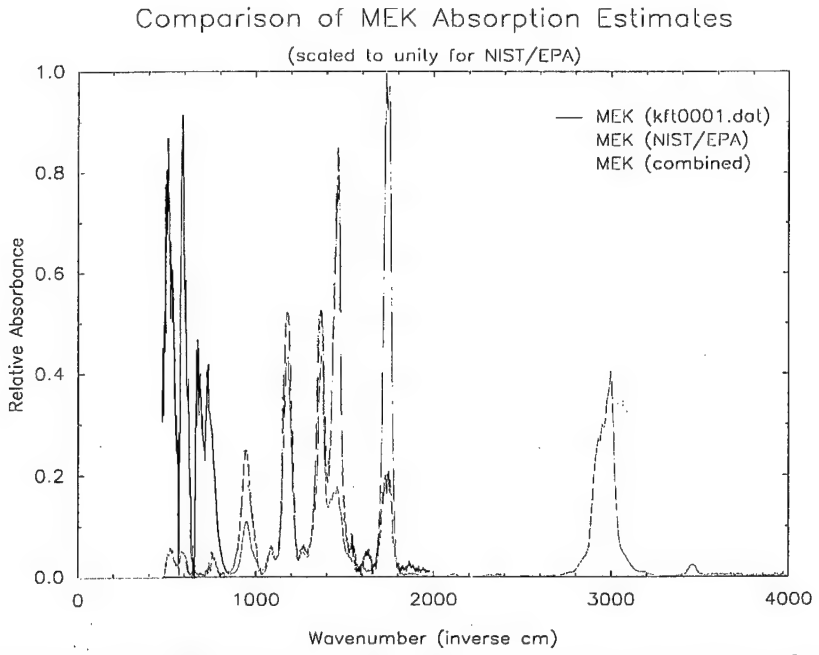

Figure 29. Comparison of MEK Absorbance Estimates. Estimates of the absorbance for MEK obtained from the Kroutil datafile `kft0001.dat` were combined with NIST/EPA absorption values in the outer spectral regions to create a combined revised estimate of the absorbance for MEK.

5.3 Mixtures of Gases

We created one test cube for the Rauss_Howden simulation that contained various mixtures of gases. For this cube, we selected four gases representing various pesticides and precursors (or simulators) of chemical nerve gas agents. We combined absorbances in equal percentages (50:50 or 25:25:25:25) as linearly additive spectral mixtures.

Mixture 1 was a 50:50 percentage mix of chloroethanol and thiodiglycol, two precursors to the development of the chemical blister agent, mustard gas. Absorption spectra (from the Sprouse database) for these two gases are shown in Figure 30 (full scale), and in Figure 31 (expanded over the 800–1300 cm^{-1} spectral region).

Mixture 2 was a 50:50 mix of dimethyl-methyl-phosphonate (DMMP) and diethyl-methyl-phosphonite (DEMP), two simulation agents for chemical nerve agents. Absorption spectra (from the Sprouse database) for these two gases are shown in Figure 32 (full scale), and in Figure 33 (expanded over the 800–1300 cm^{-1} spectral region).

Mixture 3 was a 25:25:25:25 mix of all four of these agents. Absorption spectra for all four gases are superposed in Figure 34 (expanded over the 800–1300 cm^{-1} spectral region only).

Table 2 indicates into which cloud of Figure 19 each mixture was inserted. Each mixture was inserted at the same total radiance contributions as defined earlier for acetone and SF_6 (1 percent, 10 percent, 50 percent and 100 percent of the total *mixture* ratio).

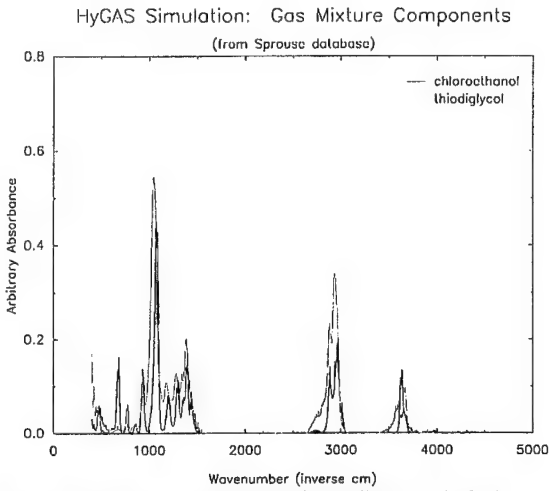

Figure 30. Gases selected for Mixture 1, full spectral range.

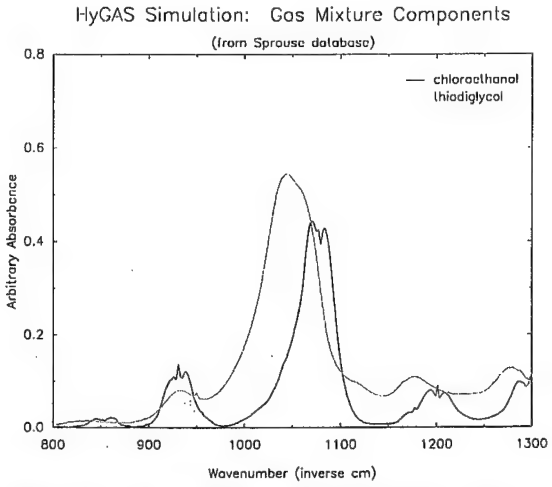

Figure 31. Gases selected for Mixture 1, 800–1200 cm^{-1} only.

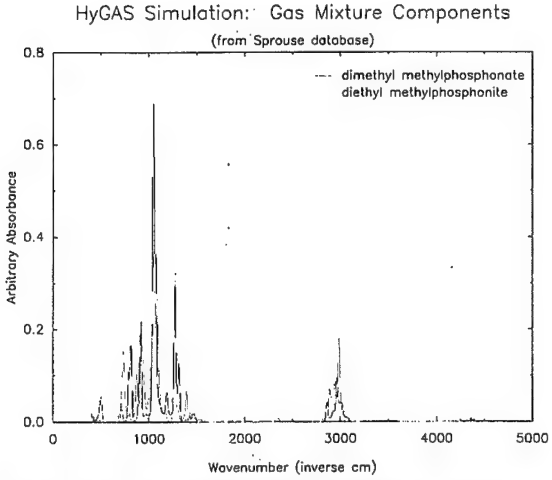

Figure 32. Gases selected for Mixture 2, full spectral range.

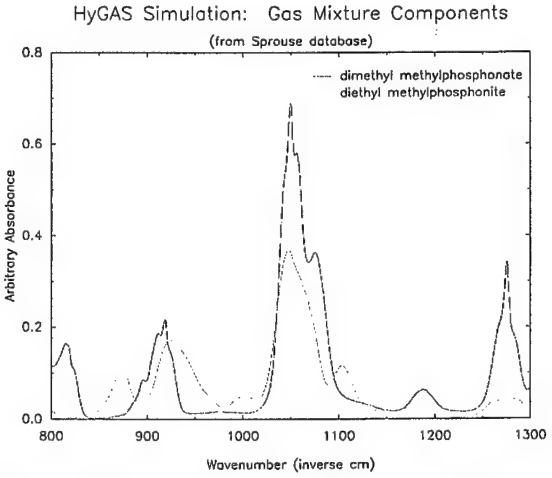

Figure 33. Gases selected for Mixture 2, 800–1200 cm^{-1} only .

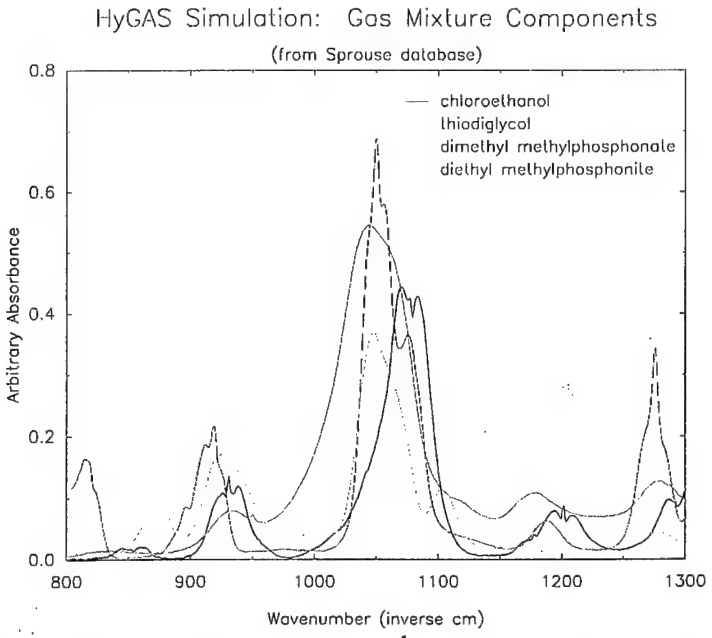

Figure 34. Gases selected for Mixture 3, 800–1200 cm^{-1} only. All four gases were combined at equal radiance contribution.

Table 2. Identification of gas mixtures inserted into each cloud numbered in Figure 19.

Large cloud	Small cloud	Gas Mixture Inserted	Absorption or Emission
1	5	Mixture 1 (chloroethanol + thiodiglycol)	Emission
2	6	Mixture 2 (dimethyl-methyl-phosphonate + diethyl-methyl-phosphonite)	Emission
3	7	Mixture 3 (all four of the above)	Emission
4	8	none	n/a

6. Summary

A summary of the simulation image cubes delivered with HyGAS is given in Table 3.

Table 3. Summary of simulation image cubes delivered with HyGAS.

Image cube name	Gases Inserted	Notes
SE_Kahoolawe_event_locator		overlay (value = 1) marks center of each "gas event"
SE_Kahoolawe_gas_masks		overlay (values = 1–4, 5–8, 9–12, 13–16) for contour levels of clouds
SE_Kahoolawe_Kroutil	Acetone, SF_6	interferograms
SE_Kahoolawe_Rauss	Acetone, SF_6	spectra
SE_Kahoolawe_Rauss_2	none	spectra
SE_Kahoolawe_Rauss_3	Mixtures	spectra

APPENDIX D

Neural Net Notes

The implementation of a backpropagation neural net as the HyGAS module for spectral identification was based on research initially carried out by Patrick Rauss at the U.S. Army Research Laboratory. Rauss implemented a backpropagation network that successfully identified 65 spectra from Sprouse Scientific in the presence of large amounts (e.g. 200 percent) of random noise. Rauss's work is fully described in a paper he submitted to the 1994 Army Science Conference. [A preprint of this paper[1] is attached at the end of this appendix.]

1. Choice of Software

Rauss implemented his neural net with software from the company HNC, Inc. His choice was made several years ago when there were fewer players in the market, and was largely based on a desire to use hardware that was specifically manufactured for neural net computations (HNC's Balboa accelerator board). In an effort to be fully compatible with Rauss, and thus ease the transfer of knowledge, we initially sought to use identical HNC software for HyGAS. Despite much effort on our part, and by Rauss (amid claims to the contrary by HNC, after we had purchased the HNC software *NeuroSoft*), we discovered that the code written by Rauss would not run without purchase of the $10,000 HNC Balboa board. Furthermore, after much frustration, it was revealed that Rauss's software might not even run on the newest Balboa board, having been coded for an earlier discontinued version. This, plus the fact that the HNC software was very user unfriendly and complicated, and that the Rauss code was in a research state and essentially undocumented, resulted in a decision to look for other software. Since backpropagation nets are the most basic of neural nets, we expected a commercially available neural net software package would work in place of the HNC software.

After inquiring on the internet, several options were considered. One highly recommended package was *Matlab* by The MathWorks, Inc. Our limited experience with basic *Matlab* suggested this package was very easy to use and well supported. After receiving a trial copy and a manual from the MathWorks, we determined that *Matlab*'s *Neural Net Toolbox* could be used to identically replicate the network that Rauss had devised. Initially, our intention was to acquire the trained network (i.e. weights) from Rauss and use them in *Matlab*. However, Rauss was unable to export his weights out of the HNC format. As such, we undertook the added time-intensive task of training the new network in addition to our original plan of interfacing a neural net search function into HyGAS.

2. Introduction to Backpropagating Networks

Backpropagation nets are named after *back-propagation of error*, a widely used learning method for neural networks. Backpropagation nets are very easy to apply and useful in many practical applications. However, it should be noted that they truly are a proverbial *black box* in the sense that you never really know what the net is actually keying on.

---

[1] Rauss, P. J., *Noise Tolerance of Model-Based Neural ATR*, Army Science Conference, 1994.

Architecturally, backpropagating neural nets, like most networks, contain several layers: an input layer, an output layer, and one or more hidden layers. Each layer contains a number of nodes, where weighted combinations of inputs from the previous layer are processed through a transfer function (typically: linear, step function, or log sigmoidal) and passed to the next layer. The outputs from one layer are then used as the inputs to the next layer. As such, the structure of a backpropagation net is completely defined by its size (number of layers and number of nodes in each layer), and the type of transfer function used at each node. [See *Matlab* manual pages 2-1 through 2-12. This is an excellent description, both visually and mathematically, of neural network architecture.]

Backpropagation neural nets are *feed-forward*, supervised learning, networks. In order to function, they must be trained with known inputs and known solutions. The network weights are adjusted during this supervised training mode, using a *gradient descent* algorithm, which minimizes the errors between the outputs of the network and the known solutions. The derivatives of the error between the output of the network, and the known solutions, are backpropagated through the network as small changes to each weighting function, hence the name *backpropagation neural net.* After changes to the weights are made, the net is run again. This process iterates until the solution converges to an expectable error (e.g., sum of the square of the error SSE = .01). Once trained, backpropagation networks can very rapidly be applied to new inputs, in a feed-forward mode, with the new inputs beginning feed-forward to the network and its trained weights to produce the output solution.

Note, the solution to training a neural network (i.e. the trained net *weights*), finds a minimum in the error surface. Like most iterative techniques, this minimum is only required to be a local minimum, and may not be the global minimum; thus, it may not necessarily be the *best* solution. Also, recall that the net is minimizing the error relative to all weights. With the Sprouse_65 spectra, using 200 hidden nodes, and 449 channels, this translates to (see Script 2 below) (449*200) + (200*65) weights for a total of 102,080 parameters.

3. Training a net.

In general terms, 4 steps are required to train and apply a neural net.

Step 1. Read in data

Step 2. Set up neural net

Step 3. Train neural net

Step 4. Apply neural net

Definition of the net all occurs in Step 2. Because *Matlab* is a higher order language, the basic steps outlined above are very easily translated into a *Matlab* script as shown in Script 1 below.

3.1. Example 1: Training on four spectra with 60 percent noise.

In order to train, the size and shape of the net must be determined. Rauss had used a three-layer neural net with log sigmoidal transfer functions, 65 spectra (outputs), and a 200 node hidden layer. For a four spectra net, the number of inputs is 449 (the number of channels in the Rauss_Howden sensor) and the number of outputs is four (four different spectra). The only remaining choice is the number of nodes in the hidden layer.

We chose 20 nodes for the hidden layer. Based on Rauss's results and the examples in the *Matlab* Neural Net manual, this choice seemed reasonable. (It is an order of magnitude less hidden nodes than what was used for the actual HyGAS training for the 65 spectra). Both 10 and 40 nodes produced similar results, although the 40 nodes seemed to take longer to train. However, given that no careful studies were done, the choice of 20 nodes is rather arbitrary.

Recall that Rauss was using software from HNC. While the exact form of the Rauss network was used in our application using *Matlab*, the *Matlab* implementation for training a backpropagation net is much more sophisticated than HNC's. First, in *Matlab* it is possible to send the neural net inputs in a parallel or batch mode (see *Matlab* Neural Net manual pages 2-13 through 2-15), i.e. several sets of inputs can be sent through the net at once. Second, *Matlab* includes both weights (multiplicative constants for input) and biases (additive constants) for each node, while HNC only had weights. Finally, Matlab includes a learning rate option in its back propagation network. As described in Chapter 5 (see text and demos) of the *Matlab* Neural Net manual, the learning rate determines the size of the changes to the weights that are made at each iteration.

For training, Rauss would send a different set of spectra at each iteration, and simply iterate until the solution converged to a certain error level. For HyGAS training, we chose to use a more sophisticated implementation using Matlab's adaptive learning rate (*trainbpx*) training. To begin, the weights are set to small random numbers (as was done in the *Matlab* example `App CR1`, below, and as was done by Rauss) and the biases are set to zero. The initial learning rate was set to the Matlab value of `0.01` with an error goal of `0.001`. For the four spectra example, the two sets of inputs were trained in parallel: four spectra with 60 percent noise, and four spectra with 0 percent noise (as recommended by *Matlab* Neural Net manual, example *App CR1*). The network iterated on these inputs, and displayed results every 20 iterations (`disp_freq=20`). A maximum of 5,000 iterations also was set (`max_epoch=5000`).

Using the adaptive training rate, at each iteration, the training rate is altered based on the results of the previous iteration. As described in the `trainbpx` reference (*Matlab* Neural Net manual, page 13-135) and "Improving Backpropagation" (p. 5-25 through 5-32), the learning rate increases by a default of `1.05` times if the error ratio between iterations is less than the default value of `1.04`. If it is greater than the error ratio, the learning rate decreases by a default value of `0.7`. An additional parameter, the momentum which governs the sensitivity to small variations in the error surface, also was left at the default setting of `0.9`.

To summarize, the example four spectra net was trained using adaptive learning rate backpropagating neural net (`trainbpx`). The default values were used and the error goal was set to SSE=.001. The Matlab script given in Script 1 shows all the Matlab calls.

In addition to the example given in Script 1, an example of character recognition which is VERY similar in format is given in the *Matlab Neural Net* manual: `App CR1` (pp. 11-40 through 11-46). This can be run by typing `appcr1` at the Matlab prompt (>>).

The Matlab script `m-file` (Script 1) is similar to the character recognition example (`App CR1`) in the Matlab Neural Net manual (pp. 11-40 through 11-46). Refer to that example and the neural net toolbox manual for explanations. All calls are documented in the neural net toolbox manual except the following: *rand*, *zeros*, *max*, *bar*, all of which are documented in the *Matlab Reference Guide*. Note for an introduction to basic *Matlab*, see *Matlab User's Guide*.

Script 1. Matlab script for training four spectra. This script (`m-file`) is similar to the Matlab example App_CR1.

```
% Training a net with 60% random noise on 4 spectra
% Acetone, Sulfur Hexafloride, Methanol, Ethyl Acetate
%
% Step 1. read the 4 449 point spectra (second column) into cols
% of the matrix "input"

load ace.asc;
load shf.asc;
load met.asc;
load eat.asc;
input(:,1)=ace(:,2);
input(:,2)=shf(:,2);
input(:,3)=met(:,2);
input(:,4)=eat(:,2);

% make array "P" with 60% noise added
% and normalize each col to range from zero to one

P=input + 0.6*rand(449,4);
for I = 1:4,
       P(:,I)=(P(:,I)/max(P(:,I)) * 2) -1;
end

% make array "P2" with 0% noise added
% and normalize each col to range from zero to one

P2=input;
for I = 1:4,
       P2(:,I)=(P2(:,I)/max(P2(:,I)) * 2) -1;
end

% change array "P" to include both 60% noise and 0% noise

P=[P P2];

% set up correct answer array "T"

T=  [  1 0 0 0 1 0 0 0
       0 1 0 0 0 1 0 0
       0 0 1 0 0 0 1 0
       0 0 0 1 0 0 0 1];

% Step 2. set up backpropagation network with 449 inputs,
% 20 node hidden layer, 4 outputs, and log sigmodial transfer functions

R=449; S1=20; S2=4;
[W1,b1,W2,b2]=initff(P,S1,'logsig',S2,'logsig');

% set offsets to zero, weights to small random numbers,
% and set up training parameters

W1=rand(S1,R)*.001; W2=rand(S2,S1)*.001;
b1=zeros(S1,1); b2=zeros(S2,1);
disp_freq=20; max_epoch=5000; err_goal=0.001;
tp =[disp_freq max_epoch err_goal];

% Step 3. train net
```

```
[W1,b1,W2,b2,epochs,TR]=trainbpx(W1,b1,'logsig',W2,b2,'logsig', P, T, tp);

% Step 4. Apply trained net. Set up array "P" with 150% noise
% and normalize between zero and one

P=input + 1.5*rand(449,4);
for I = 1:4,
       P(:,I)=(P(:,I)/max(P(:,I)) * 2) -1;
end

% run search with 150% array "P" on trained net (W1,W2,b1,b2)

simuff(P,W1,b1,'logsig',W2,b2,'logsig');

% plot bar graph (see Matlab manual)

bar(ans);
```

In addition, Figure 1 shows the progress of training. This is default Matlab graphics that plots as you train. The top plot charts the progress of the SSE at each iteration until it reaches the error goal (dotted line). The bottom plot shows the progress of the training rate. It increases dramatically as the solution progresses. This adaptive learning rate allows for much more rapid converge of training. The net typically converges after about 160 iterations.

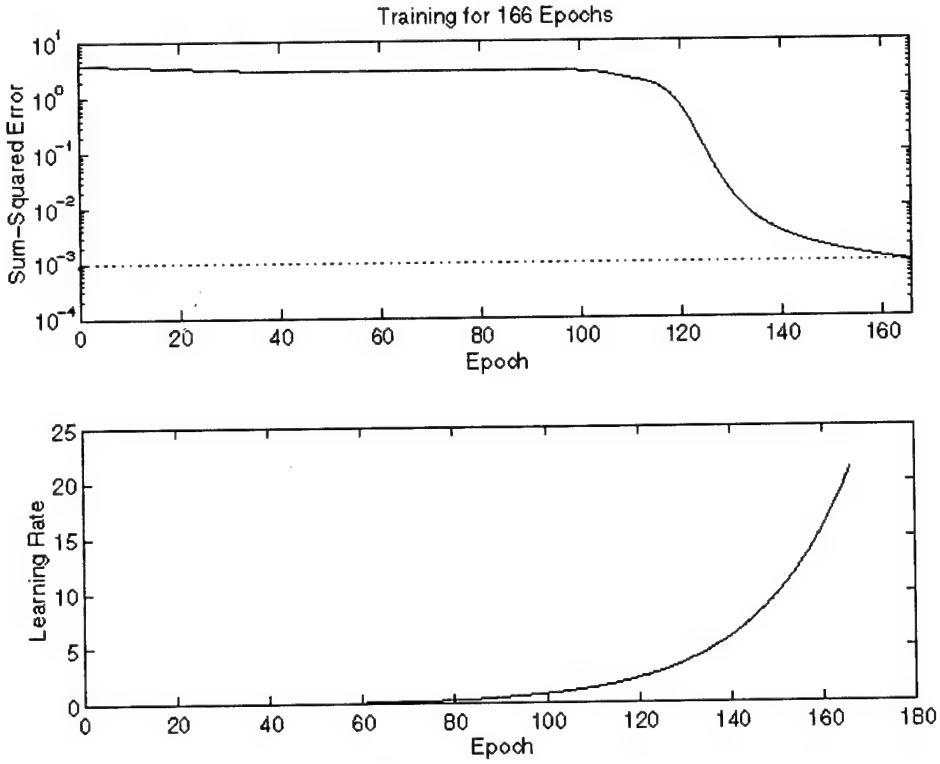

Figure 1. Neural Net training progress. This is a default Matlab plot showing the progress of training until the error goal (dotted line) is reached. The top graph plots the sum of the square of the error (SSE). The bottom graph plots the learning rate.

The four spectra selected for this example are acetone, sulfur hexafluoride, methanol and ethyl acetate. Examples of the spectra are shown in Figure 2 with 60 percent noise, and in Figure 3, with 150 percent noise. Figure 4 shows an example of passing methanol with 150 percent noise to the four-spectra net trained with 60 percent noise. The net identifies methanol with a probability of 90 percent.

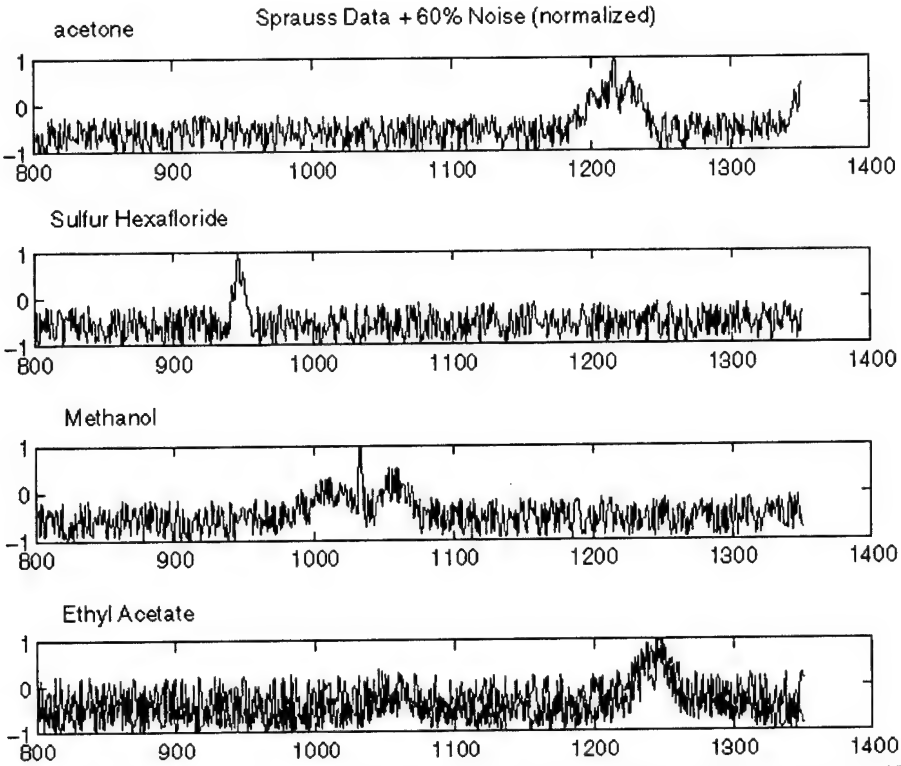

Figure 2. Spectra selected for the four spectra net with 60 percent random noise added. The four spectra selected for this test are acetone, sulfur hexafluoride, methanol and ethyl acetate.

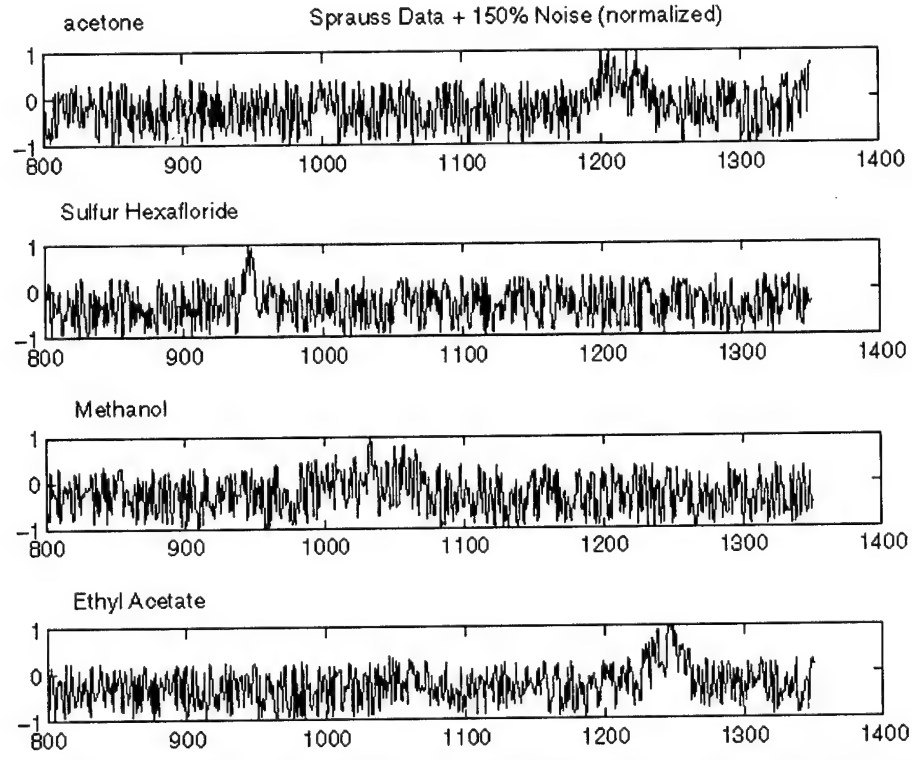

Figure 3. Spectra selected for the four spectra net with 150% random noise added. The four spectra selected for this test are acetone, sulfur hexafluoride, methanol and ethyl acetate.

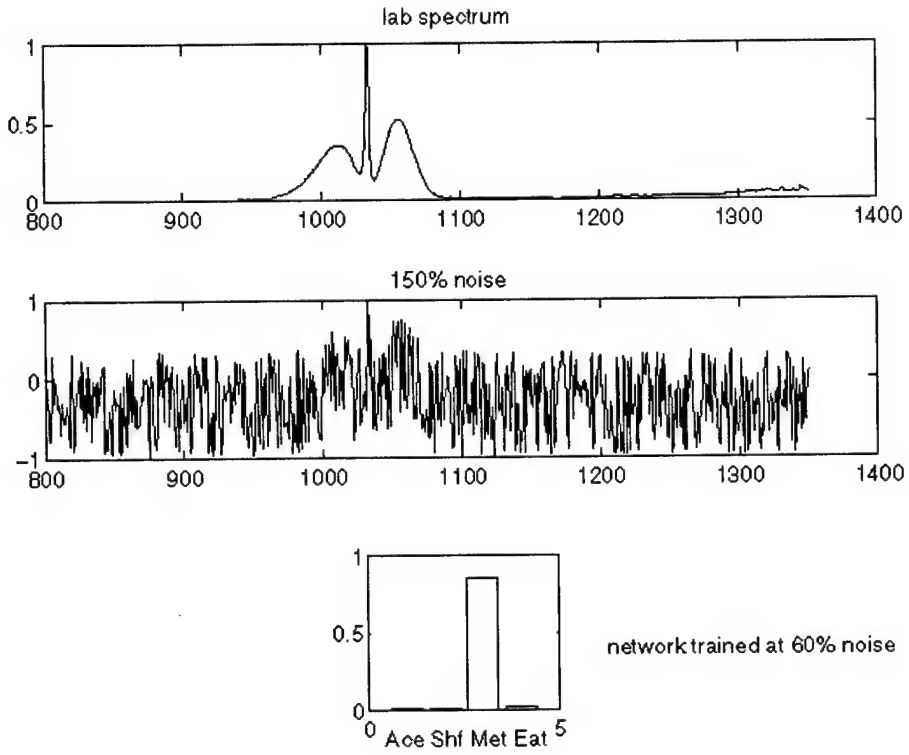

Figure 4. Sample results of passing a methanol spectrum with 150 percent noise through the four-spectra net trained with 60 percent noise.

3.2. Example 2: Training Sprouse data (65 spectra) with 100 percent noise.

Training for 65 spectra, is structurally very similar to training with four spectra, but the implementation is a bit more complicated. The only structural change is that there are now 200 nodes in the hidden layer instead of 20. The number 200 was chosen by Rauss as approximately half way between the number of inputs (449) and the number of outputs (65).

The strategy we employed to train the Sprouse data was based on Matlab examples (e.g. *appcr1*) and trail and error. Unfortunately, a careful study to determine the optimal method of training was beyond the scope of the HyGAS project. The Matlab script for training 65 spectra is given in its entirety in Script 2.

After reading the data into an array and normalizing them from zero to one, the first step in training was to train the neural net to correctly identify the 65 spectra without any noise. However, before training all 65, some experiments were carried out with 10 and 15 spectra. It was discovered that with 15 spectra the default learning rate (.01) was too high. Many iterations where required before the error when down. When the learning rate was changed to .005 the net trained in 360 iterations. Using a learning rate of .001 was too small and the net did not converge.

Step 1. Training with all 65 spectra began with the default Matlab parameters where used. However, as with the 15 spectra, the initial learning rate was too high (.01); as such it was changed to .006. In addition, with 65 spectra the net got stuck in a local minimum in the error surface at an error that was too high (SSE

on the order of 1 or 10). Changes in the momentum (0.8), and to the learning rate increase rate (1.02) and decrease rate (0.5) were made based on the nets performance and trial and error. Using these values the net was successfully trained with 0 percent noise to recognize the 65 different spectra.

Step 2. Starting with the weights determined for 0 percent noise, training the net with 60 percent noise was then attempted. Here 500 sets of 65 spectra with 60 percent random noise (different random noise in each of 500 presentations) were presented to the net. Training parameters were set tostop at SSE=0.001, a learning rate of 1.0, and learning rate increase 1.5 and decrease of 0.5. These later numbers were chosen in attempt to make the net convergence faster. By presenting the net with different sets of random noise it should "learn" which features are real. After completion of this training, the net worked pretty well when data with 60 percent or less noise was sent to it. However, it did not perform well with large noise amounts, and did not always get the right answer even with 60 percent noise.

After re-evaluating the results and the progress of the training at each of the 500 iterations, it was clear that the problem was that the net was presented with a single set of 65 spectra with one set of random values. The net iterated until a small error was reached and, in effect, memorized the given noise pattern. At the presentation of the next set of spectra with a different random noise, it adjusted the weights again to match this new set of noise "perfectly." Over the 500 iterations the length of time to converge decreased; however, the net was still learning a single set of random noise. It was clear that spectra with different sets of random noise must be presented to the net all at one. This is what is done in the Matlab example *appcr1*.

Step 3. Starting with the weights after 0 percent noise and 500 iterations of 60 percent noise, the net was then trained with 100 percent noise inputs. This time, 10 sets of 65 spectra, each with different random noise, were presented to the net at a single time. This process was repeated 500 times.

At the conclusion of this training the net performed very well. Statistical comparisons to Rauss results for a net trained at 100 percent noise were carried out. For example, the trained net was presented 1000 sets of 65 spectra with 100 percent noise and 99.89 percent of them were correctly identified (a correct id is defined as a probability of greater than 0.6 by Rauss). When the same net, trained to 100 percent, was given 1000 sets of 65 spectra with 200 percent noise 73 percent of the spectra were correctly identified. Rauss results were correct only 63 percent of the time. As such, the SETS trained network was out-performing Rauss's and was therefore deemed to be successfully trained to 100 percent noise.

Total training time for Steps 1-3 was greater than one week of CPU time on a Sparc 10-40 machine.

Script 2. Matlab script for training Spouse Library (65 spectra).

```
percent load Sprouse Data
```

```
format long e

load /scooter/home/jess/nets/work/Sprouse_449/lab_data/spec_01.prn
...
(load statements for other spectra removed for space)
...
load /scooter/home/jess/nets/work/Sprouse_449/lab_data/spec_72r.prn

waves=lab_data/spec_01(:,1);
spr=[ lab_data/spec_01(:,2) ...
lab_data/spec_02(:,2) ...
...
(statements for other spectra removed for space)
...

lab_data/spec_71(:,2) ...
lab_data/spec_72r(:,2) ];

clear lab_data/spec_01
...
(statements for other spectra removed for space)
...
clear lab_data/spec_72r

% train with 0% noise

for I = 1:65,
   sprZERO(:,I)=(spr(:,I)/max(spr(:,I)));
end

for I = 1:65,
  P(:,I)=(sprZERO(:,I)/max(sprZERO(:,I)) * 2) -1;
end

T=zeros(65,65);
for I= 1:65,
  T(I,I)=1;
end

R=449; S1=200; S2=65;

W1=rands(S1,R)*.001;
W2=rands(S2,S1)*.001;
b1=zeros(S1,1);
b2=zeros(S2,1);

disp_freq=20; max_epoch=10000; err_goal=0.001;
lr=.006;
lr_inc=1.02;
lr_dec=0.5;
momentum=0.8;
err_ratio=1.01;
tp =[disp_freq max_epoch err_goal lr lr_inc lr_dec momentum err_ratio];
[W1,b1,W2,b2,epochs,TR]= trainbpx(W1,b1,'logsig',W2,b2,'logsig', P, T, tp);
save Hygas65_449

% train 500 times with 60% noise
tp=[2 500 .001 1. 1.5 .5];

for J= 1:500,
 test= sprZERO +.60*rand(449,65);
 for I = 1:65,
    test(:,I)=(test(:,I)/max(test(:,I)) * 2) -1;
 end
 P=test;
 [W1,b1,W2,b2,epochs,TR]= trainbpx(W1,b1,'logsig',W2,b2,'logsig', P, T, tp);
end
save Hygas65_449_60

% train 500 times with 10 sets of 100% noise
for K=1:500;
  test= sprZERO;
  for I = 1:65,
    test(:,I)=(test(:,I)/max(test(:,I)) * 2) -1;
  end
  T2=T; P2=test;
  for J = 1:10,
     test= sprZERO +rand(449,65);
    for I = 1:65,
            test(:,I)=(test(:,I)/max(test(:,I)) * 2) -1;
```

```
    end
    T2=[T2, T];
     P2=[P2,test];
  end
  [W1,b1,W2,b2,epochs,TR]= trainbpx(W1,b1,'logsig',W2,b2,'logsig', P2, T2, tp);
  save Hygas_449_100_5
end

simuff(test,W1,b1,'logsig',W2,b2,'logsig');
bar(ans);
```

4. *Interface with HyGAS*

The trained neural net can be used to identify spectra within HyGAS, both in interactive HyGAS and as a stand alone HyGAS function. Spectra can be input from HIPS data sets. If you wish to run a new spectrum through the neural net, it is recommended that the HIPS function *ASCII to hips* be used to transform ASCII data into HIPS format. Using the stand alone Neural Net function (on the HyGAS menu), the spectrum, or any subset of any HIPS file, can be sent to Matlab for identification against the Sprouse library. Spectra also can be sent from interactive HyGAS.

The Matlab script called when the HyGAS neural net routine is used is listed in Script 3. With the exception of the one line which calls the trained neural net (*simuff*), all other calls are to routines described in the Matlab Reference Guide. For an introduction to basic Matlab see the Matlab User's Guide. On-line help is available by typing help (recommend setting "*more on*" prior to help).

Script 3: Matlab script for executing HyGAS Neural Net Identification Routine.

```
echo off
% make sure to NOT echo this script to screen

% Load trained neural net
clear

% load trained_NN (saved weights and biases, spectra and names of spectra)
load '/usr/HIPS/DATA/hygas/neural_net/trained_NN'

% Load unknown spectrum
clc, disp(' '), disp(' ')
fname = ['unknown'];
eval(['load ',fname])
spec=eval(fname);,spec=spec(:,2);,spec=spec-min(spec);, spec=spec/max(spec)*2-1;

% Run unknown through neural net
ident=simuff(spec,W1,b1,'logsig',W2,b2,'logsig'); ident=ident*100;
[a(:,2),a(:,1)]=sort(ident);, a=flipud(a);

% renormalize spectrum between zero and one
spec=spec+1;, spec=spec/2;

% Clear or open new figure and set size
figure('Position', [20 100 600 700], 'NumberTitle', 'off', 'Name', 'Neural Net
Identifications');

repeat='Y';
while repeat(1)=='Y';

% number of id's with prob. ?.05%
num=size(find(ident>.05),1);

clc,disp(' '), disp(' ')
disp(['The Neural Net has identified ',int2str(num),' possible spectral matches']);

disp(' '), disp(' ')
disp('The best identification will be displayed...')

% Plot unknown spectrum
```

```
subplot(311),plot(waves,spec), title('Unknown Spectrum','color','y')
xlabel('Wavenumber'), ylabel('Arbitrary'), zoom on

n=1;
while n <= num;
  % Plot id'ed spectrum
  subplot(312),plot(waves, sprZERO(:,a(n,1)),'c'),axis([800 1300 0 1])
  xlabel('Wavenumber'), ylabel('Arbitrary')
  title(['Spectrum #', int2str(a(n,1)),':  ',names(a(n,1),:), ' Probability:  ',
num2str(a(n,2)),'%'],'color', 'c')

  % Plot probability bar graph
  subplot(313),bar(ident,'r'),hold on
  [x,y]=bar(a(n,1),ident(a(n,1)));,patch(x,y,'c');bar(ident,'r')
  xlabel('Spectrum Number'), ylabel('Probability (percent)')
  title('Neural Net Identifications from Sprouse Library','color','r'),
  hold off

  % Ask if want to see next spectrum
  in=upper(input('  Display next best identification? ([Y] or N) ', 's'));
  if size(in)==0, in='Y';, end
  if in(1)=='N', break, end
  clc;

  % Check to see if there are any more possible spectra
  if n==num
    disp(' ');
    disp('            No more significant identifications');
  end
  n=n+1;
end

% Ask if want to see all possible id's
disp(' '), disp (' ')
in=upper(input('  Would you like to see all the possible identifications at once ?
([Y] or N) ', 's'));
if size(in)==0, in='Y';, end
if in(1)=='Y'
 % Plot id'ed spectrum
  subplot(312), plot(waves,[sprZERO(:,a(1:num,1))]),axis([800 1300 0 1])
  xlabel('Wavenumber'), ylabel('Arbitrary')
  title(['All Significant Spectral Identifications'],'color', 'w')

 % Plot probability bar graph
  clrs='ymcrgbymcrgb';,
  subplot(313), bar(ident),hold on
  for I=1:num,
    [x,y]=bar(a(I,1),ident(a(I,1)));
    patch(x,y,clrs(I));
    bar(a(I,1),ident(a(I,1)),clrs(I));
  end
  hold off
  xlabel('Spectrum Number'), ylabel('Probability (percent)')
  title('Neural Net Identifications from Sprouse Library'), hold off
end

repeat=upper(input('  Repeat with same unknown??  (Y or [N]) ', 's'));
if size(repeat)==0, repeat='N';, end
end;

disp(' '), disp(' ')
disp('    Hit any key to end ');
pause;
close
exit
```

References

For additional background reading please refer to the following references:

1. *The Matlab Neural Net Toolbox Manual.* (Chapter 2, Chapter 5, Chapter 11, Chapter 13 reference for each function).

2. Pao, Y. H. (1989). *Adaptive Pattern Recognition and Neural Networks.* Addison-Wesley Publishing Company, Inc. (ISBN 0-201-12584-6). [Chapter 5 is the chapter on backpropagation.]

3. Zurada, Jacek M. (1992). *Introduction to Artificial Neural Systems*. West Publishing Co., Minn. (ISBN 0-314-93391-3).

4. Rauss, P. J., *Noise Tolerance of Model-Based Neural ATR*, Army Science Conference, 1994.

APPENDIX E

Gas Coefficient datafiles (GFI)

The gas coefficient datafiles (GFI) supplied by Kroutil must be converted into a HIPS gas coefficient library for use with HyGAS. Kroutil gas coefficient datafiles consist of two files per gas:

- discrim.inc
- filter.inc

These files must be edited, renamed, and put into a HIPS gas coefficient library directory structure to be used by HyGAS. The HIPS gas coefficient library directory structure is a set of two ASCII files, `discrim.dat` and `matrix.dat`, for each gas (Table 1). Example listings of these files for the gas acetone are given in Tables 2 and 3. Tables 4 and 5 list the contents of the corresponding original Kroutil datafiles (`discrim2.inc` and `filter2.inc`), from which the HIPS format files were derived. The HIPS format files are essentially identical to the Kroutil format files except for the various text and delimiters included in the Kroutil format files. These files can be edited with any basic text editor (the unix editor *vi*, for example) to eliminate the extraneous characters and convert them into the appropriate format for a HIPS gas coefficient library.

Table 1. HIPS gas coefficient library directory structure for HyGAS. Two gases, acetone and MEK, are included in this library. For each gas, two files are required, `discrim.dat` and `matrix.dat`. These files are derived from the original Kroutil (GFI) gas coefficient files.

```
$DOD_DIR/LIBRARY/gas_coeff:
acetone/  mek/

$DOD_DIR/LIBRARY/gas_coeff/acetone:
discrim.dat    matrix.dat

$DOD_DIR/LIBRARY/gas_coeff/mek:
discrim.dat    matrix.dat
```

Table 2. Example listing of coefficient file `discrim.dat`, in HIPS LIBRARY format, for acetone. This file is an edited version of the Kroutil file `discrim2.inc`, with extraneous text and delimiters omitted. The directory path for this file is `$DOD_DIR/LIBRARY/gas_coeff/acetone/discrim.dat`.

```
DSC_PASS2   3

  0.255064427599E-01 -0.100223590863E+00  0.722094869816E-01 -0.142908176255E+00
  0.387147592090E-01 -0.457688511587E-01  0.666723427025E-02  0.549303296116E-01
  0.258666742417E-01 -0.212534755364E-01 -0.103640863615E+00 -0.559873687706E-01
  0.132637271432E+00  0.502642931654E-01  0.332738630764E-01  0.523635334859E-01
  0.598746214260E-01  0.150038462318E-01 -0.835000074861E-02  0.115685910825E+00
  0.165066618553E+00 -0.114054530389E+00 -0.205823953136E-01  0.232152045068E-01
 -0.131858943693E+00  0.637355738641E-01 -0.122147355276E+00 -0.857994199088E-01
  0.159371004400E+00  0.102976263443E-01  0.767992388321E-01 -0.233144268574E-01
  0.979633002935E-01  0.221635127670E-01  0.161372486974E+00 -0.269019616799E-01
  0.958158125967E-01  0.841308470954E-01 -0.156920307132E+00 -0.879165542670E-01
 -0.258287362639E-02 -0.601471533969E-01 -0.332554181388E-01 -0.111826354490E+00
 -0.289261012898E-01  0.473731139511E-01 -0.260164056446E+00 -0.233879562651E-01
 -0.929342169892E-01  0.784293005025E-01  0.216282949761E+00  0.254596104360E+00
 -0.167438598595E+00 -0.881685235927E-01  0.683509934382E-01  0.187501416347E+00
  0.838604617509E-02  0.117718865282E+00  0.107572029849E+00  0.295386248388E-01
 -0.202390989196E-01  0.228619532166E+00 -0.165103113350E+00  0.166548328975E+00
 -0.251028496591E+00 -0.579447628456E-01 -0.182230039431E+00  0.105784232004E-01
 -0.725527284989E-01  0.330257203365E-01 -0.231574364978E-01 -0.356553700872E+00
 -0.331275681979E-01 -0.190941008139E+00  0.179050771354E-01 -0.379976689544E-01

 -0.357965106959E-01  0.119100186870E+00 -0.900599843442E-01  0.115123635121E+00
 -0.647137418031E-01 -0.939717920180E-02  0.109589516217E-02 -0.665734014134E-01
 -0.370555296481E-01  0.295352969089E-01  0.548867357606E-01  0.189388089648E-01
 -0.176314247900E+00 -0.460318335240E-01 -0.401569769807E-01 -0.161381060623E-01
 -0.495743201599E-01  0.796236113431E-01 -0.298391601965E-01 -0.121853324038E+00
 -0.145388906472E+00  0.105533459843E+00  0.218486056773E-01 -0.180579436232E-01
  0.174394302729E+00 -0.369477209668E-01  0.151492038486E+00  0.485349809708E-01
 -0.210638318559E-01  0.416969233036E-01 -0.971743725030E-01  0.623083430228E-01
 -0.637615505731E-01  0.384754766785E-01 -0.118422155253E+00  0.247649479350E-01
  0.721583749183E-01 -0.605239719287E-01  0.131441086843E+00 -0.262444797033E-01
  0.426741308381E-01  0.730620477275E-01 -0.266738619558E-01  0.812446931285E-01
 -0.834953677806E-01 -0.401252683728E-01  0.267371138615E+00 -0.981385754649E-02
  0.557271023379E-01 -0.281699701110E-01 -0.194439636751E+00 -0.245005018391E+00
  0.201692352373E+00  0.100750642375E+00 -0.226237742653E-01 -0.181974488528E+00
 -0.230493436995E+00 -0.147155398170E+00 -0.141767138171E+00 -0.195309191030E-01
  0.127421532959E-02 -0.177754857593E+00  0.153990540410E+00 -0.165229032664E+00
  0.173478461659E+00  0.337022662869E-01  0.249467144945E+00 -0.838320460537E-04
  0.127523859075E+00 -0.392260937136E-01 -0.165371481317E-01  0.354859303885E+00
 -0.537122544969E-03  0.197973863676E+00  0.310175610672E-01  0.278376586637E-02

  0.337203328963E-01  0.663643187794E-01 -0.184144339744E-01  0.775679708455E-01
 -0.118503481788E+00  0.174415884093E+00 -0.743865397372E-01 -0.102301751537E-01
  0.701043661654E-01 -0.927293157894E-02  0.620590909402E-04 -0.280260904996E-01
 -0.800262038557E-02  0.227950995048E-01 -0.348017402841E-01 -0.969547374083E-01
  0.244426512089E-01 -0.238370688319E-01  0.580607056254E-01  0.624240867667E-01
 -0.595031868769E-01  0.390825169046E-01  0.264139043127E-01 -0.514682745211E-01
 -0.108610084453E+00 -0.100615778466E+00 -0.199534278243E+00 -0.212508844590E-01
 -0.304637554614E+00 -0.737705631065E-01 -0.227848748717E-01 -0.559899963071E-01
 -0.127114041859E-01 -0.830212522959E-01 -0.346322131680E-02 -0.374465354167E-01
 -0.356836746305E+00  0.312541990968E-01 -0.774033392719E-01  0.103727586439E+00
 -0.801815774759E-01 -0.833973141320E-01  0.874200226720E-01 -0.539542815425E-01
  0.168673169924E+00 -0.567242727350E-01  0.150959313668E+00  0.113419273771E+00
  0.163836911984E+00 -0.144077681767E+00 -0.980426648633E-01  0.225974965482E+00
 -0.361475039063E-01  0.876631456549E-01 -0.951545673173E-01 -0.107308897987E+00
  0.398950993174E+00 -0.762634114671E-01 -0.142491796039E+00 -0.223220966486E-01
 -0.615980654478E-01  0.658476099302E-02  0.149022791355E+00 -0.197757552055E+00
  0.209709870474E+00 -0.828110245068E-01 -0.586938394549E-01  0.276909381842E-01
 -0.537560045664E-01 -0.174811194025E-01  0.276273073276E-01 -0.551741292532E-01
  0.143327296997E-01  0.206151588338E+00 -0.396652738377E-01 -0.217814779983E-02


 -0.277739894096E-01 -0.145518027452E-01 -0.139372943357E-01
```

Table 3. Example listing of coefficient file `matrix.dat`, in HIPS LIBRARY format, for acetone. This file is an edited version of the Kroutil file `filter2.inc`, with extraneous text and delimiters omitted. The directory path for this file is `$DOD_DIR/LIBRARY/gas_coeff/acetone/matrix.dat`.

```
SEG_LENGTH   76
SEG_OFFSET   85

  11   11   13   10    9    5   10    6   10    6   14
   7    8    7    9   12    8   11    9    6   10   11
  11    9    5    5    7   11   11    6   11    9    9
  11    9    6    8    8   12    6    3    8    9    9
   6   11    5    8   10    8    6    5    5    9    5
  12    5   11    5    7    9    9    6    5    6    8
   3    9    8    6    6    3    9    3   11    8

 -64  -61  -51  -50  -32  -23  -19  -13   -8   -5    0

 -78  -71  -55  -37  -33  -30  -22  -15  -10   -5   -1

 -68  -60  -35  -30  -26  -25  -24  -18  -13  -10   -7
  -3   -2

 -80  -77  -57  -55  -35  -22  -12   -8   -7   -3

 -35  -31  -30  -27  -18  -13   -8   -7    0

 -69  -60  -57  -10   -5

 -83  -75  -65  -39  -38  -33  -30  -20  -10    0

 -20  -15  -12  -10   -5    0

 -79  -78  -72  -69  -60  -40  -15  -10   -5    0

 -40  -35  -23  -18  -13   -7

 -83  -81  -65  -50  -43  -32  -25  -18  -15  -10   -7
  -4   -1    0

 -86  -79  -65  -43  -39  -10   -5

 -80  -70  -64  -43  -28  -12   -7   -2

 -87  -65  -42  -17  -15  -10   -3

 -86  -60  -45  -40  -30  -26  -17  -10   -3

 -69  -68  -47  -37  -23  -22  -18  -15   -8   -7   -3
   0

 -93  -85  -80  -70  -48  -47  -34   -8

 -88  -48  -39  -35  -30  -25  -18  -17  -10   -5    0
```

```
 -82  -79  -70  -20  -17  -10   -6   -5    0

 -65  -50  -35  -15   -3    0

 -99  -72  -42  -28  -25  -20  -15  -10   -5    0

 -78  -73  -70  -50  -45  -20  -13  -12   -5   -1    0

 -98  -74  -59  -51  -38  -30  -22  -15  -10   -3   -2

 -87  -75  -67  -25  -15  -11   -5   -1    0

 -78  -53  -30  -17    0

 -46  -30  -25   -7    0

 -78  -55  -50  -42  -18   -6   -2

 -95  -58  -43  -35  -20  -19  -15   -8   -4   -3    0

 -90  -80  -58  -57  -44  -33  -30  -20  -10   -5    0

 -63  -58  -33  -22  -10   -5

 -95  -52  -36  -30  -24  -23  -17  -16  -10   -5   -2

 -93  -85  -63  -60  -23  -18  -13   -8    0

 -94  -84  -63  -48  -27  -22  -10   -5    0

 -99  -87  -42  -26  -25  -21  -15  -11  -10   -5    0

 -68  -63  -50  -38  -29  -18  -15  -10    0

 -35  -29  -28  -15   -7    0

 -82  -65  -60  -28  -18  -13   -7    0

 -75  -68  -53  -40  -27  -15  -10   -3

 -90  -83  -31  -30  -20  -16  -15  -12   -7   -4   -3
   0

 -73  -68  -66  -12   -5    0
```

```
-44  -40  -12

-93  -70  -33  -21  -17  -10   -7    0

-80  -73  -32  -17  -14  -13  -10   -5    0

-78  -37  -23  -22  -18  -15  -10   -5    0

-78  -73  -58  -10   -5   -1

-82  -45  -37  -31  -22  -18  -17  -10   -7   -3    0

-98  -75  -70  -26  -25

-85  -78  -67  -37  -17  -12   -8   -5

-91  -79  -40  -30  -25  -20  -15  -10   -5    0

-83  -78  -65  -15  -10   -9   -5    0

-70  -50  -42  -22   -8    0

-80  -75  -72  -31  -12

-97  -83  -68  -42   -5

-96  -51  -47  -30  -25  -22  -15  -10   -3

-83  -71  -12   -5   -2

-86  -62  -55  -27  -20  -17  -13  -12   -8   -7   -3
  0

-80  -36  -20  -17  -13

-95  -88  -47  -30  -29  -18  -17  -13  -10   -5    0

-92  -57  -50  -38   -3

-88  -20  -14  -13   -8   -7    0

-54  -53  -40  -35  -23  -16  -15   -8   -3

-99  -41  -35  -30  -20  -15  -10   -5    0
```

```
-93  -69  -34  -23   -7    0

-59  -43  -35  -28   -8

-95  -90  -25  -21   -7   -2

-85  -66  -65  -57  -37  -13  -10   -5

-90  -46  -12

-98  -89  -72  -34  -26  -15  -13   -8    0

-90  -68  -60  -40  -22  -18  -12   -5

-100  -95  -28  -15   -8   -5

-75  -70  -20  -12   -3    0

-95  -51  -32

-77  -70  -20  -18  -15  -13  -10   -5    0

-65  -45  -23

-98  -33  -28  -27  -23  -20  -15  -10   -7   -3    0

-80  -75  -67  -37  -18  -17   -5    0


-0.6614879E-02  -0.1429926E-01   0.1880962E-01   0.4904101E-01
-0.5967685E-01   0.9309760E-01  -0.3967213E-01   0.5029122E-01
-0.7570823E-01  -0.9420925E-01   0.1056719E+00


-0.3887421E-02  -0.3144222E-02  -0.2708863E-01   0.4338598E-01
 0.3446739E-01   0.7237891E-01  -0.3861937E-01  -0.6701618E-01
 0.6618018E-01  -0.9265281E-01  -0.5974102E-01


-0.1015457E-02   0.1787316E-01  -0.5627253E-01   0.2446596E-01
 0.4138545E-01  -0.4920137E-01   0.8277126E-01  -0.5583157E-01
 0.5483646E-01   0.7511845E-01   0.7321317E-01   0.5719284E-01
-0.5573704E-01


 0.3706080E-02   0.4192878E-02   0.2192246E-01  -0.2125863E-01
-0.8888560E-01  -0.4599749E-01  -0.3867546E-01  -0.8356100E-01
 0.5090259E-01   0.7988496E-01


-0.5007708E-01  -0.2835327E-01   0.5709929E-01   0.3569544E-01
-0.8053026E-01   0.6206589E-01  -0.5520297E-01   0.5194590E-01
```

```
 0.7264247E-01

 0.4696982E-02   0.1344796E-01   0.4094194E-01   0.1405365E+00
-0.1029181E+00

 0.2858981E-02   0.4921757E-02  -0.1507979E-01  -0.2491641E-01
-0.8683238E-01   0.4160152E-01   0.6842425E-01   0.3372858E-01
 0.8530207E-01   0.8224385E-01

 0.5356384E-01  -0.8929932E-01  -0.4202133E-01   0.9691476E-01
-0.1476151E+00   0.8123142E-01

 0.3891838E-02   0.4115778E-02   0.1523170E-01   0.9186109E-02
 0.2767959E-01   0.6692114E-01  -0.5258305E-01   0.7912263E-01
-0.8534696E-01   0.1040969E+00

 0.6037670E-01  -0.6883714E-01   0.4781083E-01  -0.7646285E-01
 0.9738579E-01   0.3017977E-01

-0.8358268E-02  -0.1078631E-01  -0.1974960E-01   0.3368537E-01
 0.3764563E-01  -0.7846859E-01  -0.5252290E-01  -0.7839710E-01
-0.4286567E-01   0.7466000E-01   0.4668713E-01   0.3656130E-01
-0.4346279E-01   0.9671300E-01

 0.3909264E-02   0.2749227E-02  -0.4503471E-01   0.6308652E-01
-0.5864193E-01   0.4538230E-01  -0.8220814E-01

 0.1718440E-02   0.6382233E-02   0.1334275E-01   0.5420069E-01
-0.6019428E-01  -0.9237481E-01   0.6849685E-01  -0.1243653E+00

 0.4034336E-02  -0.5621848E-01  -0.5721593E-01   0.3324445E-01
-0.7362759E-01   0.1308168E+00   0.1009267E+00

-0.8879554E-03   0.1323899E-01  -0.6358895E-01   0.4966516E-01
 0.4289684E-01   0.4098634E-01   0.2913818E-01   0.7054655E-01
 0.6150728E-01

-0.1363695E-01  -0.2093042E-01   0.9327054E-02   0.4563500E-01
 0.7180022E-01  -0.5832529E-01  -0.6202235E-01  -0.6733461E-01
-0.8133513E-01   0.7626045E-01   0.7296384E-01   0.8405028E-01

 0.1785205E-02   0.3876256E-02  -0.5187889E-02   0.3658513E-01
-0.5824666E-01   0.3553154E-01   0.4898361E-01  -0.8159473E-01

-0.2441164E-02  -0.3309193E-01  -0.2949855E-01  -0.4857912E-01
 0.3897524E-01  -0.6927840E-01  -0.5184076E-01   0.5133453E-01
 0.1029789E+00  -0.7937372E-01   0.7691066E-01

 0.9691402E-02   0.1573787E-01   0.4049329E-01   0.5797600E-01
 0.4341811E-01   0.1044834E+00   0.5589737E-01  -0.6136465E-01
 0.1266025E+00
```

```
-0.2911289E-01   0.6536022E-01  -0.9595171E-01  -0.2635118E-01
 0.5173032E-01   0.5038553E-01

 0.5064464E-03  -0.1938821E-01  -0.2045006E-01  -0.3502310E-01
-0.5073417E-01   0.6181104E-01  -0.6143093E-01   0.1017410E+00
-0.5733096E-01   0.1099021E+00

-0.6450505E-02   0.1197766E-01  -0.6577452E-02   0.4924058E-01
-0.5118743E-01   0.5812128E-01   0.9391383E-01  -0.3865344E-01
-0.5250741E-01  -0.6554410E-01   0.8407435E-01

 0.2801587E-02   0.1673847E-01   0.2395294E-01  -0.3958954E-01
-0.2367036E-01   0.5159958E-01  -0.4911932E-01  -0.8399504E-01
 0.8474098E-01   0.5365313E-01  -0.6453564E-01

-0.5055159E-02  -0.2326774E-01   0.1894546E-01  -0.5114691E-01
-0.9815212E-01  -0.4697780E-01  -0.1217237E+00  -0.3119738E-01
 0.1016141E+00

-0.4417848E-02   0.7742098E-01   0.4264242E-01   0.5359055E-01
 0.7687466E-01

-0.4329887E-01   0.1245421E+00  -0.2846893E-01   0.1347317E+00
 0.1279109E+00

-0.2226657E-01  -0.5160971E-01   0.3648871E-01  -0.3594881E-01
-0.8736341E-01   0.8779839E-01  -0.7271840E-01

-0.9175061E-03  -0.4004556E-01   0.4991431E-01  -0.4166025E-01
 0.5223776E-01  -0.6164364E-01  -0.9030090E-01  -0.5116666E-01
 0.5738448E-01   0.5955560E-01   0.1010771E+00

-0.6161666E-02   0.2162465E-01  -0.1690745E-01   0.1458709E-01
 0.2280459E-01   0.2883639E-01   0.3736303E-01   0.8033267E-01
 0.1166013E+00  -0.1032388E+00   0.4823207E-01

 0.1872556E-01  -0.7729628E-01   0.4621783E-01  -0.4012094E-01
 0.5902296E-01  -0.7037951E-01

 0.3155643E-02  -0.2826733E-01   0.3062426E-01   0.4021729E-01
 0.6401054E-01   0.8385868E-01   0.4622849E-01   0.8073462E-01
 0.7923588E-01  -0.6105518E-01  -0.5418089E-01

-0.5417099E-02  -0.1790018E-01   0.2421645E-01   0.3651322E-01
 0.4757639E-01  -0.3285359E-01   0.9041086E-01  -0.7359436E-01
 0.6656604E-01

-0.6927019E-02   0.1583141E-01   0.5772311E-01  -0.4546625E-01
 0.5429167E-01  -0.7121480E-01   0.7531629E-01  -0.6427686E-01
 0.5058303E-01

 0.3349290E-02   0.2598547E-01   0.2603641E-01   0.2869117E-01
-0.5560236E-01  -0.4124419E-01  -0.9738243E-01  -0.2900641E-01
```

```
 0.9336783E-01  -0.4642718E-01   0.6119101E-01

-0.2144716E-01   0.5859940E-01   0.4104657E-01  -0.2838143E-01
-0.2947324E-01  -0.3557045E-01  -0.5517643E-01   0.6514291E-01
 0.9176975E-01

-0.7765751E-01  -0.5638416E-01  -0.9008388E-01  -0.7788346E-01
 0.9086886E-01   0.8660997E-01

-0.1137784E-01  -0.4058158E-01   0.3245270E-01  -0.4292451E-01
-0.8402064E-01   0.8908543E-01   0.4711056E-01   0.6691652E-01

-0.3579511E-01  -0.5865894E-01   0.6133667E-01   0.3006370E-01
 0.5329183E-01  -0.4610473E-01   0.8270162E-01   0.4395046E-01

 0.7641728E-02  -0.1113240E-01  -0.3335683E-01   0.5433084E-01
 0.6818714E-01   0.3371345E-01  -0.9338174E-01  -0.4668515E-01
 0.6782711E-01   0.3186922E-01   0.6549584E-01   0.6918482E-01

 0.3299118E-01  -0.4227466E-01   0.3103725E-01  -0.5033476E-01
-0.6719448E-01   0.8481884E-01

 0.3336797E-01   0.9236907E-01  -0.1593052E+00

 0.8157173E-02   0.5168252E-01   0.3905740E-01  -0.5900268E-01
 0.7004637E-01   0.4552325E-01   0.8388874E-01   0.9758771E-01

 0.4147324E-01   0.7269266E-01  -0.4770963E-01   0.3419052E-01
 0.4878791E-01   0.5932455E-01   0.5388714E-01  -0.8102848E-01
 0.1162714E+00

 0.1873459E-01   0.3837034E-01   0.6504966E-01  -0.5953367E-01
-0.5975812E-01  -0.9290178E-01   0.5676722E-01  -0.8950090E-01
 0.9507764E-01

-0.2894814E-01   0.5057938E-01  -0.1808140E-01   0.5988654E-01
-0.1028527E+00  -0.5846804E-01

 0.3291355E-01  -0.4437537E-01   0.6803057E-01  -0.4815017E-01
-0.4711590E-01  -0.5060849E-01   0.7042320E-01   0.6447795E-01
 0.4678527E-01   0.8806979E-01   0.4878302E-01

-0.8771360E-02  -0.5994582E-01   0.3814937E-01   0.8554896E-01
-0.4169315E-01

-0.3657513E-01  -0.8251550E-01   0.4399715E-01   0.5526234E-01
 0.7571201E-01  -0.6371758E-01  -0.7080819E-01  -0.7365576E-01

 0.1195100E-01   0.2362175E-01   0.4317594E-01   0.5466008E-01
-0.6546786E-01   0.9262113E-01  -0.4062239E-01   0.7532982E-01
-0.5964542E-01   0.7468928E-01
```

```
 0.1619453E-01  -0.4108550E-01  -0.2260301E-01  -0.5597401E-01
 0.8142098E-01  -0.3302361E-01  -0.8204678E-01   0.5921208E-01

 0.4304931E-01   0.7605813E-01  -0.8353233E-01  -0.7646306E-01
-0.5347725E-01   0.7866547E-01

 0.2850488E-01  -0.6485684E-01  -0.2479879E-01  -0.8661002E-01
-0.5764616E-01

-0.5424140E-02   0.5348583E-01  -0.9035242E-01  -0.8372557E-01
-0.5181130E-01

-0.1670526E-01  -0.5824187E-01   0.3338574E-01   0.5332801E-01
-0.7521041E-01  -0.3403812E-01  -0.6603187E-01   0.6710238E-01
 0.5244897E-01

 0.7116876E-01   0.4290202E-01  -0.9650268E-01  -0.7159492E-01
-0.5531762E-01

 0.2118123E-01  -0.3916537E-01  -0.5624462E-01   0.7524978E-01
 0.4825355E-01   0.4298079E-01   0.9778190E-01  -0.5122039E-01
-0.4737237E-01   0.6585310E-01   0.6630810E-01   0.4685323E-01

 0.6657317E-01   0.8633183E-01   0.4640199E-01   0.6243679E-01
 0.5254362E-01

-0.2462394E-01  -0.4815776E-01   0.3934532E-01   0.4348452E-01
-0.4063642E-01  -0.5861045E-01   0.6549107E-01   0.6442931E-01
 0.4171386E-01  -0.6112875E-01   0.9744171E-01

-0.1573435E-01   0.7631516E-01   0.8629898E-01  -0.1102906E+00
 0.1027282E+00

-0.2956824E-01   0.7718813E-01   0.3606934E-01   0.9468325E-01
-0.6346736E-01   0.6661998E-01   0.1173735E+00

 0.5552817E-01   0.6476392E-01   0.4064802E-01  -0.8114761E-01
 0.7275619E-01   0.4035515E-01  -0.5406699E-01  -0.9764583E-01
 0.8995514E-01

 0.1331168E-01  -0.2581197E-01  -0.4927886E-01   0.5133463E-01
 0.6809124E-01  -0.4226324E-01   0.4753117E-01  -0.6921270E-01
 0.6723411E-01

 0.5604440E-01  -0.7229649E-01   0.5320710E-01   0.8676874E-01
 0.6210139E-01   0.9611095E-01

-0.3191814E-01   0.6595018E-01  -0.9802993E-01  -0.3899986E-01
-0.7033533E-01

-0.4227392E-01   0.1422027E-01  -0.6879323E-01  -0.7103910E-01
```

```
 0.5515100E-01  -0.7020096E-01


-0.3566328E-01   0.4954189E-01  -0.4300747E-01   0.3426962E-01
 0.4974108E-01   0.7415684E-01   0.5711441E-01  -0.7182895E-01


 0.6140056E-01   0.7111893E-01  -0.4804461E-01


-0.2997365E-01  -0.4629572E-01  -0.3989322E-01   0.4538489E-01
 0.5980771E-01  -0.7202677E-01   0.4854868E-01  -0.6519832E-01
 0.8260079E-01


 0.2926636E-01  -0.5817771E-01   0.5397728E-01   0.5684553E-01
-0.3359030E-01  -0.5425525E-01  -0.6073613E-01  -0.7547803E-01


 0.3502282E-01  -0.1358177E-01  -0.5018083E-01  -0.8992089E-01
-0.5606518E-01  -0.6158898E-01


-0.4238006E-01   0.6123731E-01   0.3187495E-01  -0.8657039E-01
 0.5340118E-01   0.1051042E+00


-0.5427403E-01  -0.5890925E-01  -0.3562557E-01


 0.3972447E-01   0.2197290E-01   0.7261248E-01  -0.4201903E-01
-0.7315820E-01   0.1360201E-01   0.5520076E-01  -0.8179243E-01
 0.7224426E-01


-0.7109583E-01  -0.1303928E+00   0.4776314E-01


-0.2063328E-01   0.2734613E-01  -0.3529310E-01   0.3259774E-01
 0.3253571E-01   0.8483794E-01  -0.7366542E-01   0.5688202E-01
 0.5682221E-01   0.5374562E-01   0.7876849E-01


 0.4776524E-01  -0.1507547E-01   0.2400588E-01   0.3280406E-01
-0.5068491E-01   0.6211805E-01  -0.8781512E-01   0.9945956E-01


 0.8259140E-01  -0.4758021E-01   0.4089225E-01   0.1639756E-01
-0.6876206E-01   0.2273056E-01   0.3819146E-01  -0.3721802E-01
-0.5713508E-01   0.2394236E-01  -0.6512219E-01  -0.2191193E-01
 0.6342072E-01  -0.3024785E-01  -0.3814323E-01   0.3050360E-01
 0.3170719E-01  -0.2565768E-01  -0.5481426E-01   0.3873283E-01
-0.3035126E-01  -0.3384014E-01   0.9957474E-01  -0.3666606E-02
-0.5692184E-01  -0.5636183E-01   0.6097601E-01  -0.3236854E-01
-0.3393197E-01   0.1826495E-01   0.3305293E-01  -0.1825163E-01
-0.7350731E-02   0.3190426E-02  -0.1362626E-01  -0.4761601E-01
 0.3119041E-01   0.3703185E-01  -0.4902850E-01   0.2156271E-01
 0.2257008E-01  -0.2476735E-01  -0.1802885E-01   0.3251489E-01
-0.1129883E-01   0.5745488E-02   0.5650065E-01   0.2234104E-01
-0.4830371E-01   0.2498304E-01   0.6292367E-01  -0.5668922E-01
 0.1234409E-01   0.4732342E-01  -0.5023522E-01   0.6448446E-02
-0.4441234E-03  -0.1959216E-01   0.3735405E-01   0.6997063E-01
 0.4517583E-02  -0.2926396E-01   0.3523561E-01   0.6521603E-01
-0.4535277E-01  -0.3852353E-01   0.1808334E-01   0.1675636E-04
-0.3392704E-01   0.1460649E-01  -0.7783228E-02  -0.1373911E-01
 0.7815688E-02   0.9795678E-01  -0.1906542E-02   0.2516573E-01
```

Table 4. Example listing of coefficient file `discrim2.inc`, as supplied by Kroutil (GFI), for acetone. This is the original Kroutil file `discrim2.inc`. The equivalent HyGAS directory path for this file is `/d2/hygas/Kroutil/new/mtrx/discrim2.inc`.

```
#define DSC_PASS2  3
float dsc_coefs2[DSC_PASS2][SEG_LENGTH2] =
{
  {
  0.255064427599E-01, -0.100223590863E+00,  0.722094869816E-01, -0.142908176255E+00,
  0.387147592090E-01, -0.457688511587E-01,  0.666723427025E-02,  0.549303296116E-01,
  0.258666742417E-01, -0.212534755364E-01, -0.103640863615E+00, -0.559873687706E-01,
  0.132637271432E+00,  0.502642931654E-01,  0.332738630764E-01,  0.523635334859E-01,
  0.598746214260E-01,  0.150038462318E-01, -0.835000074861E-02,  0.115685910825E+00,
  0.165066618553E+00, -0.114054530389E+00, -0.205823953136E-01,  0.232152045068E-01,
 -0.131858943693E+00,  0.637355738641E-01, -0.122147355276E+00, -0.857994199088E-01,
  0.159371004400E+00,  0.102976263443E-01,  0.767992388321E-01, -0.233144268574E-01,
  0.979633002935E-01,  0.221635127670E-01,  0.161372486974E+00, -0.269019616799E-01,
  0.958158125967E-01,  0.841308470954E-01, -0.156920307132E+00, -0.879165542670E-01,
 -0.258287362639E-02, -0.601471533969E-01, -0.332554181388E-01, -0.111826354490E+00,
 -0.289261012898E-01,  0.473731139511E-01, -0.260164056446E+00, -0.233879562651E-01,
 -0.929342169892E-01,  0.784293005025E-01,  0.216282949761E+00,  0.254596104360E+00,
 -0.167438598595E+00, -0.881685235927E-01,  0.683509934382E-01,  0.187501416347E+00,
  0.838604617509E-02,  0.117718865282E+00,  0.107572029849E+00,  0.295386248388E-01,
 -0.202390989196E-01,  0.228619532166E+00, -0.165103113350E+00,  0.166548328975E+00,
 -0.251028496591E+00, -0.579447628456E-01, -0.182230039431E+00,  0.105784232004E-01,
 -0.725527284989E-01,  0.330257203365E-01, -0.231574364978E-01, -0.356553700872E+00,
 -0.331275681979E-01, -0.190941008139E+00,  0.179050771354E-01, -0.379976689544E-01,
  },
  {
 -0.357965106959E-01,  0.119100186870E+00, -0.900599843442E-01,  0.115123635121E+00,
 -0.647137418031E-01, -0.939717920180E-02,  0.109589516217E-02, -0.665734014134E-01,
 -0.370555296481E-01,  0.295352969089E-01,  0.548867357606E-01,  0.189388089648E-01,
 -0.176314247900E+00, -0.460318335240E-01, -0.401569769807E-01, -0.161381060623E-01,
 -0.495743201599E-01,  0.796236113431E-01, -0.298391601965E-01, -0.121853324038E+00,
 -0.145388906472E+00,  0.105533459843E+00,  0.218486056773E-01, -0.180579436232E-01,
  0.174394302729E+00, -0.369477209668E-01,  0.151492038486E+00,  0.485349809708E-01,
 -0.210638318559E-01,  0.416969233036E-01, -0.971743725030E-01,  0.623083430228E-01,
 -0.637615505731E-01,  0.384754766785E-01, -0.118422155253E+00,  0.247649479350E-01,
  0.721583749183E-01, -0.605239719287E-01,  0.131441086843E+00, -0.262444797033E-01,
  0.426741308381E-01,  0.730620477275E-01, -0.266738619558E-01,  0.812446931285E-01,
 -0.834953677806E-01, -0.401252683728E-01,  0.267371138615E+00, -0.981385754649E-02,
  0.557271023379E-01, -0.281699701110E-01, -0.194439636751E+00, -0.245005018391E+00,
  0.201692352373E+00,  0.100750642375E+00, -0.226237742653E-01, -0.181974488528E+00,
 -0.230493436995E+00, -0.147155398170E+00, -0.141767138171E+00, -0.195309191030E-01,
  0.127421532959E-02, -0.177754857593E+00,  0.153990540410E+00, -0.165229032664E+00,
  0.173478461659E+00,  0.3370226628695-01,  0.249467144945E+00, -0.838320460537E-04,
  0.127523859075E+00, -0.392260937136E-01, -0.165371481317E-01,  0.354859303885E+00,
 -0.537122544969E-03,  0.197973863676E+00,  0.310175610672E-01,  0.278376586637E-02,
  },
  {
  0.337203328963E-01,  0.663643187794E-01, -0.184144339744E-01,  0.775679708455E-01,
 -0.118503481788E+00,  0.174415884093E+00, -0.743865397372E-01, -0.102301751537E-01,
  0.701043661654E-01, -0.927293157894E-02,  0.620590909402E-04, -0.280260904996E-01,
 -0.800262038557E-02,  0.227950995048E-01, -0.348017402841E-01, -0.969547374083E-01,
  0.244426512089E-01, -0.238370688319E-01,  0.580607056254E-01,  0.624240867667E-01,
 -0.595031868769E-01,  0.390825169046E-01,  0.264139043127E-01, -0.514682745211E-01,
 -0.108610084453E+00, -0.100615778466E+00, -0.199534278243E+00, -0.212508844590E-01,
 -0.304637554614E+00, -0.737705631065E-01, -0.227848748717E-01, -0.559899963071E-01,
 -0.127114041859E-01, -0.830212522959E-01, -0.346322131680E-02, -0.374465354167E-01,
 -0.356836746305E+00,  0.312541990968E-01, -0.774033392719E-01,  0.103727586439E+00,
 -0.801815774759E-01, -0.833973141320E-01,  0.874200226720E-01, -0.539542815425E-01,
  0.168673169924E+00, -0.567242727350E-01,  0.150959313668E+00,  0.113419273771E+00,
  0.163836911984E+00, -0.144077681767E+00, -0.980426648633E-01,  0.225974965482E+00,
 -0.361475039063E-01,  0.876631456549E-01, -0.951545673173E-01, -0.107308897987E+00,
  0.398950993174E+00, -0.762634114671E-01, -0.142491796039E+00, -0.223220966486E-01,
 -0.615980654478E-01,  0.658476099302E-02,  0.149022791355E+00, -0.197757552055E+00,
  0.209709870474E+00, -0.828110245068E-01, -0.586938394549E-01,  0.276909381842E-01,
 -0.537560045664E-01, -0.174811194025E-01,  0.276273073276E-01, -0.551741292532E-01,
  0.143327296997E-01,  0.206151588338E+00, -0.396652738377E-01, -0.217814779983E-02,
  },
};
```

```
float dsc_intercepts2[DSC_PASS2] =
{
 -0.277739894096E-01, -0.145518027452E-01, -0.139372943357E-01,
};
```

Table 5 Example listing of coefficient file `filter2.inc`, as supplied by Kroutil (GFI), for acetone. This is the original Kroutil file `filter2.inc`. The equivalent HyGAS directory path for this file is `/d2/hygas/Kroutil/new/mtrx/filter2.inc`.

```
#define MFLT_LENGTH2   14
#define SEG_LENGTH2    76
#define SEG_OFFSET2    85
char hdmsg2[10] = "ACETONE   ";
int flt_length2[SEG_LENGTH2] =
{
   11,   11,   13,   10,    9,    5,   10,    6,   10,    6,   14,
    7,    8,    7,    9,   12,    8,   11,    9,    6,   10,   11,
   11,    9,    5,    5,    7,   11,   11,    6,   11,    9,    9,
   11,    9,    6,    8,    8,   12,    6,    3,    8,    9,    9,
    6,   11,    5,    8,   10,    8,    6,    5,    5,    9,    5,
   12,    5,   11,    5,    7,    9,    9,    6,    5,    6,    8,
    3,    9,    8,    6,    6,    3,    9,    3,   11,    8,
};

int flt_offsets2[SEG_LENGTH2][MFLT_LENGTH2] =
{
  {
  -64,  -61,  -51,  -50,  -32,  -23,  -19,  -13,   -8,   -5,    0,
  },
  {
  -78,  -71,  -55,  -37,  -33,  -30,  -22,  -15,  -10,   -5,   -1,
  },h
  {
  -68,  -60,  -35,  -30,  -26,  -25,  -24,  -18,  -13,  -10,   -7,
   -3,   -2,
  },
  {
  -80,  -77,  -57,  -55,  -35,  -22,  -12,   -8,   -7,   -3,
  },
  {
  -35,  -31,  -30,  -27,  -18,  -13,   -8,   -7,    0,
  },
  {
  -69,  -60,  -57,  -10,   -5,
  },
  {
  -83,  -75,  -65,  -39,  -38,  -33,  -30,  -20,  -10,    0,
  },
  {
  -20,  -15,  -12,  -10,   -5,    0,
  },
  {
  -79,  -78,  -72,  -69,  -60,  -40,  -15,  -10,   -5,    0,
  },
  {
  -40,  -35,  -23,  -18,  -13,   -7,
  },
  {
  -83,  -81,  -65,  -50,  -43,  -32,  -25,  -18,  -15,  -10,   -7,
   -4,   -1,    0,
  },
  {
  -86,  -79,  -65,  -43,  -39,  -10,   -5,
  },
  {
  -80,  -70,  -64,  -43,  -28,  -12,   -7,   -2,
  },
  {
  -87,  -65,  -42,  -17,  -15,  -10,   -3,
  },
  {
  -86,  -60,  -45,  -40,  -30,  -26,  -17,  -10,   -3,
  },
  {
  -69,  -68,  -47,  -37,  -23,  -22,  -18,  -15,   -8,   -7,   -3,
    0,
  },
  {
  -93,  -85,  -80,  -70,  -48,  -47,  -34,   -8,
  },
  {
  -88,  -48,  -39,  -35,  -30,  -25,  -18,  -17,  -10,   -5,    0,
  },
  {
  -82,  -79,  -70,  -20,  -17,  -10,   -6,   -5,    0,
  },
  {
  -65,  -50,  -35,  -15,   -3,    0,
  },
  {
  -99,  -72,  -42,  -28,  -25,  -20,  -15,  -10,   -5,    0,
  },
  {
  -78,  -73,  -70,  -50,  -45,  -20,  -13,  -12,   -5,   -1,    0,
  },
  {
  -98,  -74,  -59,  -51,  -38,  -30,  -22,  -15,  -10,   -3,   -2,
  },
  {
  -87,  -75,  -67,  -25,  -15,  -11,   -5,   -1,    0,
  },
  {
  -78,  -53,  -30,  -17,    0,
  },
  {
  -46,  -30,  -25,   -7,    0,
  },
  {
  -78,  -55,  -50,  -42,  -18,   -6,   -2,
  },
  {
  -95,  -58,  -43,  -35,  -20,  -19,  -15,   -8,   -4,   -3,    0,
  },
  {
  -90,  -80,  -58,  -57,  -44,  -33,  -30,  -20,  -10,   -5,    0,
  },
  {
  -63,  -58,  -33,  -22,  -10,   -5,
  },
  {
  -95,  -52,  -36,  -30,  -24,  -23,  -17,  -16,  -10,   -5,   -2,
  },
  {
  -93,  -85,  -63,  -60,  -23,  -18,  -13,   -8,    0,
  },
  {
  -94,  -84,  -63,  -48,  -27,  -22,  -10,   -5,    0,
  },
  {
  -99,  -87,  -42,  -26,  -25,  -21,  -15,  -11,  -10,   -5,    0,
  },
  {
  -68,  -63,  -50,  -38,  -29,  -18,  -15,  -10,    0,
  },
  {
  -35,  -29,  -28,  -15,   -7,    0,
  },
  {
  -82,  -65,  -60,  -28,  -18,  -13,   -7,    0,
  },
  {
  -75,  -68,  -53,  -40,  -27,  -15,  -10,   -3,
  },
```

```
  {
  -90,  -83,  -31,  -30,  -20,  -16,  -15,  -12,   -7,   -4,   -3,
    0,
  },
  {
  -73,  -68,  -66,  -12,   -5,    0,
  },
  {
  -44,  -40,  -12,
  },
  {
  -93,  -70,  -33,  -21,  -17,  -10,   -7,    0,
  },
  {
  -80,  -73,  -32,  -17,  -14,  -13,  -10,   -5,    0,
  },
  {
  -78,  -37,  -23,  -22,  -18,  -15,  -10,   -5,    0,
  },
  {
  -78,  -73,  -58,  -10,   -5,   -1,
  },
  {
  -82,  -45,  -37,  -31,  -22,  -18,  -17,  -10,   -7,   -3,    0,
  },
  {
  -98,  -75,  -70,  -26,  -25,
  },
  {
  -85,  -78,  -67,  -37,  -17,  -12,   -8,   -5,
  },
  {
  -91,  -79,  -40,  -30,  -25,  -20,  -15,  -10,   -5,    0,
  },
  {
  -83,  -78,  -65,  -15,  -10,   -9,   -5,    0,
  },
  {
  -70,  -50,  -42,  -22,   -8,    0,
  },
  {
  -80,  -75,  -72,  -31,  -12,
  },
  {
  -97,  -83,  -68,  -42,   -5,
  },
  {
  -96,  -51,  -47,  -30,  -25,  -22,  -15,  -10,   -3,
  },
  {
  -83,  -71,  -12,   -5,   -2,
  },
  {
  -86,  -62,  -55,  -27,  -20,  -17,  -13,  -12,   -8,   -7,   -3,
    0,
  },
  {
  -80,  -36,  -20,  -17,  -13,
  },
  {
  -95,  -88,  -47,  -30,  -29,  -18,  -17,  -13,  -10,   -5,    0,
  },
  {
  -92,  -57,  -50,  -38,   -3,
  },
  {
  -88,  -20,  -14,  -13,   -8,   -7,    0,
  },
  {
  -54,  -53,  -40,  -35,  -23,  -16,  -15,   -8,   -3,
  },
  {
  -99,  -41,  -35,  -30,  -20,  -15,  -10,   -5,    0,
  },
  {
  -93,  -69,  -34,  -23,   -7,    0,
  },
  {
  -59,  -43,  -35,  -28,   -8,
  },
  {
  -95,  -90,  -25,  -21,   -7,   -2,
  },
  {
  -85,  -66,  -65,  -57,  -37,  -13,  -10,   -5,
  },
  {
  -90,  -46,  -12,
  },
  {
  -98,  -89,  -72,  -34,  -26,  -15,  -13,   -8,    0,
  },
  {
  -90,  -68,  -60,  -40,  -22,  -18,  -12,   -5,
  },
  {
 -100,  -95,  -28,  -15,   -8,   -5,
  },
  {
  -75,  -70,  -20,  -12,   -3,    0,
  },
  {
  -95,  -51,  -32,
  },
  {
  -77,  -70,  -20,  -18,  -15,  -13,  -10,   -5,    0,
  },
  {
  -65,  -45,  -23,
  },
  {
  -98,  -33,  -28,  -27,  -23,  -20,  -15,  -10,   -7,   -3,    0,
  },
  {
  -80,  -75,  -67,  -37,  -18,  -17,   -5,    0,
  },
};

float flt_coefs2[SEG_LENGTH2][MFLT_LENGTH2] =
{
  {
  -0.6614879E-02,  -0.1429926E-01,   0.1880962E-01,   0.4904101E-01,
  -0.5967685E-01,   0.9309760E-01,  -0.3967213E-01,   0.5029122E-01,
  -0.7570823E-01,  -0.9420925E-01,   0.1056719E+00,
  },
  {
  -0.3887421E-02,  -0.3144222E-02,  -0.2708863E-01,   0.4338598E-01,
   0.3446739E-01,   0.7237891E-01,  -0.3861937E-01,  -0.6701618E-01,
   0.6618018E-01,  -0.9265281E-01,  -0.5974102E-01,
  },
  {
  -0.1015457E-02,   0.1787316E-01,  -0.5627253E-01,   0.2446596E-01,
   0.4138545E-01,  -0.4920137E-01,   0.8277126E-01,  -0.5583157E-01,
   0.5483646E-01,   0.7511845E-01,   0.7321317E-01,   0.5719284E-01,
```

```
-0.5573704E-01,
},
{
 0.3706080E-02,   0.4192878E-02,   0.2192246E-01,  -0.2125863E-01,
-0.8888560E-01,  -0.4599749E-01,  -0.3867546E-01,  -0.8356100E-01,
 0.5090259E-01,   0.7988496E-01,
},
{
-0.5007708E-01,  -0.2835327E-01,   0.5709929E-01,   0.3569544E-01,
-0.8053026E-01,   0.6206589E-01,  -0.5520297E-01,   0.5194590E-01,
 0.7264247E-01,
},
{
 0.4696982E-02,   0.1344796E-01,   0.4094194E-01,   0.1405365E+00,
-0.1029181E+00,
},
{
 0.2858981E-02,   0.4921757E-02,  -0.1507979E-01,  -0.2491641E-01,
-0.8683238E-01,   0.4160152E-01,   0.6842425E-01,   0.3372858E-01,
 0.8530207E-01,   0.8224385E-01,
},
{
 0.5356384E-01,  -0.8929932E-01,  -0.4202133E-01,   0.9691476E-01,
-0.1476151E+00,   0.8123142E-01,
},
{
 0.3891838E-02,   0.4115778E-02,   0.1523170E-01,   0.9186109E-02,
 0.2767959E-01,   0.6692114E-01,  -0.5258305E-01,   0.7912263E-01,
-0.8534696E-01,   0.1040969E+00,
},
{
 0.6037670E-01,  -0.6883714E-01,   0.4781083E-01,  -0.7646285E-01,
 0.9738579E-01,   0.3017977E-01,
},
{
-0.8358268E-02,  -0.1078631E-01,  -0.1974960E-01,   0.3368537E-01,
 0.3764563E-01,  -0.7846859E-01,  -0.5252290E-01,  -0.7839710E-01,
-0.4286567E-01,   0.7466000E-01,   0.4668713E-01,   0.3656130E-01,
-0.4346279E-01,   0.9671300E-01,
},
{
 0.3909264E-02,   0.2749227E-02,  -0.4503471E-01,   0.6308652E-01,
-0.5864193E-01,   0.4538230E-01,  -0.8220814E-01,
},
{
 0.1718440E-02,   0.6382233E-02,   0.1334275E-01,   0.5420069E-01,
-0.6019428E-01,  -0.9237481E-01,   0.6849685E-01,  -0.1243653E+00,
},
{
 0.4034336E-02,  -0.5621848E-01,  -0.5721593E-01,   0.3324445E-01,
-0.7362759E-01,   0.1308168E+00,   0.1009267E+00,
},
{
-0.8879554E-03,   0.1323899E-01,  -0.6358895E-01,   0.4966516E-01,
 0.4289684E-01,   0.4098634E-01,   0.2913818E-01,   0.7054655E-01,
 0.6150728E-01,
},
{
-0.1363695E-01,  -0.2093042E-01,   0.9327054E-02,   0.4563500E-01,
 0.7180022E-01,  -0.5832529E-01,  -0.6202235E-01,  -0.6733461E-01,
-0.8133513E-01,   0.7626045E-01,   0.7296384E-01,   0.8405028E-01,
},
{
 0.1785205E-02,   0.3876256E-02,  -0.5187889E-02,   0.3658513E-01,
-0.5824666E-01,   0.3553154E-01,   0.4898361E-01,  -0.8159473E-01,
},
{
```

```
-0.2441164E-02,  -0.3309193E-01,  -0.2949855E-01,  -0.4857912E-01,
 0.3897524E-01,  -0.6927840E-01,  -0.5184076E-01,   0.5133453E-01,
 0.1029789E+00,  -0.7937372E-01,   0.7691066E-01,
},
{
 0.9691402E-02,   0.1573787E-01,   0.4049329E-01,   0.5797600E-01,
 0.4341811E-01,   0.1044834E+00,   0.5589737E-01,  -0.6136465E-01,
 0.1266025E+00,
},
{
-0.2911289E-01,   0.6536022E-01,  -0.9595171E-01,  -0.2635118E-01,
 0.5173032E-01,   0.5038553E-01,
},
{
 0.5064464E-03,  -0.1938821E-01,  -0.2045006E-01,  -0.3502310E-01,
-0.5073417E-01,   0.6181104E-01,  -0.6143093E-01,   0.1017410E+00,
-0.5733096E-01,   0.1099021E+00,
},
{
-0.6450505E-02,   0.1197766E-01,  -0.6577452E-02,   0.4924058E-01,
-0.5118743E-01,   0.5812128E-01,   0.9391383E-01,  -0.3865344E-01,
-0.5250741E-01,  -0.6554410E-01,   0.8407435E-01,
},
{
 0.2801587E-02,   0.1673847E-01,   0.2395294E-01,  -0.3958954E-01,
-0.2367036E-01,   0.5159958E-01,  -0.4911932E-01,  -0.8399504E-01,
 0.8474098E-01,   0.5365313E-01,  -0.6453564E-01,
},
{
-0.5055159E-02,  -0.2326774E-01,   0.1894546E-01,  -0.5114691E-01,
-0.9815212E-01,  -0.4697780E-01,  -0.1217237E+00,  -0.3119738E-01,
 0.1016141E+00,
},
{
-0.4417848E-02,   0.7742098E-01,   0.4264242E-01,   0.5359055E-01,
 0.7687466E-01,
},
{
-0.4329887E-01,   0.1245421E+00,  -0.2846893E-01,   0.1347317E+00,
 0.1279109E+00,
},
{
-0.2226657E-01,  -0.5160971E-01,   0.3648871E-01,  -0.3594881E-01,
-0.8736341E-01,   0.8779839E-01,  -0.7271840E-01,
},
{
-0.9175061E-03,  -0.4004556E-01,   0.4991431E-01,  -0.4166025E-01,
 0.5223776E-01,  -0.6164364E-01,  -0.9030090E-01,  -0.5116666E-01,
 0.5738448E-01,   0.5955560E-01,   0.1010771E+00,
},
{
-0.6161666E-02,   0.2162465E-01,  -0.1690745E-01,   0.1458709E-01,
 0.2280459E-01,   0.2883639E-01,   0.3736303E-01,   0.8033267E-01,
 0.1166013E+00,  -0.1032388E+00,   0.4823207E-01,
},
{
 0.1872556E-01,  -0.7729628E-01,   0.4621783E-01,  -0.4012094E-01,
 0.5902296E-01,  -0.7037951E-01,
},
{
 0.3155643E-02,  -0.2826733E-01,   0.3062426E-01,   0.4021729E-01,
 0.6401054E-01,   0.8385868E-01,   0.4622849E-01,   0.8073462E-01,
 0.7923588E-01,  -0.6105518E-01,  -0.5418089E-01,
},
{
-0.5417099E-02,  -0.1790018E-01,   0.2421645E-01,   0.3651322E-01,
 0.4757639E-01,  -0.3285359E-01,   0.9041086E-01,  -0.7359436E-01,
```

```
 0.6656604E-01,
},
{
-0.6927019E-02,   0.1583141E-01,   0.5772311E-01,  -0.4546625E-01,
 0.5429167E-01,  -0.7121480E-01,   0.7531629E-01,  -0.6427686E-01,
 0.5058303E-01,
},
{
 0.3349290E-02,   0.2598547E-01,   0.2603641E-01,   0.2869117E-01,
-0.5560236E-01,  -0.4124419E-01,  -0.9738243E-01,  -0.2900641E-01,
 0.9336783E-01,  -0.4642718E-01,   0.6119101E-01,
},
{
-0.2144716E-01,   0.5859940E-01,   0.4104657E-01,  -0.2838143E-01,
-0.2947324E-01,  -0.3557045E-01,  -0.5517643E-01,   0.6514291E-01,
 0.9176975E-01,
},
{
-0.7765751E-01,  -0.5638416E-01,  -0.9008388E-01,  -0.7788346E-01,
 0.9086886E-01,   0.8660997E-01,
},
{
-0.1137784E-01,  -0.4058158E-01,   0.3245270E-01,  -0.4292451E-01,
-0.8402064E-01,   0.8908543E-01,   0.4711056E-01,   0.6691652E-01,
},
{
-0.3579511E-01,  -0.5865894E-01,   0.6133667E-01,   0.3006370E-01,
 0.5329183E-01,  -0.4610473E-01,   0.8270162E-01,   0.4395046E-01,
},
{
 0.7641728E-02,  -0.1113240E-01,  -0.3335683E-01,   0.5433084E-01,
 0.6818714E-01,   0.3371345E-01,  -0.9338174E-01,  -0.4668515E-01,
 0.6782711E-01,   0.3186922E-01,   0.6549584E-01,   0.6918482E-01,
},
{
 0.3299118E-01,  -0.4227466E-01,   0.3103725E-01,  -0.5033476E-01,
-0.6719448E-01,   0.8481884E-01,
},
{
 0.3336797E-01,   0.9236907E-01,  -0.1593052E+00,
},
{
 0.8157173E-02,   0.5168252E-01,   0.3905740E-01,  -0.5900268E-01,
 0.7004637E-01,   0.4552325E-01,   0.8388874E-01,   0.9758771E-01,
},
{
 0.4147324E-01,   0.7269266E-01,  -0.4770963E-01,   0.3419052E-01,
 0.4878791E-01,   0.5932455E-01,   0.5388714E-01,  -0.8102848E-01,
 0.1162714E+00,
},
{
 0.1873459E-01,   0.3837034E-01,   0.6504966E-01,  -0.5953367E-01,
-0.5975812E-01,  -0.9290178E-01,   0.5676722E-01,  -0.8950090E-01,
 0.9507764E-01,
},
{
-0.2894814E-01,   0.5057938E-01,  -0.1808140E-01,   0.5988654E-01,
-0.1028527E+00,  -0.5846804E-01,
},
{
 0.3291355E-01,  -0.4437537E-01,   0.6803057E-01,  -0.4815017E-01,
-0.4711590E-01,  -0.5060849E-01,   0.7042320E-01,   0.6447795E-01,
 0.4678527E-01,   0.8806979E-01,   0.4878302E-01,
},
{
-0.8771360E-02,  -0.5994582E-01,   0.3814937E-01,   0.8554896E-01,
-0.4169315E-01,
```

```
},
{
-0.3657513E-01,  -0.8251550E-01,   0.4399715E-01,   0.5526234E-01,
 0.7571201E-01,  -0.6371758E-01,  -0.7080819E-01,  -0.7365576E-01,
},
{
 0.1195100E-01,   0.2362175E-01,   0.4317594E-01,   0.5466008E-01,
-0.6546786E-01,   0.9262113E-01,  -0.4062239E-01,   0.7532982E-01,
-0.5964542E-01,   0.7468928E-01,
},
{
 0.1619453E-01,  -0.4108550E-01,  -0.2260301E-01,  -0.5597401E-01,
 0.8142098E-01,  -0.3302361E-01,  -0.8204678E-01,   0.5921208E-01,
},
{
 0.4304931E-01,   0.7605813E-01,  -0.8353233E-01,  -0.7646306E-01,
-0.5347725E-01,   0.7866547E-01,
},
{
 0.2850488E-01,  -0.6485684E-01,  -0.2479879E-01,  -0.8661002E-01,
-0.5764616E-01,
},
{
-0.5424140E-02,   0.5348583E-01,  -0.9035242E-01,  -0.8372557E-01,
-0.5181130E-01,
},
{
-0.1670526E-01,  -0.5824187E-01,   0.3338574E-01,   0.5332801E-01,
-0.7521041E-01,  -0.3403812E-01,  -0.6603187E-01,   0.6710238E-01,
 0.5244897E-01,
},
{
 0.7116876E-01,   0.4290202E-01,  -0.9650268E-01,  -0.7159492E-01,
-0.5531762E-01,
},
{
 0.2118123E-01,  -0.3916537E-01,  -0.5624462E-01,   0.7524978E-01,
 0.4825355E-01,   0.4298079E-01,   0.9778190E-01,  -0.5122039E-01,
-0.4737237E-01,   0.6585310E-01,   0.6630810E-01,   0.4685323E-01,
},
{
 0.6657317E-01,   0.8633183E-01,   0.4640199E-01,   0.6243679E-01,
 0.5254362E-01,
},
{
-0.2462394E-01,  -0.4815776E-01,   0.3934532E-01,   0.4348452E-01,
-0.4063642E-01,  -0.5861045E-01,   0.6549107E-01,   0.6442931E-01,
 0.4171386E-01,  -0.6112875E-01,   0.9744171E-01,
},
{
-0.1573435E-01,   0.7631516E-01,   0.8629898E-01,  -0.1102906E+00,
 0.1027282E+00,
},
{
-0.2956824E-01,   0.7718813E-01,   0.3606934E-01,   0.9468325E-01,
-0.6346736E-01,   0.6661998E-01,   0.1173735E+00,
},
{
 0.5552817E-01,   0.6476392E-01,   0.4064802E-01,  -0.8114761E-01,
 0.7275619E-01,   0.4035515E-01,  -0.5406699E-01,  -0.9764583E-01,
 0.8995514E-01,
},
{
 0.1331168E-01,  -0.2581197E-01,  -0.4927886E-01,   0.5133463E-01,
 0.6809124E-01,  -0.4226324E-01,   0.4753117E-01,  -0.6921270E-01,
 0.6723411E-01,
},
```

```
  {
   0.5604440E-01,  -0.7229649E-01,   0.5320710E-01,   0.8676874E-01,
   0.6210139E-01,   0.9611095E-01,
  },
  {
  -0.3191814E-01,   0.6595018E-01,  -0.9802993E-01,  -0.3899986E-01,
  -0.7033533E-01,
  },
  {
  -0.4227392E-01,   0.1422027E-01,  -0.6879323E-01,  -0.7103910E-01,
   0.5515100E-01,  -0.7020096E-01,
  },
  {
  -0.3566328E-01,   0.4954189E-01,  -0.4300747E-01,   0.3426962E-01,
   0.4974108E-01,   0.7415684E-01,   0.5711441E-01,  -0.7182895E-01,
  },
  {
   0.6140056E-01,   0.7111893E-01,  -0.4804461E-01,
  },
  {
  -0.2997365E-01,  -0.4629572E-01,  -0.3989322E-01,   0.4538489E-01,
   0.5980771E-01,  -0.7202677E-01,   0.4854868E-01,  -0.6519832E-01,
   0.8260079E-01,
  },
  {
   0.2926636E-01,  -0.5817771E-01,   0.5397728E-01,   0.5684553E-01,
  -0.3359030E-01,  -0.5425525E-01,  -0.6073613E-01,  -0.7547803E-01,
  },
  {
   0.3502282E-01,  -0.1358177E-01,  -0.5018083E-01,  -0.8992089E-01,
  -0.5606518E-01,  -0.6158898E-01,
  },
  {
  -0.4238006E-01,   0.6123731E-01,   0.3187495E-01,  -0.8657039E-01,
   0.5340118E-01,   0.1051042E+00,
  },
  {
  -0.5427403E-01,  -0.5890925E-01,  -0.3562557E-01,
  },
  {
   0.3972447E-01,   0.2197290E-01,   0.7261248E-01,  -0.4201903E-01,
  -0.7315820E-01,   0.1360201E-01,   0.5520076E-01,  -0.8179243E-01,
   0.7224426E-01,
  },
  {
  -0.7109583E-01,  -0.1303928E+00,   0.4776314E-01,
  },
  {
  -0.2063328E-01,   0.2734613E-01,  -0.3529310E-01,   0.3259774E-01,
   0.3253571E-01,   0.8483794E-01,  -0.7366542E-01,   0.5688202E-01,
   0.5682221E-01,   0.5374562E-01,   0.7876849E-01,
  },
  {
   0.4776524E-01,  -0.1507547E-01,   0.2400588E-01,   0.3280406E-01,
  -0.5068491E-01,   0.6211805E-01,  -0.8781512E-01,   0.9945956E-01,
  },
};

float flt_intercepts2[SEG_LENGTH2] =
{
   0.8259140E-01,  -0.4758021E-01,   0.4089225E-01,   0.1639756E-01,
  -0.6876206E-01,   0.2273056E-01,   0.3819146E-01,  -0.3721802E-01,
  -0.5713508E-01,   0.2394236E-01,  -0.6512219E-01,  -0.2191193E-01,
   0.6342072E-01,  -0.3024785E-01,  -0.3814323E-01,   0.3050360E-01,
   0.3170719E-01,  -0.2565768E-01,  -0.5481426E-01,   0.3873283E-01,
  -0.3035126E-01,  -0.3384014E-01,   0.9957474E-01,  -0.3666606E-02,
  -0.5692184E-01,  -0.5636183E-01,   0.6097601E-01,  -0.3236854E-01,
  -0.3393197E-01,   0.1826495E-01,   0.3305293E-01,  -0.1825163E-01,
  -0.7350731E-02,   0.3190426E-02,  -0.1362626E-01,  -0.4761601E-01,
   0.3119041E-01,   0.3703185E-01,  -0.4902850E-01,   0.2156271E-01,
   0.2257008E-01,  -0.2476735E-01,  -0.1802885E-01,   0.3251489E-01,
  -0.1129883E-01,   0.5745488E-02,   0.5650065E-01,   0.2234104E-01,
  -0.4830371E-01,   0.2498304E-01,   0.6292367E-01,  -0.5668922E-01,
   0.1234409E-01,   0.4732342E-01,  -0.5023522E-01,   0.6448446E-02,
  -0.4441234E-03,  -0.1959216E-01,   0.3735405E-01,   0.6997063E-01,
   0.4517583E-02,  -0.2926396E-01,   0.3523561E-01,   0.6521603E-01,
  -0.4535277E-01,  -0.3852353E-01,   0.1808334E-01,   0.1675636E-04,
  -0.3392704E-01,   0.1460649E-01,  -0.7783228E-02,  -0.1373911E-01,
   0.7815688E-02,   0.9795678E-01,  -0.1906542E-02,   0.2516573E-01,
};
```

RAUSS

Noise Tolerance of Model-Based Neural ATR

Mr. Patrick J. Rauss
U. S. Army Research Laboratory
Sensors, Signatures, Signal and Information Processing Directorate
ATR Research Branch
AMSRL SS SK RAUSS
10221 Burbeck Rd. Ste. 430
Ft. Belvoir, VA 22060-5806

Introduction:

Model-based automatic target recognition (ATR) is the focus of much attention. One approach is the use of artificial neural networks (NNs) that have been trained with model data. This paper will present the results of a research effort entitled Neural Networks Applied to Infrared Signal Processing. This project evolved from an effort to automatically identify infrared chemical spectra collected in the field with a Fourier Transform Infrared Spectrometer (FTIR). A number of common spectroscopic analysis techniques were investigated and found unable to tolerate the level of noise common to this sensor system.[1] Due to the poor performance of the common techniques a new approach was required. A literature search was undertaken, as well as discussions with other Army organizations, to identify methods to pull signals out of a high noise environment. A number of promising methods were identified and subsequently ruled out due to constraints on the program hardware. Several sources mentioned NN's tolerance to noise, suggesting these may be a promising approach.

Overview:

The neural network chosen to investigate was the simple back propagation of error, or backprop (BP), network. The BP network is a supervised network. The architecture used in this work consists of

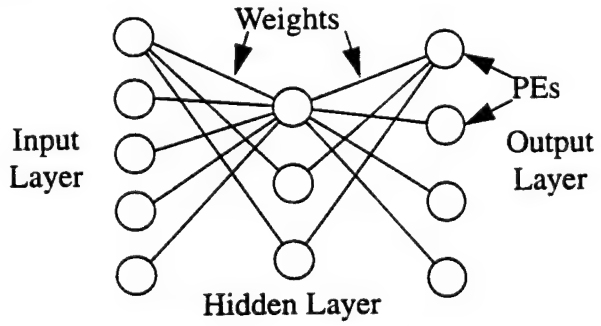

Figure 1: Three layer NN
Note: For clarity only one node is shown fully interconnected in each layer.

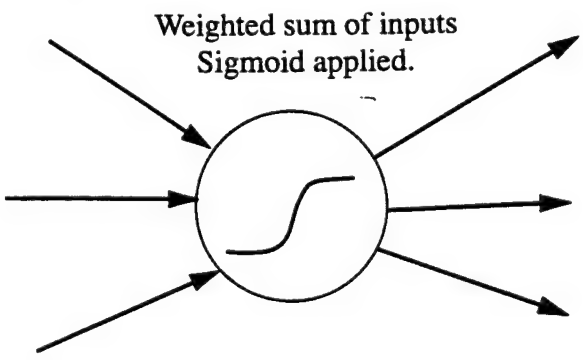

Figure 2: Processing Element

three layers; input, hidden, and output. The input layer consists of 571 nodes. These nodes are fully connected to 200 processing elements (PEs) in the hidden layer. The hidden-layer PEs are fully connected to 66 output-layer PEs (see fig. 1). The NN is given an input and told what the required response or truth is. The network compares its response to the desired response, computes an error, and propagates the error correction back through the layers. The PEs take the sum of the weighted inputs and apply a nonlinear thresholding function. The function used in this work is the logistic sigmoid function, as shown in figure 2. The output of the PE depends upon the activation of the sigmoid function.

The current environment used for this work consists of a VME BALBOA i860 neural accelerator board and NeuroSoft software from HNC, Inc., hosted on a SUN 630MP. The program is written in C with function calls to NeuroSoft.

The goal of this effort is to identify an unknown infrared spectrum as one of a library of 66 spectra or as an unknown/unidentifiable. The structure of this NN with 66 output nodes, one for each class, has been shown to give Bayesian a posteriori probabilities, once trained, if the training requires the nodes to respond in a binary fashion: true = 1 and false = 0.[2,3] The neural network is trained on a library of 66 spectra that were collected in a laboratory with a laboratory-grade FTIR configured to collect at the same resolution as the fieldable sensor. The library data has no noticeable noise in the signal.

The problem with training an NN in this fashion is its ability to memorize. In this environment the training of an NN continues until some Mean Squared Error (MSE) threshold is crossed. That is, over the last complete pass through the training file did the MSE drop below the set threshold; if so, training is complete. Equation (1) shows the MSE calculation used by this package.

$$MSE = \frac{1}{N} \sum_{k=1}^{N} \sum_{i=1}^{M} (t_i - z_i)^2 \qquad (1)$$

where k indexes the iterations, one iteration being the presentation of one spectrum; N is the number of consecutive iterations of the network since the last error calculation, here set to 66 (check MSE after each training pass through the library); i indexes the PE's; M is the total number of PE's; t is the truth value for the ith PE, and z is the output of the ith PE.

The difficulty lies in answering the question: What is a suitable MSE threshold? The MSE threshold could be set to zero, which would require the network to train until it exactly reproduced the required outputs. However, in this case that would mean the NN memorized the original spectral inputs, and exact reproductions of these spectra would be required to get a proper response from the network. The problem is the actual sensor will have quite a bit of noise in it, which would confuse a network trained to this level.

Alternatively one could train only to a relatively high MSE: however, this network would have poor recognition qualities in general or would identify some of the spectra well and others not at all. The objective is to find an optimal MSE which identifies all the spectra but is not trained so far that it needs an exact reproduction of the spectra it was trained on before it registers a match.

In order to avoid having to collect the library with the fieldable sensor or to extensively preprocess the collected data, the approach was taken to add random noise to every input point to 'fuzz up' the model data. The questions are how much noise can be added before the network will no longer learn and how well will an NN trained in this manner perform on sensor data. Figure 3 shows an example of the original library spectra and the resultant noisy spectra. This approach also forces the network to become very robust by compelling it to focus only on the most robust features of the data set. The network will not focus only on peak location or relative intensities between specific peaks because these values will

continuously vary during training.

Approach:

The following procedure was used to train the networks discussed in this paper. A network was initialized with small near- zero random weights. A noise level was chosen. This level is a percentage of the height of the preprocessed library spectrum. The preprocessing simply normalizes each spectrum between 0 and 1. The noise is added to the spectrum just before presentation to the NN. The resulting noisy spectrum is then normalized again to either a 0 to 1 or -1 to 1 range and fed to the NN for training. This paper primarily focuses on the -1 to 1 range as this range appeared to train faster in preliminary work.

The noisy spectra are renormalized in order to make the baseline of the spectra vary somewhat. Of course, the amount of noise added will influence how much the baseline varies. There was some concern that the NN may only recognize spectra with a baseline on the zero or -1 line and thus not recognize sensor data that can have a varying baseline due to background subtraction methods; figure 4 shows an example of very bad baseline from sensor data.

Once training is begun the MSE is monitored every complete pass through the training library. When the MSE drops below 0.1 the network state is saved. Training is then continued from the current state to the next threshold. The thresholds used in this effort are 0.1, 0.01, 0.001, and 0.0001. Four thresholds were chosen to allow an investigation into what would be a good MSE level for training. Too much

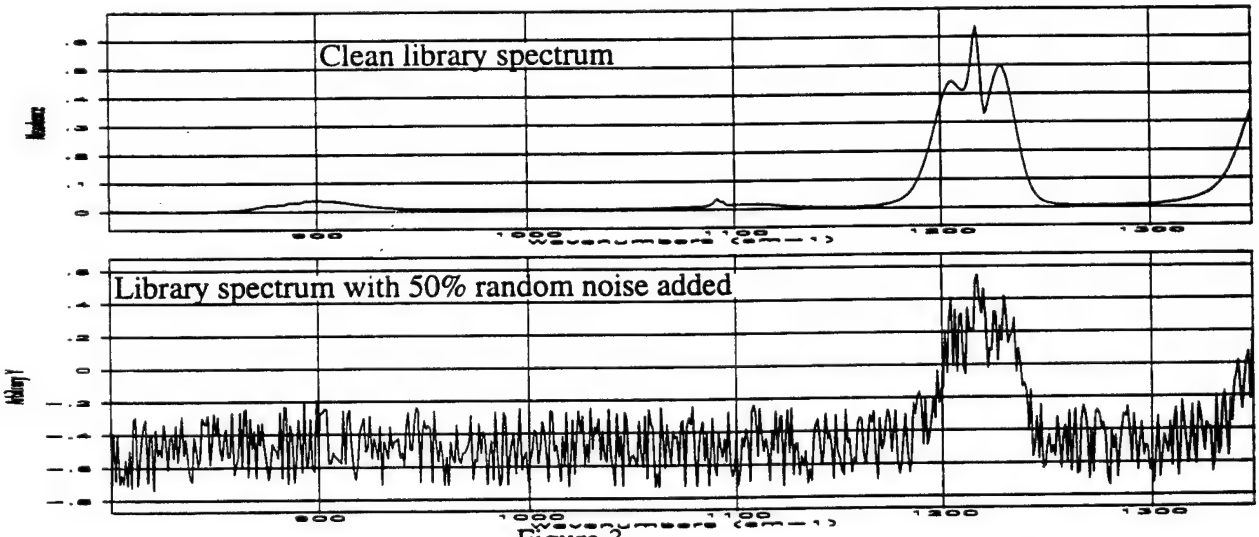

Figure 3

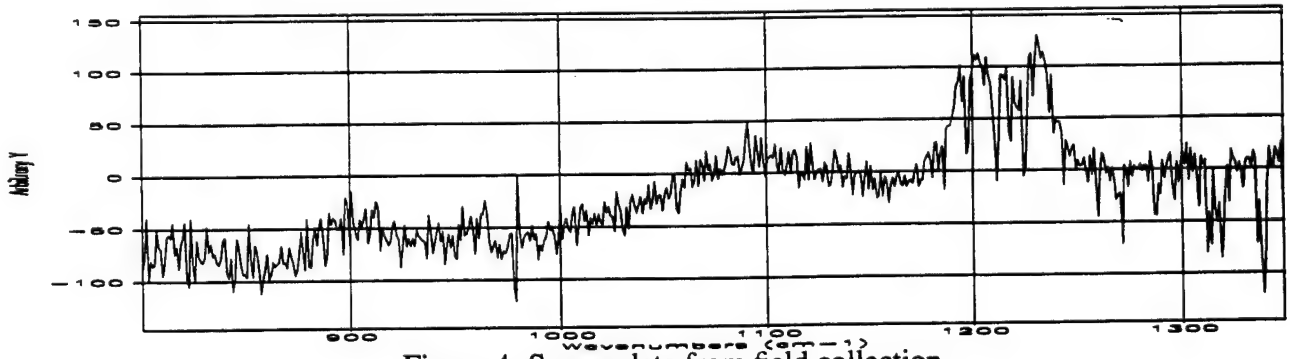

Figure 4: Sensor data from field collection.

training, even if there is a slight improvement of performance, can be a waste of resources.

Networks have been completely trained on the following noise levels: 20% (2), 50%, 60%, 70%, 80%, 90%, 100% (7), 140%, 150% (2), and 200%. The (2) indicates that two networks were trained starting in different random areas of weight space. This was done to ensure that a trained network did not just "happen" to start in a weight space area near a solution. The seven different networks for 100% noise are the result of an error in the computer code, which defaulted to 100% noise for any value entered greater than 100%. This error was corrected and networks trained recently to 140%, 150%, and 200% noise levels.

In order to determine the noise tolerance of the trained networks a statistics collection routine was written that uses the library spectra trained with, as a test. The library spectra are used at this stage because a truth file exists that is used to determine a correct hit. Starting with 0% noise added, the library is run through the trained network with learning turned off. A threshold of 60% is set for a confidence-level check. The output nodes are sorted and the largest response is checked. If it does not cross the threshold, the presentation is classified as NoCross. If it crosses or equals the threshold it is checked for

```
Network trained with 100% noise
Threshold level is   0.6
Ambiguity level is  0.4

Noise level is 0  Percent.
--------1----------2----------3----------4----------5----------6-----
0       0   0    2000   1    2000   2    2000   3    2000   4    2000   5
1    2000   6    2000   7    2000   8    2000   9    2000  10    2000  11
2    2000  12    2000  13    2000  14    2000  15    2000  16    2000  17
3    2000  18       0  19    2000  20    2000  21    2000  22    2000  23
4    2000  24    2000  25    2000  26    2000  27    2000  28    2000  29
5    2000  30    2000  31    2000  32    2000  33    2000  34    2000  35
6       0  36    2000  37    2000  38    2000  39    2000  40    2000  41
7    2000  42    2000  43    2000  44    2000  45    2000  46    2000  47
8       0  48    2000  49    2000  50    2000  51    2000  52    2000  53
9    2000  54    2000  55    2000  56    2000  57    2000  58    2000  59
10   2000  60    2000  61    2000  62    2000  63    2000  64    2000  65
False alarms below .
0       0   0       0   1       0   2       0   3       0   4       0   5
1       0   6       0   7       0   8       0   9       0  10       0  11
2       0  12       0  13       0  14       0  15       0  16       0  17
3       0  18       0  19       0  20       0  21       0  22       0  23
4       0  24       0  25       0  26       0  27       0  28       0  29
5       0  30       0  31       0  32       0  33       0  34       0  35
6       0  36       0  37       0  38       0  39       0  40       0  41
7       0  42       0  43       0  44       0  45       0  46       0  47
8       0  48       0  49       0  50       0  51       0  52       0  53
9       0  54       0  55       0  56       0  57       0  58       0  59
10      0  60       0  61       0  62       0  63       0  64       0  65
Multi crossing total       0 No crossing total    8000
Total false alarms       0
Total correct 124000          Total number presented 132000
False alarm rate is 0.000000 Correct hit rate is 93.939394
```

Figure 5: Sample output of statistics collection program.

correctness against the truth file. If it is incorrect the False counter is incremented and the node number of the false spectra is logged in an incorrect hit table (see fig. 5 for an example). If the largest responding node is the correct identification, the Correct counter is incremented and the node number of the spectra is incremented (fig. 5). One further check is made at this point. An ambiguity level is set when the program starts. For most of this work it is 0.4. This means that if a correct hit is logged a comparison is made with the next highest responding node. If they are less than 0.4 apart the multi-cross counter is incremented.

Figure 5 shows the output of the statistics collection program for a network trained with 100% random noise and trained to 0.1 MSE. The noise level indicated in figure 5 is the noise level presented to the trained network, here 0%. The next block of numbers are the correct hit registers for each spectra, showing here 2000 presentations for each spectra. The left-most column is a row index. The next number to the right is the number of hits, and the following number to the right is the spectrum number. The next block down are the false alarms of each spectra. Below are the number of multi crossings, no crossings of the threshold, total number of false alarms, total number of correct hits, total number of spectra presented, and the false alarm and correct hit rates in percentages.

Once the program has presented the desired number of spectra, the results are written to disk and the program then increments the noise level 10% and repeats for the same number of total passes. The program continues until it completes collecting results on the upper noise level bound that was set. For this work the upper bound is 200% noise.

Results:

The first observation to be made upon examination of the statistics files collected thus far shows that training to an MSE of 0.1 is insufficient to ensure complete training. At this level, at least three of the spectra are not correctly classified (see fig. 5). In most cases the spectra not identified correctly are not identified at all, as in the results shown in figure 5. In a few cases one of the spectra is consistently classified incorrectly as another spectrum.

The second observation noted is shown in figure 6. Up to the noise trained on there is little or no difference between the performance of networks trained to an MSE of 0.01, 0.001, or 0.0001. This observa-

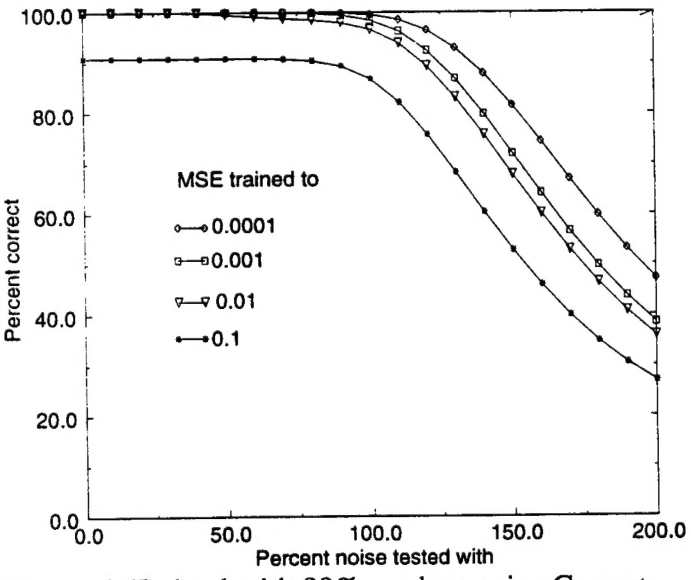

Figure 6: Trained with 80% random noise-Correct

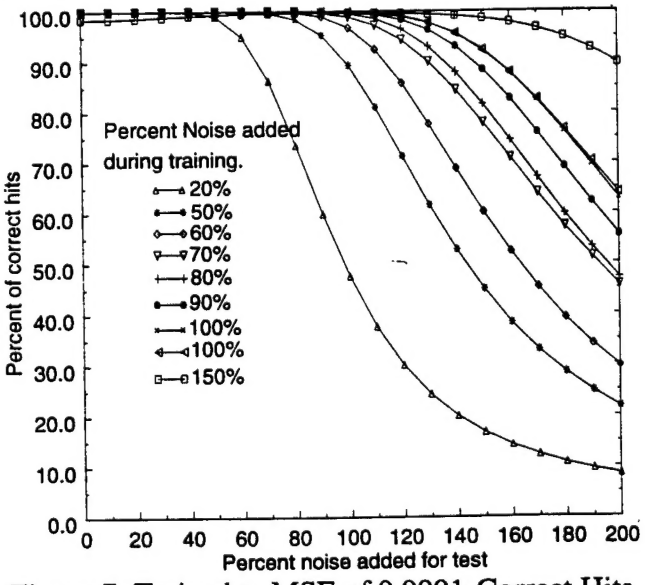

Figure 7: Trained to MSE of 0.0001-Correct Hits.

tion holds for networks trained with up to 100% noise. On networks trained with noise levels between 100% and 150% noise, networks trained to an MSE of 0.0001 incorrectly identify one spectrum at low noise levels. This can be seen in figure 7 as the slight dip at the low noise end of the 150% curve and also in figure 8. As the noise level during testing increases, the network begins to correctly identify this spectrum more regularly until the performance of the entire network begins to degrade at higher noise levels. The exact training noise level where this begins has not been identified yet, since statistics have not yet been collected for all the nets trained on noise levels between 100% and 150%, although figure 8 shows a similar effect for the network trained with 140% noise. This activity may indicate some over training of the network, so it appears that at least for high noise training levels an MSE of 0.001 is more useful.

With the 60% confidence threshold before classifying a node active, the false alarm rate remains very low even as the classification performance decays (see figs. 8 and 9). Figure 8 also shows the incorrect classification of a single spectrum by nets trained with high noise and trained to an MSE of 0.0001 when processing low noise spectra. By comparing figures 8 and 9 we see that by using nets trained to an MSE of 0.001, in general, there is very little increase in false alarms, except for nets trained with very little noise.

Preliminary results of collecting statistics with no thresholds set (i.e. finding the node with the largest magnitude) show that some networks generalize well out to nearly three times the noise level they were trained on (fig. 10). Also note that the false alarm rate also increases much faster because every presentation requires an identification (fig. 11). At this time no information is available to indicate how close the next highest node is under these conditions. Nor is information collected on the intensity of the best node. It is likely that both of these values would show low node response and little difference between best and second best hits at very high noise test levels.

Conclusions:

The results to date show that by training with noise added to the model signal a neural network can be generated which has high noise tolerance. For this data set, a reasonable noise level to train with appears to lie between 100% and 140% and training to an MSE of 0.001 appears adequate.

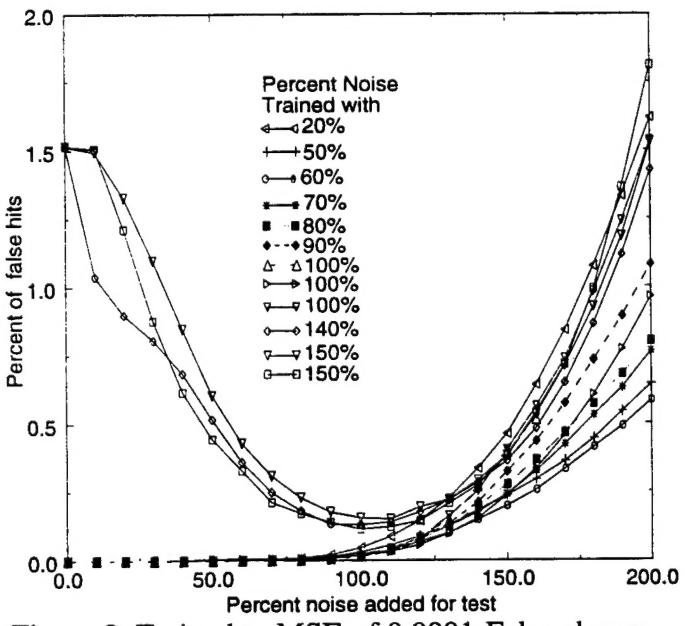

Figure 8: Trained to MSE of 0.0001-False alarms.

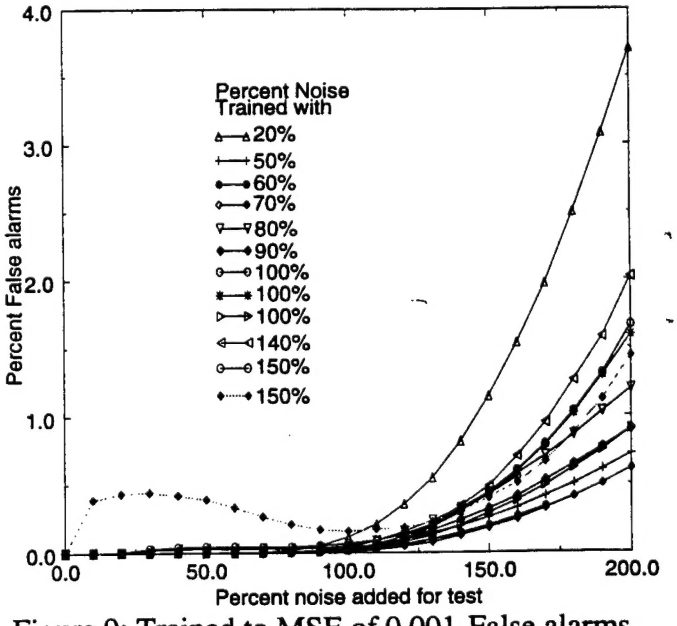

Figure 9: Trained to MSE of 0.001-False alarms.

Preliminary indications of the NNs performance on sensor data are encouraging, but only a small number, <20, of sensor spectra have been run through a network trained with 50% noise. The results were mixed as expected because some of the sensor data had very skewed baselines.

Finally, by requiring a minimum confidence level for identification one can suppress many false alarms down to 1 to 2% and maintain very high classification rates.

Future Efforts:

A more thorough test of performance with sensor data will be conducted shortly. The data is currently undergoing background subtraction and will be formatted for input into the trained networks. A small rewrite of the statistics software may be needed to properly record the results to allow a determination of the best noise level to train on for sensor data identification.

Also further statistics will be collected out to higher noise levels to determine if the networks all begin exhibit a linear roll-off at high noise levels as seen for the 50% network in figure 10. Optimal confidence thresholds will also be determined

Shortly, these techniques will be applied to Forward Looking Infrared (FLIR) imagery in order to develop a FLIR ATR system that exhibits the high classification rates displayed under this effort. Application of this technique to FLIR ATR should not only allow training with a model or simulated data, but should also improve the performance of the ATR under dynamic battlefield conditions.

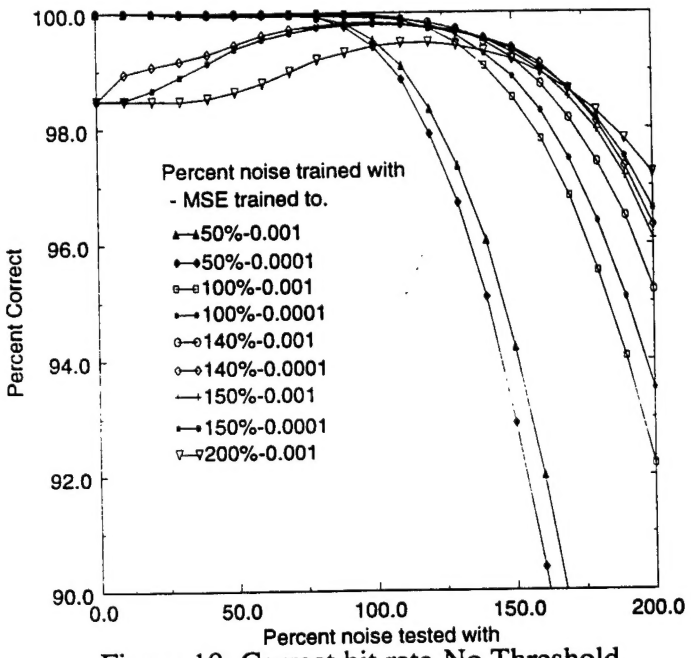

Figure 10: Correct hit rate-No Threshold.

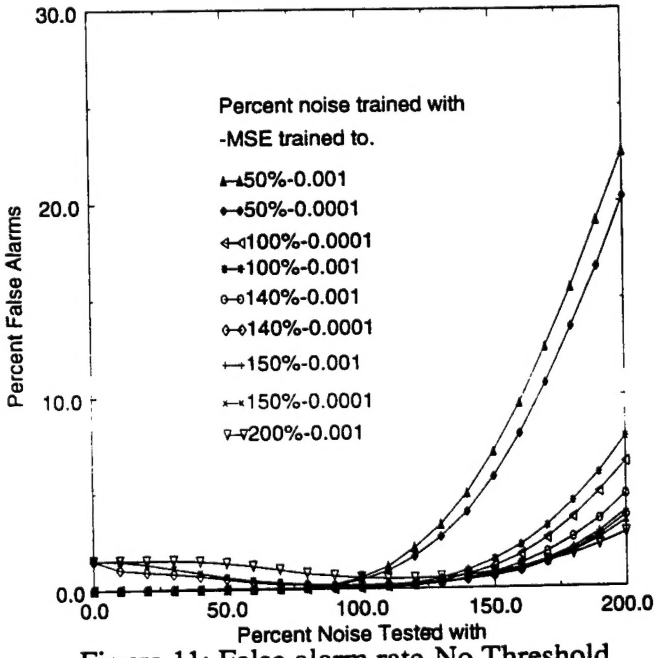

Figure 11: False alarm rate-No Threshold.

Bibliography:

1. P. Rauss, *Automatic Recognition of Spectral Components using Neural Networks,* Proceedings of the Second Automatic Target Recognizer Systems and Technology Conf., (GACIAC 1992), p 169.
2. M. Richard, R. Lippman, *Neural Network Classifiers Estimate Bayesian a posteriori Probabilities,* Neural Networks, (MIT Press), 1991 **V3**, p 461.
3. J. Hamphire and B. Pearlmutter, *Equivalence Proofs for Multi-Layer Perceptron Classifier and the Bayesian Discriminant Function,* Proceedings of the 1990 Connectionist Models Summer School, Touretzky, Elman, Senjnowski, and Hinton, Eds., (Morgan Kaufman, 1990).